

International Workshop on Physics of Active Fault



Abstracts

26-27 Feb., 2002
Tsukuba, Japan
NIED



www.bosai.go.jp/Fault_WS/



NIED National Research Institute for Earth Science and Disaster Prevention

Preface

Recent in-situ downhole measurements and coring through active faults have been providing us with new insights on the physical property of fault zones. We would like to share this knowledge and to discuss the current state of the art on fault zone physical studies from various angles.

The purpose of the workshop is mainly to discuss scientific issues related to active fault zones, especially on the importance of drilling project through the fault zone as well as to discuss the requirements to the fault zone drilling from points of view of numerical simulation and experimental studies. We would also be happy if we could discuss the future direction of active fault drilling project.

Important keyword of the workshop would be "**Stress and Strength of Active Fault**". This workshop consists of four sessions targeting the keyword.

The organization committee prepared some "Key Questions" in order to help focus the discussion during the workshop. All invited speakers should be required to reply at least one of the questions. Also invited speakers will be able to use part of their talk to give us their perspective on the questions.

Session 1: Downhole Measurements

- What is the optimum strategy to measure stress and detect changes by in-situ downhole measurements?
- What kind of methodology is needed to obtain the characteristic feature of active faults?

Session 2: Surface-based Observation

- What are the key measurements to be made through long term observations and coordinated experiments?
- What kinds of additional information will be needed to characterize the nature of an active fault?

Session 3: Numerical Modeling

- What are the key parameters for numerical modeling that can be obtained through drilling and related experiments?
- Are there hypotheses can be tested through drilling?

Session 4: Core Analyses and Experiments

- What information can we obtain about the rheological properties of active faults and the dynamics of earthquake slip from drilling holes?
- How can we estimate the age of past earthquakes and fault slip episodes? Is there any way to discriminate between aseismic and seismic slip based on the analysis of recovered fault rocks?

We, the organization committee, sincerely hope that this workshop will be of benefit to all the participants and will initiate to develop a new research field.

February 26, 2002

Ryuji Ikeda, Chair of the Workshop
Eiichi Fukuyama, Co-chair of the Workshop

Program

February 26

8:30 Registration

8:50 Opening Address (Katayama, T., president of NIED)

9:00 **S0-1** Ikeda, R.:

Introduction of the Workshop and Outline of the NIED Project

Session I Downhole Measurements

(Chaired by Hickman & Ikeda)

9:10 **S1-1** *Ikeda, R., K. Omura, T. Matsuda, and Y. Iio:

Spatial and Temporal Variation of Crustal Stress around Active Faults Inferred from In-situ Measurements

9:30 **S1-2** *Engeser, B., L. Wohlgemuth, and J. Kück:

Wellbore Instabilities - Detriment or Benefit? Experiences of the Integrated Stress Measurement Strategy in the KTB-Boreholes

9:50 **S1-3** Ellsworth, W. L.:

The Long Valley Exploratory Well: A Deep Geophysical Observatory at the Center of a Restless Caldera

10:10 Coffee Break

10:40 **S1-5** Ito, H.:

Seismogenic Zone Drilling - Nojima, Chelungpu and Nankai -

11:00 **S1-6** *Hickman, S. H., W. L. Ellsworth, and M. D. Zoback:

The San Andreas Fault Observatory at Depth: Studying the Physics of Earthquakes through Fault Zone Drilling

11:20 **S1-7** *Cornet, F. H., P. Bernard, I. Moretti, G. Borm, and I. Vardoulakis:

The Corinth Rift Laboratory Project

11:40 **S1-8** Ando, M.:

Results from Drilling Observation on Active Faults in Japan, Taiwan and South Africa - Comments on Future Drilling Programs

12:00 Discussion for Session I

12:20 Photo

12:30 Lunch & Posters

Session II Surface-based Observation

(Chaired by Ellsworth & Horiuchi)

- 14:30 **S2-1** *Nishigami, K., K. Tadokoro, T. Mizuno, Y. Kano, Y. Hiramatsu, and S. Nagai:
Fault-Zone Structure and Its Temporal Change of the Nojima Fault, Japan, Estimated
from Repeated Water Injection Experiments and Borehole Seismic Observations
- 14:50 **S2-2** *Kuwahara, Y. and H. Ito:
Fault Damaged Zone Deduced by Trapped Waves and Its Relation to Breakdown Pro-
cesses of Earthquake Faults
- 15:10 **S2-3** *Li, Y.-G., K. Aki, J. E. Vidale, S. M. Day, and D. D. Oglesby:
Characterization of Spatial and Temporal Variations of Landers and Hector Mine Rup-
ture Zones by Fault-Zone Trapped Waves
- 15:30 **S2-4** *Reches, Z. and O. Dor:
Rupture Zone at Focal Depth: Structural Analysis of Three Earthquakes (M=5.1, 3.7
and 4.2) in Deep Gold Mines, South Africa
- 15:50 Coffee Break
- 16:00 **S2-5** *Iio, Y., S. Horiuchi, K. Yamamoto, Y. Kobayashi, S. Ohmi, R. Ikeda, E.
Yamamoto, H. Sato, and H. Ito:
Three Dimensional P and S wave Velocity Structures in the Aftershock area of the
1984 Western Nagano Prefecture, Japan Earthquake - Implications for the Relationship
between Structures and Earthquake Occurrences -
- 16:20 **S2-6** *Horiuchi, S., K. Takai, Y. Iio, and S. Zheng:
High Sampling Frequency Seismic Array at Ootaki, Nagano Prefecture - Stress Drop
Distribution and Seismic Velocity Change -
- 16:40 **S2-7** Toda, S.:
The Paradox of the Overabundance of Historical Earthquakes on Class C Faults: Pos-
sible Mechanism for Earthquakes on Low Stressing Rate Faults
- 17:00 **S2-8** *Ogawa, Y., M. Mishina, and Y. Mitsuhata:
Magnetotelluric Soundings over Seismically Active Regions, NE Japan
- 17:20 **S2-9** *Rabbel, W., Th. Beilecke, G. Borm, K. Bram, D. Fischer, A. Frank, H.
Gebrande, J. Kück, E. Lüschen, D. Okaya, and S. Smithson:
Seismic Properties of a Major Fault Zone at 7-8.5km Depth: Results from Vertical
Seismic Profiling at the Superdeep Continental Drillhole KTB (South Germany)
- 17:40 Discussion for Session II
- 19:00 Reception at Sansui-tei

February 27

Session III Numerical Modeling

(Chaired by Cocco & Fukuyama)

8:50 **S3-1** Fukuyama, E.:

Numerical Modeling of Dynamic Rupture Propagation along a Fault: Which Parameters are Critical?

9:10 **S3-2** *Aochi, H. and R. Madariaga:

Fault Geometry in Numerical Simulation of Earthquake Rupture: Implication to a Complex Fault Jog

9:30 **S3-3** *Cocco, M. and A. Bizzarri:

Traction Behavior within the Cohesive Zone during a Dynamic Crack Propagation: Absorbed Fracture Energy and Fault Constitutive Properties

9:50 **S3-4** *Shibazaki, B., C. Marone, and S. Yoshida:

Nucleation Process, and the Associated Convection current, in a Fault Model with Dilatancy and Fluid Movements

10:10 **S3-5** Yamashita, T.:

Mechanical Effects of Fluid Migration in a Fault Zone on Seismic Activity

10:30 Discussion for Session III

10:50 Coffee Break

Session IV-1 Core Analyses and Experiments (1)

(Chaired by Lockner & Omura)

11:00 **S4-1** *Yamamoto, K., N. Sato, and Y. Yabe:

Elastic Property of Damaged Zone Inferred from In-Situ Stress near Fault: The Changes in Seismic Wave Velocities Caused by Faulting

11:20 **S4-2** *Masuda, K. and K. Fujimoto:

Effects of Water, Strain-Rate, and Heterogeneity on Rock Strength: Experimental Study on Strength of Fault Zone Materials

11:40 **S4-3** *Lockner, D. A., D. Moore, H. Tanaka, R. Ikeda, and H. Ito:

Permeability and Strength of Borehole Core Samples from the Nojima Fault

12:00 Lunch & Posters

13:40 **S1-4** *Pezard, P. A., H. Ito, K. Fujimoto, T. Ohtani, T. Kiguchi, A.-M. Boullier, M. Zamora, B. Célérier, B. Ildefonse, C. Lussac, and P. Glover:

Geophysical Structure of the Nojima Fault in the GSJ Hirabayashi Hole, One Year after the 1995 Nanbu Earthquake (M=7.2)

14:00 **S4-4** *Shimamoto, T., T. Hirose, K. Mizoguchi, and T. Fukuchi:

Frictional Heating and High-Velocity Frictional Properties of Faults

14:20 **S4-5** *Otsuki, K. and N. Monzawa:

Comminution and Fluidization of Fault Gouge: Their Implications to Fault Slip Behavior

14:40 **S4-6** *Omura, K., H. Tanaka, K. Kobayashi, T. Arai, S. Hirano, R. Ikeda, T. Matsuda, K. Shimada, and T. Tomita:

Fault Rock Distribution and Physical Properties of the Nojima Fault Fracture Zone - Analysis of Core Samples and Well Logging in the Hirabayashi NIED Borehole -

15:00 **S4-7** *Matsuda, T., R. Ikeda, and K. Omura:

Fracture-Zone Conditions on an Active Fault that Has Just Moved: Analysis of the Hirabayashi NIED Drill Core on the Nojima Fault that Ruptured in the 1995 Kobe Earthquake, Southwest Japan

15:20 Coffee Break

Session IV-2 Core Analyses and Experiments (2)

(Chaired by Boullier & Matsuda)

15:30 **S4-10** *Ohtani, T., H. Tanaka, K. Fujimoto, and H. Ito:

Fault Rocks and Hydrothermal Alteration of the Nojima Fault, Southwest Japan

15:50 **S4-8** *Boullier, A.-M., K. Fujimoto, T. Ohtani, H. Ito, P. Pezard, M. Dubois, and B. Ildefonse:

Textual Evidences for Ancient and Recent Earthquakes on the Nojima Fault

16:10 **S4-9** *Fujimoto, K., A. Ueda, T. Ohtani, H. Ito, and H. Tanaka:

Geochemical Characteristics of Fault Rocks along the Nojima Fault: Implications for the Fluid in the Fault Zone

16:30 **S4-11** *Chester, F. M., J. S. Chester, J. E. Wilson, and D. L. Kirschner:

Paleostress and Slip Distribution in Large-Displacement Faults of the San Andreas System, California

16:50 **S4-12** *Tanaka, H., A. Sakaguchi, K. Ujiie, C. Y. Wang, W. M. Chen, H. Ito and M. Ando:

Geological and Geophysical Logging Results of Shallow Drilling Penetrating into Chelungpu Fault Zone, ROC, Taiwan

17:10 Discussion for Session IV

17:30 Global Discussion

17:50 Closing Address (Ishida, M., Research Supervisor of NIED)

Posters for Session I

P1-1 Ogasawara, H., H. Ishii, S. Moriyama, Y. Iio, and SA Group:

A Preliminary Report on Continuous 24-bit 25-Hz Strain Monitoring on Seismogenic Faults of $M \sim 3$ in Deep Gold Mines

P1-2 Ogasawara, H.:

A Key Point of Potential Future Hypocenter Fault Studies in Deep Mines: A Report on a Scientific Tour of RaSim5

P1-3 Mizuno, T. and K. Nishigami:

Deep Structure of the Nojima Fault Estimated by a Borehole Observation of Trapped-Waves

P1-4 Kiguchi, T., H. Ito, and Y. Kuwahara:

Permeability Evaluation at the GSJ Hirabayashi Borehole in the Nojima Fault from VSP Experiment and Sonic Logging

P1-5 Nankai Trough Seismogenic Zone Research Group:

Nankai Trough Seismogenic Zone Drilling and Observatory

Posters for Session II

P2-1 Li, Y.-G., J. E. Vidale, S. M. Day, and D. D. Oglesby:

Multiple-Fault Rupture of the M7.1 Hector Mine, California, Earthquake from Fault-Zone Trapped Waves

P2-2 Zheng, S., S. Horiuchi, and M. Ando:

Stress Drop of Off-Fault Aftershocks of the 1995 Hyogo-ken Nanbu, Japan Earthquake

P2-3 Tanaka, T., H. Aoki, M. Okubo, M. Onishi, and K. Oshita:

Exploration of Subsurface Structure across the Atera Fault Zone

P2-4 Miyata, T., Y. Tanaka, R. Kayen, S. Takada, and B. J. Shih:

Ground-Penetrating Radar Image of the 1999 Rupture in Chi-Chi Earthquake, Taiwan

P2-5 Lin, C. H. and M. Ando:

Aftershocks Triggered by Released Waters due to Strong Excitation of Dynamic Stress in the 1999 Chi-Chi Earthquake of Taiwan

P2-6 Tank, S. B., Y. Honkura, N. Oshiman, M. K. Tuncer, C. Celik, and E. Tolak:

Magnetotelluric Imaging of Western Part of the North Anatolian Fault Zone

P2-7 Stork, A. L., K. Imanishi, and H. Ito:

Earthquake Scaling down to $M=0.9$ Observed at the Western Nagano Deep Borehole, Central Japan

P2-8 Imanishi, K., M. Takeo, T. Matsuzawa, H. Ito, Y. Kuwahara, Y. Iio, S. Sekiguchi, S. Horiuchi and S. Ohmi:

Source Parameters of Small Earthquakes Estimated from an Inversion Method Using Stopping Phases

P2-9 Kano, Y., K. Nishigami, and T. Yanagidani:

Seismic Observation at the Nojima Fault with a PC-Based High-Speed Waveform Acquisition System

P2-10 Zhao, S. J. and R. D. Müller:

Effect of Crustal Heterogeneities on Deformation and Stress Change Associated with Faulting

P2-11 Fukuyama, E., K. B. Olsen, and T. Mikumo:

Critical Slip-Weakening Distance Measured from Near-Fault Strong Motion Data

P2-12 Fusejima, Y., K. Mizuno, R. Imura, Y. Sugiyama, T. Yoshioka, M. Shishikura, T. Komatsubara, M. Morino, H. Kurosawa, and T. Sasaki:

Field Surveys and Trenching Surveys of Surface Ruptures Associated with 2000 Tottori-ken Seibu Earthquake, Japan

P2-13 Kubo, A. and E. Fukuyama:

Stress Field near the Fault: 2000 Western Tottori Earthquake and 2001 Northern Hyogo Swarm

Posters for Session III

P3-1 Mamada, Y., Y. Kuwahara, and H. Ito:

3D Finite-Difference Simulation of Fault Zone Waves - Application to the Fault Zone Structure of the Mozumi-Sukenobu Fault, Central Japan -

P3-2 Tada, T., E. Fukuyama, and B. Shibazaki:

Displacement and Stress Green's Functions for a Constant Slip-rate on a Quadrantal Fault

P3-3 Ando, R., T. Tada, and T. Yamashita:

Formation of the Geometry of Fault System due to Dynamic Interactions among Fault Elements

P3-4 Kase, Y., H. Horikawa, H. Sekiguchi, and K. Satake:

Simulation of Earthquake Rupture Process using Geological Information: Application to the Uemachi Fault

Posters for Session IV

P4-1 Kato, A., S. Yoshida, M. Mochizuki, and M. Ohnaka:

Experimental Study of the Shear Failure Process of Rock in Seismogenic Environments

P4-2 Wibberley, C., S. Uehara, and T. Shimamoto:

Hydrodynamic Controls on Fault Strength during Rapid Slip: Laboratory Constraints

P4-3 Shimada, K., T. Arai, S. Hirano, R. Ikeda, K. Kobayashi, T. Matsuda, K. Omura, H. Tanaka, and T. Tomita:

Preliminary Report on a Small-scale Granitic Mylonite Zone in the Hirabayashi NIED Core Penetrating the Nojima Fault

P4-4 Omura, K., T. Arai, S. Hirano, K. Kobayashi, T. Matsuda, K. Shimada, H. Tanaka, T. Tomita, and R. Ikeda:

Photographs of NIED Nojima Fault Drilling Cores at Hirabayashi Site CD-ROM Volumes

S0-1

Introduction of the Workshop and Outline of the NIED Project

R. Ikeda

Nat'l Res. Inst. Earth Science and Disaster Prevention, Tsukuba, Ibaraki, 305-0006, Japan
(Phone: +81-298-51-1611, Fax: +81-298-54-0629, E-mail: ikeda@bosai.go.jp)

Cooperative research integrated by direct observations both in a borehole and from the surface, numerical modeling, and laboratory experiments is essential to improve our understanding of the kinematics of an active fault system and to advance in earthquake hazard assessment. Recent investigations on each topic have provided us with new insights on the physics of fault zones. We would like to share this knowledge and discuss the current state-of-art research on fault zone physical studies from various angles.

This workshop was planned through various experiences by the NIED project. We have been conducting "Fault zone drilling" under the special research project of "Research on mechanisms of earthquake occurrence." Through this project we have studied spatial and temporal stress variation and the earthquake generation process. We have focused our study in the Kanto-Tokai area, the Central Japan active fault region and the Western Nagano seismogenic region. We could obtain regional and depth profiling of the stress states in these areas. The Neodani fault, which moved at the time of the great 1891 Nobi earthquake, M8.0, was the first target in 1993 for the NIED fault zone drilling project. After the occurrence of the 1995 Kobe earthquake, it has been widely recognized that direct measurements in fault zones by drilling is important for the understanding of earthquake occurrence. The investigation in and around the Nojima fault appeared on the surface on Awaji Island, and it goes without saying that the Kobe earthquake produced a lot of physical and geological aspects worthy of research. The overall goal of the NIED project corresponds to the purpose of this workshop.

At present we are promoting the project with four sub-themes, which are strongly related to the target and keywords of this workshop. (1) In-situ downhole measurements of stress, and geophysical exploration near the fault zone: large active faults, Neodani, Atotsugawa, Atera and Gohukuji in the Chubu district of central Japan, are drilling targets. In-situ experiments, field and laboratory analysis of fault and material properties, and observations of boreholes have been conducted. (2) Study on the dynamics of intraplate earthquakes by seismic observation and geophysical exploration near the fault: observational studies, micro-seismic observation and resistivity measurements have been conducted in and around the source region of the 1984 Western Nagano Prefecture earthquake (M6.8). A model for the occurrence of intraplate earthquakes is proposed. The essential parts of the model are stress accumulations due to a seismic slip on the downward extension of the fault into the lower crust, and stress release due to inelastic deformation in the upper crust. (3) Numerical modeling of an earthquake fault zone: rupture processes have been studied by numerical simulations. We are now preparing to propagate this simulation to an actual fault zone defined by in-situ measurements physical factors. (4) Experimental and analytical studies of fault zone materials: we analyze the physical and chemical properties of the fault-zone rock retrieved from the borehole. We have also planned to conduct laboratory experiments using the rock cores under the conditions of high temperature and high pressure.

S1-1

Spatial and Temporal Variation of Crustal Stress around Active Faults Inferred from In-situ Measurements

R. Ikeda¹, K. Omura¹, T. Matsuda¹, and Y. Iio²

1. Nat'l. Res. Inst. Earth Science and Disaster Prevention, Tsukuba, Ibaraki, 305-0006, Japan (Phone: +81-298-51-1611, Fax: +81-298-54-0629, E-mail: ikeda@bosai.go.jp, omura@bosai.go.jp, mtatsuo@bosai.go.jp)

2. Earthquake Research Institute, Univ. Tokyo, Yayoi, Bunkyo, Tokyo, 113-0033 Japan (Phone: +81-3-5841-5787, Fax: +81-3-5689-7234, E-mail: iio@eri.u-tokyo.ac.jp)

In-situ downhole measurements and coring within and around an active fault zone are needed to better understand the structure and material properties of fault rocks as well as the physical state of active faults. Particularly, the relationship between the stress concentration state and the heterogeneous strength of an earthquake fault zone is important to estimate earthquake-generating mechanisms. It is necessary to compare some active faults in different conditions of the chrysalis stage and their relation to subsequent earthquake occurrence. In the "Active Fault Zone Drilling Project in Japan," the Nojima fault which appeared on the surface by the 1995 Great Kobe earthquake (M=7.2) and the Neodani fault which appeared by the 1891 Nobi earthquake, the greatest inland earthquake M=8.0 in Japan, have been drilled through their fault fracture zones. A similar experiment conducted on and research of the Atera fault, of which some parts have seemed to be dislocated by the 1586 Tensyo earthquake, is promoted.

In these boreholes, the stress states in and around the fault fractured zones were obtained from in-situ stress measurements by the hydraulic fracturing method. Important phenomena such as rapid stress drop in the fault fracture zones were observed in the Neodani well (1300 m deep) and the Nojima well (1800 m) of the fault zone drillings, as well as in the Ashio well (2,000 m) in the focal area. In the Atera fault project, we have conducted integrated investigations by surface geophysical survey and drilling around the Atera fault. Four boreholes (400 m to 600 m deep) were located on a line crossing the fracture zone of the Atera fault. We noted that the stress magnitude decreases in the area closer to the center of the fracture zone. Furthermore the orientation of the maximum horizontal compressive stress was almost in a North-South direction, just reverse of the fault moving direction. These results support the idea that the differential stress is extremely small at narrow zones adjoining fracture zones. We also noted that the frictional strength of the crust adjacent to the faults is high and the level of shear stress in the crust adjacent to the faults is principally controlled by the frictional strength of rock. We argue that the stress state observed in these sites exists only if the faults are quite "weak." It is important to examine these results comparing them with faults in other tectonic environments.

As a temporal variation of stresses, crustal stress was recorded from 1978 to before the Kobe earthquake in and around the area where the earthquake occurred. By examining this data, the change in tectonic stress gradually increased prior to the earthquake. After the earthquake, the same boreholes were once again used to obtain new data. From these measurements, we were able to determine that there was a definite drop in the crustal stress in the area and that there was a change in the direction of the principal stresses. It was also made obvious that continual measuring of the absolute stress magnitude is essential in the area for earthquake prediction.

S1-2

Wellbore Instabilities - Detriment or Benefit? Experiences of the Integrated Stress Measurement Strategy in the KTB- Boreholes

B. Engeser¹, L. Wohlgemuth², J. Kück³

1. Niedersächsisches Landesamt für Bodenforschung, D30655 Hannover, Stilleweg 2, Germany (Phone: +49-511-643-2497, E-mail: bernhard.engeser@bgr.de)
2. GeoForschungsZentrum Potsdam, ICDP Operational Support Group, D14473 Potsdam, Telegraphenberg, Germany (Phone: +49-331-288-1080, E-mail: wohlgem@gfz-potsdam.de)
3. GeoForschungsZentrum Potsdam, ICDP Operational Support Group, D14473 Potsdam, Telegraphenberg, Germany (Phone: +49-9681-91182, E-mail: jkueck@gfz-potsdam.de)

Borehole instabilities number among the most serious problems in commercial and scientific drilling projects. The monetary value of time delay and lost equipment directly caused by wellbore failures is estimated at over 500 million \$ per year worldwide. In the KTB project borehole instabilities turned out to be the key obstacle for reaching the target depth of 10 km within the scope of time and budget. The time delay due to borehole stability problems amounted to 468 days equivalent to more than 20 mill \$. On the other hand wellbore failures bear valuable information on in situ parameters for determining the crustal stress state. Use of this information together with a variety of measurements and experiments carried out in the drillholes and the field lab was part of the so called KTB Integrated Stress Measurement Strategy (ISMS). Successful utilization requires a thorough monitoring and understanding of the technical impact factors supplemented by comprehensive core analysis and borehole logging.

The phenomena of wellbore failures encountered in the KTB pilot hole and superdeep hole can be described as:

- borehole breakouts due to compressive shear failure
- drilling induced tensile wall fractures
- shear failure on pre-existing faults
- caliper enlargements in fault zones caused by drilling fluid induced weakening of cataclastic rocks

Drilling operation in the depth section below 7500 m was extremely hindered by undergauge hole sections. Most likely these pseudo-ductile convergency phenomena have to be interpreted as brittle shear failures on unfavourably oriented planes of weakness caused by the high horizontal stress anisotropy in the range of 2. The destabilisation processes showed a clearly time dependent behaviour most likely caused by drilling fluid induced pore pressure diffusion in connection with physico-chemical weakening processes.

A cornerstone for the deduction of a complete stress profile at KTB drillsite were hydraulic fracturing experiments conducted in both boreholes. A technically challenging combined hydrofrac/induced seismicity experiment subsequent to the drilling phase was carried out successfully at a depth of more than 9 km. With the results of this experiment a lower bound for the magnitude of S_{h} at a mid crustal depth could be established for the first time. The results correspond with the assumed existence of the crust being at a critical state of shear fracture equilibrium.

With both holes cased a globally unique deep crustal laboratory is available for further scientific investigations. Besides of a long-term injection experiment already conducted in the superdeep borehole a cross hole hydraulic experiment is in the planning stage at present. It is believed that a comprehensive stress measurement strategy together with a 2- borehole site configuration as applied in the KTB project could be of benefit for investigation and understanding the physics of in situ processes going on at active fault sites.

S1-3

The Long Valley Exploratory Well: A Deep Geophysical Observatory at the Center of a Restless Caldera

W. L. Ellsworth
U.S. Geological Survey
Menlo Park, CA 94305, USA
ellswrth@usgs.gov

The Long Valley Exploratory Well (LVEW) is a 3-km-deep scientific drill hole into the center of the resurgent dome of Long Valley caldera in eastern California. Long Valley is situated at the western margin of the Great Basin extensional tectonic province, a region dominated by a combination of normal and strike-slip faulting and volcanism. The current unrest in Long Valley caldera began in 1980 with an intense earthquake sequence that included four **M** 6 earthquakes accompanied by a 25-cm, dome-shaped uplift of the resurgent dome in the center of the caldera. The subsequent unrest has been characterized by recurring earthquake swarm activity and continued uplift of the resurgent dome, the center of which now stands nearly 80 cm higher than in 1979.

The drilling of LVEW was originally undertaken to investigate the potential for near-magmatic temperature energy extraction by the Department of Energy (DOE), and drilling was completed to a depth of 2313 m in 1991. The direction of the LVEW project changed in 1996 when LVEW was transferred from the DOE to the U.S. Geological Survey. A new drilling phase occurred in 1998 under the auspices of the International Continental Drilling Program (ICDP) in which the hole was continuously cored from 2188 to 2996 m depth. The core contained numerous fault zones, both sealed and very fresh, as well as many indicators of the stress orientation in the formation.

The final phase of the ICPD project will be the conversion of the well into a permanent deep geophysical observatory. The scientific goals of the observatory are to make quantitative observations of active tectonic processes operating at mid-crustal depths in the caldera from continuous strain, seismic and pore pressure measurements in the seismogenic volume beneath the resurgent dome. The observatory will be fully integrated into the surface monitoring networks operated by the U.S. Geological Survey, and will be used to track processes occurring directly above the inflating magma chamber driving any future episodes of unrest in the caldera. Installation of the observatory is scheduled for June 2002.

Hydrological testing and geophysical logging were carried out in 2000-2001 in preparation for the observatory instrumentation. LVEW has a very strong response to earth tides, with a tidal water level range of 20 cm. It has also proven to be an excellent facility for the testing of deep borehole seismometers during campaigns in 1992, 1997-1998 and 2000-2002. High frequency recordings of earthquakes during the 1997-1998 seismic crisis in the caldera provided unique information on the nature of seismic swarms in the south moat of the caldera, as well as important new information on the energy scaling of earthquakes.

S1-4

**GEOPHYSICAL STRUCTURE OF THE NOJIMA FAULT
IN THE GSJ HIRABAYASHI HOLE,
ONE YEAR AFTER THE 1995 NANBU EARTHQUAKE (M=7.2)**

P.A. PEZARD¹, H. ITO², K. FUJIMOTO², T. OHTANI², T. KIGUCHI², A.-M. BOULLIER³,
M. ZAMORA⁴, B. CÉLÉRIER¹, B. ILDEFONSE¹, C. LUSSAC¹, P. GLOVER¹.

¹ISTEEM (CNRS), Montpellier, France, ²GSJ (AIST), Tsukuba, Japan, ³LGIT (CNRS),
Grenoble, France, ⁴IPG (Université de Paris 7), Paris, France.

The Nojima fault located on Awaji island, Japan, to the SE of Kobe, was drilled (Ohtani et al., 2000) through at shallow depth one year after the 1995 Nanbu earthquake (M=7.2). Cores and downhole measurements collected from the in the Hirabayashi hole by the Geological Survey of Japan (GSJ) have been analyzed to describe the structure of the fault in relation to dynamic parameters such as fluid flow and deformation in the vicinity of the hole.

Electrical resistivity and pore fluid. The in-situ physical properties are related, in this transpressional context, to changes in alteration and fracturing intensity of the penetrated granodiorite. A monotonic decrease in electrical resistivity, density and acoustic velocities is recorded between fresher granodiorites in the upper part of the hole and the recent rupture (or "co-axial") zone, near 625 m. This low-frequency signal reflects, over a few tens of m (in terms of true fault thickness), a distribution of the deformation away from the central part of the fault. Core analyses performed at varying fluid salinity have provided measurements of electrical formation factor and surface conductivity for over 50 samples (Pezard et al., 2000). The comparison of this data to in-situ samples and measurements reveals the presence of at least two types of pore fluids in the near vicinity of the fault. A low salinity fluid ($C_w = 0.06$ S/m) sampled in the hole in front of the fault zone (Sato et al., 2000), and a more saline pore fluid ($C_w = 1.20$ S/m) inferred as present in the fresh granodiorite, a few meters away from the fault. This contrast implies the presence of a relationship between structure and fluid salinity in low porosity crystalline rocks. As a consequence, permeability and electrical conductivity are inversely correlated in such an environment.

Acoustic images and deformation. BoreHole Televiewer acoustic scans in the GSJ Hirabayashi hole reveal only a few damaged cross sections in front of fracture zones, in an otherwise very much "intact" borehole (Celerier et al., 2000). Borehole breakouts are not identified as generally expected in such a shallow borehole. Drilling-induced slip on active faults were also investigated to look for traces of the 1995 rupture. Less than 30 locations with such borehole wall displacements were identified, among which 24 were located within the postulated 1995 earthquake rupture zone, from 623 to 635 m. Most planes dip to the SE, and most slip directions are oriented NE-SW. However, this set of 24 planes and slip vectors is found to be incompatible with a single homogeneous stress system.

Structure of the main fault zone. To the first order, these deformations of the borehole surface point to a 1.2 m-thick zone still deforming one year after the Nanbu earthquake. The 30 cm-thick gouge thought to include the plane of rupture (Tanaka et al., 2000) is located at the top of this zone. The gouge itself is constituted with mm-scale structures including pseudo-tachylites and characterized by physical properties such as a local drop to zero of shear velocity. The layered nature of the gouge associated with changes in grain size between layers may provide the mechanism to store a significant overpressure before or after the earthquake, increasing

locally the porosity in a significant manner and explaining the absence of shear resistance of the material. The base of this 1.2 m-thick zone is constituted with a 5 to 8 cm-thick gouge zone, also dipping steeply ($> 80^\circ$) to the SE. Between these two gouge layers, a more homogeneous rock with regularly spaced fractures dipping less steeply ($30 - 40^\circ$) to the SE are found. These fractures appear to be open in 1996, and are geometrically consistent with the reverse movement on the fault during the 1995 earthquake.

Shear-wave anisotropy and stress field orientation. As the in-situ stress field orientation could not be determined from breakout analyses or indications of slip on active planes, the orientation of maximum shear velocity was studied and compared to elastic borehole deformations. Out of the main fault zone (above 520 m), fast shear waves and slight hole deformation directions propose a N060W direction of maximum horizontal stress (SHmax), almost orthogonal in 1995 to the N035E trace of the fault at surface. Acoustic velocity measurements on core show very little anisotropy in relatively fresh, weakly fractured rock. Closer to the inner trace of the fault (from 520 to 700 m), a more complex signal is obtained. However, acoustic and mechanical indicators still coincide in azimuth.

In all, these analyses performed at different scales, either in-situ or in the laboratory, contribute to build a geophysical description of the Nojima fault with series of nested structures from mm- to decameter-scale. Dynamic analyses of the fault behavior require to take into account this spatial complexity, as well as the time variability of some of the parameters such as stress, electrical potential, fluid flow and fluid nature.

References.

- CÉLÉRIER B., PEZARD P.A., ITO H., KIGUCHI T. (2000). Borehole wall geometry across the Nojima Fault: BHTV acoustic scans analysis from the GSJ Hirabayashi hole, Japan. In: *International workshop of the Nojima fault core and borehole data analysis* (edited by Ito, H., Fujimoto, K., Tanaka, H. & Lockner, D.) GSJ Interim report No.EQ/00/1, USGS Open-File Report 000-129. Geological Survey of Japan, Tsukuba, 233-238.
- OHTANI, T., FUJIMOTO, K., ITO, H., TANAKA, H., TOMIDA, N. & HIGUCHI, T. 2000. Fault rocks and paleo- to recent fluid characteristics from the borehole survey of the Nojima Fault rupture in the 1995 Kobe earthquake, southwest Japan. *Journal of Geophysical Research* **105** (B7), 16161-16171.
- PEZARD P.A., ITO H., HERMITTE D., REVIL A. (2000). Electrical properties and alteration of granodiorites from the GSJ Hirabayashi hole, Japan. In: *International workshop of the Nojima fault core and borehole data analysis* (edited by Ito, H., Fujimoto, K., Tanaka, H. & Lockner, D.) GSJ Interim report No.EQ/00/1, USGS Open-File Report 000-129. Geological Survey of Japan, Tsukuba, 255-262.
- SATO, T. & TAKAHASHI, M. (2000). Chemical and isotopic compositions of groundwater obtained from the GSJ Hirabayashi well. In: *International workshop of the Nojima fault core and borehole data analysis* (edited by Ito, H., Fujimoto, K., Tanaka, H. & Lockner, D.) GSJ Interim report No.EQ/00/1, USGS Open-File Report 000-129. Geological Survey of Japan, Tsukuba, 187-192.
- TANAKA, H., FUJIMOTO, K., OHTANI, T. & ITO, H. 2001. Structural and chemical characterization of shear zones in the freshly activated Nojima fault, Awaji Island, southwest Japan. *Journal of Geophysical Research* **106** (B5), 8789-8810.
- ZAMORA M., PEZARD P.A., ITO H. (2000). Anisotropy of elastic and anelastic properties of granites from the GSJ Hirabayashi hole, Japan. In: *International workshop of the Nojima fault core and borehole data analysis* (edited by Ito, H., Fujimoto, K., Tanaka, H. & Lockner, D.) GSJ Interim report No.EQ/00/1, USGS Open-File Report 000-129. Geological Survey of Japan, Tsukuba, 227-231.

S1-5

Seismogenic Zone Drilling -Nojima, Chelungpu and Nankai-

Hisao Ito

Geological Survey of Japan

National Institute of Advanced Industrial Science and Technology

AIST Tsukuba Central 7, 1-1-1 Higashi, Tsukuba, Ibaraki 305-8567, Japan

Phone +81-298-61-3757, Fax +81-298-61-3682, E-mail: hisao.itou@aist.go.jp

Seismogenic zone or fault zone drilling has potential to resolve a fundamental seismological debate about how large earthquakes occur, what kind of physical parameters control the occurrence of large earthquakes. Obtaining fresh samples (cores and fluids) of a fault that recently slipped in a large earthquake, determining in-situ physical parameters, such as pore pressures, stress, width of the fault zone and monitoring these parameters should be able to resolve these questions.

There are several seismogenic zone drilling projects in the world; Nojima fault drilling in Japan, Chelungpu fault drilling in Taiwan, seismogenic zone drilling in the Nankai Trough by ODP/IODP and SAFOD in California. We would like to briefly compare these projects; what are common among these projects and what are peculiar to each project, and what kind of technology transfer and science exchange are possible?

Nojima fault drilling: In Japan, several boreholes were drilled into the Nojima fault following the 1995 Kobe earthquake (M7.2) to study the fault properties and fault healing process.

Chelungpu fault drilling: The 1999 Chichi, Taiwan earthquake (Mw 7.7) produced surface faulting with vertical displacements of up to 8m on the Chelungpu Fault. The large amount of fault slip at or near the surface provides a unique opportunity to study the physical mechanisms involved in faulting of large earthquakes. The uniqueness of the Chelungpu fault drilling is that the 1999 Chi-Chi Earthquake produced distinct differences in rupture behavior between the northern and southern portions of the fault, so that the physics of the faulting process can be studied. The project to drill the Chelungpu fault was discussed at a recent workshop sponsored by the International Continental Scientific Drilling Program (ICDP).

Nankai: ODP (Ocean Drilling Program)/IODP(Integrated Ocean Drilling Program) have a drilling program with plans to drill into the seismogenic zone of the Nankai Trough, which has a long historical record (over 1000 years) of great earthquakes. In the Nankai drilling, we hope to answer the following scientific hypotheses and questions; 1) What kind of material and parameters control the generation and propagation of large earthquake?, 2) Are subduction Megathrusts weak fault? , 3) What are the asperity? Is there any creep event during the interseismic period? and 4) What kind of changes in properties and state of the fault zone throughout the earthquake cycle?

One of the uniqueness of the Nankai seismogenic zone drilling is that we will be able to monitor these changes during interseismic, preseismic, coseismic and postseismic periods.

S1-6

**The San Andreas Fault Observatory at Depth:
Studying the Physics of Earthquakes through Fault Zone Drilling**

Stephen Hickman¹, William Ellsworth¹ and Mark Zoback²

¹U.S. Geological Survey, 345 Middlefield Road, Menlo Park, CA 94025

²Department of Geophysics, Stanford University, Stanford, CA 94305

The San Andreas Fault Observatory at Depth (SAFOD) is a comprehensive project to drill and instrument an inclined borehole across the San Andreas Fault Zone to a total vertical depth of 4 km. SAFOD is motivated by the need to answer fundamental questions about the physical and chemical processes controlling faulting and earthquake generation within a major plate-bounding fault and is being proposed as part of the U.S. National Science Foundation's (NSF) new EarthScope initiative (see <http://www.earthscope.org>). The drill site is located on a segment of the San Andreas Fault that moves through a combination of aseismic creep and repeating microearthquakes. It lies at the extreme northern end of the rupture zone of the 1966, M=6 Parkfield earthquake, the most recent in a series of events that have ruptured the fault five times since 1857. The Parkfield region is the most comprehensively instrumented section of a fault anywhere in the world, and has been the focus of intensive study for the past two decades.

The SAFOD hole is intended to drill into – or very close to – a repeating microearthquake source. Rock and fluid samples recovered from the fault zone and country rock will be tested in the laboratory to determine their compositions, origins, deformation mechanisms, frictional behavior and physical properties. Following downhole measurement of stress, fluid pressure, heat flow and other parameters, the hole will be instrumented as a long-term geophysical observatory to monitor earthquakes, deformation, fluid pressure and ephemeral properties of the fault zone through multiple earthquake cycles. Through drilling, sampling, downhole measurements and long-term monitoring directly within the San Andreas fault zone at seismogenic depths, we will learn the composition of fault zone materials and determine the constitutive laws that govern their behavior; measure the stresses that initiate earthquakes and control their propagation; test hypotheses on the roles of high pore fluid pressure and chemical reactions in controlling fault strength and earthquake recurrence; and observe the strain and radiated wave fields in the near field of microearthquakes. Many geophysical and geological site characterization studies have already been carried out or are presently underway at the drill site. These include a large-scale temporary seismometer deployment for simultaneous earthquake relocations and tomography, a high-resolution seismic reflection and refraction profile, airborne and groundbased gravity and magnetic surveys, detailed geological mapping, magnetotelluric imaging, microearthquake relocations and source studies using permanent arrays of the U.S. Geological Survey (USGS) and U.C. Berkeley, and shallow geophysical investigations run as part of a multi-university field course.

Although drilling of the main SAFOD hole awaits Congressional approval of EarthScope, in the summer of 2002 a 2.2-km-deep vertical pilot hole will be drilled at the SAFOD site. The pilot hole will be carried out as a collaborative effort between the International Continental Drilling Program (ICDP), NSF and the USGS. Seismic instrumentation deployed in the pilot hole will facilitate precise earthquake hypocenter determinations that will guide subsequent SAFOD drilling and scientific investigations. Downhole physical properties, stress, fluid pressure and heat flow measurements will characterize the shallow crust adjacent to the fault zone. Laboratory studies of rock and fluid samples obtained from the pilot hole will help determine the nature and extent of fluid rock interaction along the San Andreas fault and the sources and transport paths for fault-zone fluids. Following drilling of the pilot hole, a major seismic reflection/refraction experiment will be conducted across the SAFOD site by U.S. and international investigators.

S1-7

The Corinth Rift Laboratory project

F.H. Cornet¹, P. Bernard¹, I. Moretti², G. Borm³ and I. Vardoulakis⁴

1. Institut de Physique du Globe de Paris (France)
2. Institut Français du pétrol (France)
3. GeoForschungZentrum – Potsdam (Germany)
4. National technical University of Athens (Greece)

The objective of the Corinth Rift Laboratory (CRL) is to integrate surface and downhole observations for a better understanding of the physics of faulting in an extensional tectonic regime, with special attention to interactions between fluids and active faults.

The Corinth Rift is opening at a rate of 1.5 cm/year, with its southern shore uplifting at a rate close to 1 mm/year. It is one of the most seismically active zones in Europe. CRL presently includes a set of five European funded projects. In addition to the DGLab drilling project concerned by instrumenting boreholes through the Aigion Fault, CORSEIS is centred on surface geophysical networks; 3F-Corinth places emphasis on geochemical and geophysical interactions between fluids and faults as well as on seismic reconnaissance and numerical modelling; AEGIS corresponds to the Information Science Technology component of the project, ASSEM develops sensors for offshore monitoring. In addition, national agencies (Plouton for Greece, GDR-Corinth for France, GRECO for Germany) bring equipment, personnel for maintenance and some academic expertise for more theoretical reflection on results obtained in situ.

The site for the DGLab drilling is located in Aigion, a city on the southern shore of the Corinth Gulf, which was hit by a magnitude 6.5 earthquake in 1995. On this site, the project aims at instrumenting two boreholes (1200 and 600 m deep), which intersect the recently activated, 8 to 10 km long, Aigion fault. Particular emphasis is placed on documenting the role of fluids on fault behaviour and the role of earthquake faulting on regional hydrogeology thanks to the continuous downhole monitoring of various parameters characteristics of the fault fluid-flow conditions.

The first year of DGLab activity has resulted in identifying the local geological structure where the boreholes are to be drilled and in producing the first draft of a local geological map together with some information on main faults structures. Four seismic profiles cumulating 33 km of seismic lines (three of them perpendicular to the Heliki and Aegion faults, one of them parallel to the faults) outline the absence of simple reflections. This is taken to be the consequence of the complexity of the regional faulting system. But refraction data provides clear identification of targeted tertiary limestone, below the recent conglomerates.

These results, together with observations from a 200 m deep drill hole, suggests that limestone will be hit around 820 m, in the northern hanging wall of Aigion fault. Dip of the nearby, 40 km long, Heliki fault has been measured at five different sites. Results outline a dip ranging from 70° when the fault remains in limestone to 55° when it is entirely in conglomerates, and about 60° when it interfaces limestone and conglomerates. The AIG10 well location has been chosen so that AIG10 intersects the faults where it passes through the carbonates rather than through the conglomerates

In addition to continuous coring and logging (in particular with borehole imaging and dipole sonic), the well will be used for vertical and oblique seismic profiles, hydraulic characterization of the fault and its surrounding and determination of stress profiles through the fault. Then permanent instrumentation will insure continuous monitoring of hydraulic characteristics. This will be obtained, in particular, through recurrent hydraulic interference tests with a neighbouring well, also intersecting the fault some 400 m away.

Discussion on the determination of stress profiles in the vicinity of the Aigion Fault

It is well established that active faults are sources of strong stress heterogeneity. Hence the goal of determining stress profiles through active faults may be either to retrieve large scale characteristic features or local variations (e.g. Scotti and Cornet, 1994, Cornet and Yin 1995). At Aigion, the stress field in the vicinity of the fault will be determined through various techniques :

- Classical hydraulic fracturing for the determination of the minimum principal stress magnitude and direction;
- The HTPF stress determination method in which the normal stress supported by fractures with various orientation may help document local stress heterogeneity as well as stress variations at various scales;
- Borehole imaging to detect borehole breakouts, if they exist. This helps constrain regional stress directions and local direction heterogeneity; some attention will also be given to breakouts width for constraining principal stress magnitudes.
- Elastic shear wave velocity anisotropy (from seismic profiles and sonic logs). It has been quite well established that shear wave anisotropy is strongly dependent on stress field . Hence anisotropy investigation helps to identify principal stress directions and their variations at various scales. This will be investigated through logs which will be repeated at various times. In addition, for frequencies in the 50-500 Hz range, the velocity anisotropy will be continuously monitored with a three component downhole seismometer.
- The regional significance of the stress determination retrieved from the AIG10 borehole will be investigated by confronting the results with focal mechanisms of local micro-seismicity. If possible, an integrated inversion of all data constraining some stress components will be undertaken for a characterization of the regional stress field.

Scotti O. and F.H. Cornet; In situ evidence for fluid induced aseismic slip events along fault zones; *Int. Jou. Rock Mech. Min.* vol. 31., nb. 4, pp 347-358; 1994.

Yin Jianmin and F.H. Cornet; Integrated stress determination by joint inversion of hydraulic tests and focal mechanisms, *Geophys. Res. Let.* , vol. 21,nb. 24, pp 2645-2648; 1994.

Cornet F.H. and Jianmin Yin; Analysis of induced seismicity for stress field determination and pore pressure mapping; *Pageoph*, vol. 145, nb 3/4, pp 677-700; 1995

S1-8

Results from drilling observations on active faults in Japan, Taiwan and South Africa: Comments on Future Drilling Programs

Masataka Ando
Research Center for Seismology and Volcanology
Graduate School of Science, Nagoya University
Furo-cho, Chikusa, Nagoya 462-8602, Japan
ando@seis.nagoya-u.ac.jp

The Atotsugawa fault system, right-lateral sense and 60 km long, is one of the most active faults in Japan. One of the important findings related to the Atotsugawa fault is fault creep which was detected geodetically by Geographical Survey Institute of Japan. For a long time it had been believed that fault creep had not occurred on active faults. The existence of fault creep was found on the basis of geodetic measurements at three small networks across the Atotsugawa fault.

Throughout one of the sub-fault branches of this fault system, a 480-m-long observation tunnel was excavated to investigate features and properties of the fault zone. This is the first research tunnel dedicated to active fault research in Japan. Several different kinds of observations have been carried out in the tunnel. One of the important results is that the widths of the fault zone estimated from different methods vary among them, 40 m to 500 m.

Regional seismological and geodetic observations were also made at and around the Atotsugawa fault system. An additional installation of high-gain short-period seismic stations was significantly improved the hypocenter accuracy in and around the fault system, revealing a clear seismic gap, which coincides with the creep detected from geodetic surveys. The deformation obtained from the GPS-array observation reveals a relatively systematic pattern, suggesting a significant amount of horizontal component normal to the fault plane. This comprehensive study of an active fault with a variety of methods reveals that the structure of a fault zone is wider than the width obtained from geological survey, say, 10 times wider, which is very important to understand strain accumulation on and around the fault zone.

A new hypocenter distribution map reveals a clear seismic gap of 10 km in length by 7 km in downward width which coincides with a creeping segment of the Atotsugawa fault. Seismicity on the periphery of the gap is also found relatively high, suggesting stress concentrations taking place in the surroundings. If this seismicity gap coincides with the creep, this segment can be likely to be a loosely contacted portion on the fault. In a similar manner, the western segment can be thought to be a strongly contacted one on the fault. These features are opposite to that of the San Andreas fault, where high seismicity is found in creeping sections rather than coupled sections. In any case such heterogeneity of the fault properties is a possible controlling factor to govern the faulting processes.

A question may arise which parameter(s) controls the mode of slip on the Atotsugawa fault? To solve the question, we propose drilling at least two boreholes to sample the creeping and coupled portions of the Atotsugawa fault. The levels of friction, fluid pressure, and stress loaded on the fault plane are an important issue that controls the fault behaviors, but currently there are almost no observations that can constrain this problem. Obtaining pieces of the fault zone and surrounding materials that show different fault behaviors will contribute greatly toward the understanding of the physics of active faults. Measurements of heat flow in the holes will provide information about the character of the friction during the interseismic period. Results from recent active fault observations on the Nojima fault, Chelungpu fault and South African gold mines will provide useful tools and ideas to investigate such a unique active fault in Japan.

S2-1

Fault-Zone Structure and its Temporal Change of the Nojima Fault, Japan, Estimated from Repeated Water Injection Experiments and Borehole Seismic Observations

K. Nishigami¹, K. Tadokoro², T. Mizuno¹, Y. Kano¹, Y. Hiramatsu³, and S. Nagai⁴

1. Disaster Prevention Research Institute, Kyoto University, Gokasho, Uji, Kyoto 611-0011, Japan (Phone: +81-774-38-4195, Fax: +81-774-38-4190, E-mail: nishigam@rcep.dpri.kyoto-u.ac.jp)
2. Research Center for Seismology and Volcanology, Nagoya University, Furo-cho, Chikusa-ku, Nagoya, Aichi 464-8602, Japan
3. Graduate School of Natural Science and Technology, Kanazawa University, Kakuma-machi, Kanazawa, Ishikawa 920-1192, Japan
4. Earthquake Research Institute, the University of Tokyo, 1-1-1 Yayoi, Bunkyo, Tokyo 113-0032, Japan

We have been trying to estimate the fault-zone structure and its temporal change of the Nojima fault, which was ruptured by the $M_{JMA}7.3$ Hyogo-ken Nanbu (Kobe) earthquake in January 1995, by repeated water injection experiments and borehole seismic observations. Water injection experiments were carried out in Feb.-Mar. 1997 and Jan.-Mar. 2000 at the DPRI 1800 m borehole drilled into the Nojima fault zone, aiming to detect a change in the fault-zone permeability related to the fault healing process. The actual injection of water was made at ~540 m depth. We estimated the permeability of the rocks around the fault-zone to be about 0.001-0.01 darcy and also detected a relative decrease in permeability by about 50% from 1997 to 2000 from several kinds of observations: the groundwater discharge and the strain in the 800-m-deep borehole close to the injection hole, and the electric self-potential on the ground. This suggests a healing of the shallow fault-zone, <~800 m depth. Induced earthquakes with magnitude -1.2 to 1.0 were observed around the injection hole, at about 2-4 km depth and about 4 days (in 1997) and 6 days (in 2000) after the beginning of each water injection. This space-time migration can be explained by a 2-D diffusion process of pore water pressure, and the 2-days delay of the commencement of induced seismicity in 2000 may suggest a decrease in the fault-zone permeability at deeper part, down to about 2-4 km depths.

Clear fault-zone trapped waves were observed in June 1995 by a linear seismic array deployed across the surface break of the Nojima fault, and the fault-zone structure was estimated as follows: width of ~20 m, velocity reduction of ~60% to the surrounding rocks, Q -value inside the fault zone of ~20, and dipping to the south-east at ~85 degrees. Seismograms recorded at the bottom of the 1800-m-deep borehole, since August 1997, also show several candidates of trapped waves, and the relatively shorter duration of trapped waves seen in the injection-induced events in 2000 suggests a recovery of velocity reduction inside the fault zone. The observation of fault-zone trapped waves has revealed that most of the earthquakes occur outside of the Nojima fault-zone, i.e., aftershocks observed in 1995 mostly occurred on the hanging wall side and the injection-induced events in 1997 and 2000 tended to occur on the footwall side. We still continue revising the systematic analyses of borehole seismograms, i.e., identifying the fault-zone trapped waves by an event-array method, which was effectively applied to the aftershocks of the 2000 Western Tottori earthquake with $M_{JMA}7.3$ in southwest Japan, and modeling the waveforms and dispersion curves of trapped waves. These results and also other generating properties of injection-induced and stationary ultra-microearthquakes around the Nojima fault will be discussed.

S2-2

Fault damaged zone deduced by trapped waves and its relation to breakdown processes of earthquake faults

Y Kuwahara and Hisao Ito

Geological Survey of Japan, National Institute of Advanced Industrial Science and Technology
AIST Tsukuba Central 7 1-1-1 Higashi, Tsukuba, Ibaraki 305-8567, Japan (Phone: +81-298-61-3972,
fax: +81-298-61-3682, E-mail: y-kuwahara@aist.go.jp)

We review the recent observations of fault low velocity zones (LVZ) using fault zone trapped waves and analyze breakdown processes for a model of plastic deformation zone at the edge of earthquake fault related to the LVZ. The existences of the LVZ have been demonstrated by analyzing the fault zone trapped waves at various active faults. These studies have shown that widths of the fault low velocity zones are ranging from an order of 10m to a few hundred meters. The trapped waves were observed not only just after the large earthquake, but more than about 100 years after the large earthquake. This indicates that the low velocity zone exists from the surface to the seismogenic depth for about 100 years with large velocity reduction of S-wave compared with the surrounding rock. In order to evaluate the effect of fault low velocity zones on the earthquake rupture processes, a model of the LVZ related to the plastic deformation around an edge of propagating earthquake rupture is proposed. In this study, the earthquake rupture process is regarded as Mode III crack propagation. Following two processes were assumed in the analysis: 1) The LVZ is identical with the fault damaged zone which acts as plastic deformation zone at the vicinity of the crack tip. 2) The size of the plastic deformation zone is given by the yield criterion of von Mises. These two assumptions give us simple relationships among the width of the low velocity zone, the breakdown stress drop at the crack tip, characteristic slip distance d_0 in friction laws and so on. The parameters applicable for the Nojima fault producing the 1995 Hyogoken-Nanbu earthquake, lead that the breakdown stress drop is 10 times larger than the static stress drop and d_0 is about 10cm, for example. It should be noted that the width of the LVZ is the observable value from the trapped wave observation even for earthquake faults before a large earthquake. Thus, the trapped wave observation has a great potential for predicting a process of large earthquakes

S2-3

Characterization of Spatial and Temporal Variations of Landers and Hector Mine Rupture Zones by Fault-Zone Trapped Waves

Yong-Gang Li¹, Keiiti Aki¹, J. E. Vidale², S. M. Day³, and D. D. Oglesby⁴

1. Department of Earth Sciences, University of Southern California, Los Angeles, CA 90089, USA (Phone: 213-740-3556, Fax: 213-740-8801, E-mail: ygli@terra.usc.edu)

2. Department of Earth & Space Sciences, University of California at Los Angeles, Los Angeles, CA 90095, USA

3. Department of Geological Sciences, San Diego State University, San Diego, 92182, USA

4. Department of Earth Sciences, University of California at Riverside, Riverside, CA 92521, USA

We deployed linear seismic arrays across and along rupture zones of the 1992 $M7.5$ Landers and 1999 $M7.1$ Hector Mine, California, earthquakes and recorded fault-zone trapped waves generated by aftershocks and near-surface explosions within the rupture zone. Observations and 3-D FD simulations of 2-7 Hz trapped waves allowed us to characterize the internal structure and physical nature of rupture zone with a high resolution at seismogenic depth. The Landers rupture zone is marked by a low velocity and low Q waveguide 250 m wide at the surface, tapering to 100-150 m at the 10 km depth, in which S velocities are reduced by 40-50% from wall-rock velocities and Q values are 20-60. At Hector Mine, the rupture zone has similar velocity reduction and Q values as the Landers rupture zone, but is 75 to 100 m wide. We interpret the distinct low-velocity waveguide on the rupture zone as being a remnant of the process zone, which is inelastic deformation around the propagating crack tip during dynamic rupture in earthquakes. The process zone width delineated by fault-zone trapped waves scales to the rupture length as predicted in published dynamic rupture models. Trapped waves also revealed multiple-fault rupture in both earthquakes. At Landers, the rupture is segmented by stepovers between pre-existing faults. At Hector Mine, a more complex set of rupture planes exists at seismogenic depth than the surface breakage. The northern Hector Mine rupture is bifurcated, in contrast to the single slip plane on the middle rupture segment, although only the west rupture branch on the north Lavic Lake fault broke to the surface while the east rupture branch was on a blind fault north of the mainshock epicenter. Our generic models for dynamic rupture with equal moment release on the northeast and northwest rupture branches but with the low shear stress in the shallow part of the northeast branch show that such a faulting bifurcation is physically plausible.

Repeated surveys using explosions at Landers and Hector Mine rupture zones indicated post-earthquake fault healing. At Landers, S velocities in fault zone increased by $\sim 1.2\%$ between 1994 and 1996, and increased further by $\sim 0.7\%$ between 1996 and 1998, indicating that the rupture zone has been strengthening after the mainshock, most likely due to the closure of cracks that opened during the 1992 earthquake. The observed fault strength recovery is consistent with a decrease of ~ 0.03 in apparent crack density within the fault zone. The ratio of decrease in travel time for P to S waves changed from 0.75 to 0.65 between 1994 and 1998, suggesting that cracks near the fault zone became more fluid saturated with time. The healing rate observed at the Landers rupture zone was not constant but decreased with time, and might be affected by the Hector Mine mainshock in 1999, which occurred only 25 km away from Landers. At Hector Mine, we found that S velocities within the rupture zone increased by 0.65-1.0% between 2000 and 2001 with the greater change on the fault in sedimentary sites than in mountains. The healing rate varies from one fault segment to another, probably due to rock material heterogeneity and non-linearity as well as stress changes along the rupture zone.

S2-4

Rupture Zones at Focal Depth: Structural Analysis of Three Earthquakes (M=5.1, 3.7 and 4.2) in Deep Gold Mines, South Africa

Z. Reches and O. Dor

Hebrew University, Jerusalem, Israel, and Stanford University, California, USA

The gold mines of South Africa are unique natural laboratories for studies of earthquake processes and fault properties. The mines provide access to active faults down to 4 km below the surface, and allow detailed analysis of earthquake rupture behavior at the focal depth. To utilize these advantages, we studied the rupture zones associated with three recent earthquakes in the mines in the western Witwatersrand basin, South Africa.

The first event is the Matjhabeng earthquake, M=5.1, April, 22, 1999, that reactivated the Dagbreek fault, Welkom area; this fault slipped at least 1km during the Archaean. We mapped the 1999 rupture zone at a few sites at 1370m below ground surface; maximum distance between the sites is 1300m. In the most comprehensively mapped site we found more than 20 fresh, newly formed slip-surfaces in addition to ~1.0m thick Archaean pyrophanitic gouge. These slip surfaces form a 27m wide rupture-zone (a minimum width). During the earthquake, the new slip-surfaces slipped 0.5cm to 6.5cm each, forming 0.5-5cm thick zones of crushed quartzite ranging from white 'rock powder' to pebble-size fragments. We also found a drill-rod that was abandoned inside the Archaean gouge. The rod was cut during the earthquake into four pieces by localized slip along three separate slip-surfaces within the gouge; the cumulative normal-oblique slip is 12cm.

The second rupture zone was formed by the M=3.7 earthquake in October, 1997, in Hartebeestfontein mine, Klerksdorp area. This event occurred within unfaulted massive quartzite layers, at a distance of about 80m from the mining face. About a year later, the newly formed fault zone was "mined" and we mapped it at 1950m depth. The rupture-zone was traced laterally for 100m (minimum length) and it displays a 7-9m wide highly complex structure with up to six major, fresh faults with cumulative dip-slip of up to 37cm. The fresh gouge-zones here are wide (1-10cm) and similar in composition (rock powder and rock fragments) to those mentioned above.

The third case is the M=4.2 earthquake in August, 1, 2001, along the 5-Shaft fault in ARM5 mine, Klerksdorp area; this fault displays ~320 m of vertical displacement of Archaean age. We conducted mapping, surveying and sampling in seven levels within this mine about five weeks after the event. The width of the rupture zone is 4-10 m, the internal slip surfaces are relatively smooth, and rock powder is not as abundant as in the other two events. We determined the localized slip from displaced markers (2-10 cm slip), and Geodetic measurements (EDM) of the total displacement across the rupture zone (~30 cm). Two creep meters that were installed across two of the nine slip-surfaces at one site both moved during the earthquake by 1.8 cm and 8.9 cm in horizontal and vertical directions.

Our analysis revealed that even a single event on an existing fault zone generates wide rupture zone (4m to 27m or more) with highly intricate fracture pattern. We interpret these observations as indicating that failure of solid, intact rock (rather than frictional sliding along existing surfaces) was the dominant slip mechanism during these earthquakes.

S2-5

**Three-dimensional P and S wave velocity structures in the aftershock area
of the 1984 Western Nagano prefecture, Japan Earthquake
–Implications for the relationship between structures and earthquake occurrences–**

Yoshihisa Iio¹, Shigeki Horiuchi², Kiyohiko Yamamoto³, Yoji Kobayashi⁴, Shiro Ohmi⁵,
Ryuji Ikeda², Eiji Yamamoto², Haruo Sato³, and Hisao Ito⁶

¹Earthquake Research Institute, the University of Tokyo, Yayoi 1-1-1, Bunkyo-ku, Tokyo, Japan, 113-0032(Phone: +81-3-5841-5787, Fax: 81-3-5689-7234, e-mail: iio@eri.u-tokyo.ac.jp). ²National Research Institute for Earth Science and Disaster Prevention, Tsukuba, Japan 305-0006. ³Graduate school of Science, Tohoku University, Sendai, Japan 980-8578. ⁴Institute for Geoscience, University of Tsukuba, Tsukuba, Ibaragi, Japan 305-0006. ⁵Disaster Prevention Research Institute, Kyoto University, Uji, Japan 611-0011. ⁶Institute of Geoscience, Geological Survey of Japan/National Institute of Advanced Industrial Science and Technology, Tsukuba, Japan 305-8567.

Three-dimensional P and S wave velocity structures in the aftershock area of the 1984 Western Nagano Prefecture Earthquake, central Japan (Ms6.8), were determined from a tomographic inversion of travel time data obtained by a dense network installed in the area. In this area, very shallow events occur even immediately beneath the surface, up to a depth of about 2 km from the surface. Microseismic activities are still very high about 18 years after the Ms6.8 earthquake. The network was first operated with six stations in June 1995, and now it consists of 56 stations. The data from three-component seismometers are magnified by amplifiers at two different gains and AD-converted with a sampling frequency of 10kHz.. The clock is adjusted to the GPS time signal every two hours within a precision of 1 ms. Average noise levels of each station are $1-10 \times 10^{-8}$ m/s.

Employing the iterative inversion method of Thurber (1983), we inverted travel time data to determine three-dimensional Vp and Vs structures and hypocenters simultaneously. The data set consist of, about 56000 seismic wave arrivals observed at 38 stations from about 1600 local earthquakes occurring between May 1 and October 31 of 1997. S arrivals were manually determined in both cases. Picking errors in P wave were less than 0.005 s because of the high sampling rate of 10 kHz, while those in S wave onsets were greater than that because of P wave coda.

We investigated the relationship between the obtained structures are compared with the present seismicity and the source process of the Ms6.8 earthquake. We found that microearthquakes tend to occur around the regions where Vp/Vs ratios are large. Further, it seems that the region in and around the maximum slip of the Ms6.8 earthquakes is characterized by very low Vp/Vs ratios. These maybe suggest that a water-assisted process control earthquake occurrences.

S2-6

High sampling frequency seismic array at Ootaki, Nagano Prefecture – Stress drop distribution and seismic velocity change –

Shigeaki Horiuchi¹, Kaori Takai¹, Yoshihisa Iio² and Sihua Zheng³

1. National Research Institute for Earth Science and Disaster Prevention (E-mail: horiuchi@bosai.go.jp)
2. Earthquake Research Institute, the University of Tokyo
3. Center for Analysis and Prediction, China Seismological Bureau, China

We determined stress drops for 15,000 events occurring in an earthquake swarm area at Ootaki, western part of Nagano Prefecture, Japan, where a seismic array network was operated with a sampling frequency of 10 KHz. We found from the comparison of accelerograms for same events observed by two borehole stations that P waves for about 0.03 sec are similar to each other while the two borehole stations are 3 km apart. It is also found that events occurring in a small region have various waveforms. This observation shows that the source process of micro-earthquakes is complex and the complexity can be detected by the borehole seismometers. However, there are almost no distinctions among the initial part of P waves for different events recorded by a surface station. We determined source parameters together with site-response functions by the use of P wave spectrum for the borehole stations. Obtained stress drops show that there is a large spatial variation in the stress drop distribution. We compared the stress drop distribution with that of resistivity and found that low stress drop earthquakes occur in the area of low resistivity. It is also found that stress drops increase with magnitude. Plots of stress drops for a small magnitude range show that there is no clear tendency of stress drop increase against focal depths. We calculate average magnitudes by dividing study area into small blocks and compared their spatial distribution with that of stress drops. The comparison shows that average stress drops are small in regions where average magnitudes are small.

Two or three earthquakes with magnitudes from 3.5 to 4 occur annually beneath the seismic array. We are engaging to detect seismic velocity change associated with the occurrence of these earthquakes. Even if seismic velocity in a region with a diameter of 1km changes by 1 %, it changes P and S wave travel times by only about 2 and 3 msec, respectively. We measured P wave arrival times with accuracy of about 1 msec for events occurring in a small region and calculated relative hypocenters for many pair of events with using P wave arrival time differences. Average residuals of the relative hypocenter location are less than 1 m sec for pair events with hypocentral distances less than a few hundred meters. Average residuals increase with hypocentral distances of pair events, showing the existence of heterogeneity in seismic velocity in the focal area. This result shows that we can detect very small velocity change by making a high sampling frequency seismic observation.

S2-7

The Paradox of the overabundance of historical earthquakes on Class C Faults:
Possible Mechanism for Earthquakes on Low
Stressing Rate Faults

S. Toda¹

1. Active Fault Research Center, Geological Survey of Japan, AIST, Site 7, Higashi 1-1-1, Tsukuba,
305-8567, Japan (Phone: +81-298-61-2480, Fax: +81-298-52-3461, E-mail: s-toda@aist.go.jp)

We propose a possible earthquake mechanism to explain the high rate of historical earthquakes on the so-called “class C faults” in inland Japan faults with very low slip rates.

Active faults inland Japan are categorized into three slip-rate classes, A (1mm/yr), B (0.1-1mm/yr, and C (0.01-0.1mm/yr). Since we have an empirical relation between magnitude and surface slip, one would expect that a surface-rupturing earthquake is produced every 1,000 years by a class A fault, and every 100,000 years by a class C fault. Because 6 out of 17 surface-rupturing events since the 1891 Nobi earthquake are identified to have struck on class C faults, the number of class C faults would need be a hundred times greater than A class faults to be compatible with their slip rate difference. However, the Active Fault Map identifies ~100 class A faults, and ~700 class C faults, rather than the expected 10000 needed to explain their high rate of activity.

To seek a resolution for this, we focus on the Takayama region of central Japan, where many class C faults are underlain and surrounded by several class A strike-slip faults. Recent trench excavations reveal these class A faults have 1-5 mm/yr of slip rates and 1000-2000-year inter-event times. We model these earthquakes in an elastic half-space and find typical ~10-bars stress decreases on the class C faults caused by class A ruptures. Thus the stress accumulation pattern on these class C faults would show a zigzag shape, with gradual stress increases and sudden stress decreases. The net stress accumulation rate would be much slower than the inherent rate. We find that if the inherent stressing rate on class C faults is half of that on the class A faults, the recurrence interval is ~10 times longer (~10,000 years). We can also add the effect of the rate- and state-friction on the regional seismicity rate in the stress accumulation process. Because the of sudden stress decreases and long aftershock durations, the chances to trigger class C faulting would be lowered, resulting in larger stress accumulations with time. This might explain why faults with long recurrence intervals have larger stress drop, as Kanamori and Allen (1986) found. If the model is correct, areas where class C faults should be severely restricted, we would not expect that the number of class C faults will be dramatically increased by further investigations.

Magnetotelluric Soundings over Seismically Active Regions, NE Japan

Yasuo Ogawa

Volcanic Fluid Research Center, Tokyo Institute of Technology, Tokyo, 152-8551, Japan
(Phone:+81-3-5734-2639, Fax:+81-3-5734-2492, E-mail:oga@ksvo.titech.ac.jp)

Masaaki Mishina

Tohoku University, Sendai,

Yuji Mitsuhashi

National Institute of Advanced Industrial Science and Technology, Tsukuba 305-8567, Japan

Recent MT studies in NE Japan over seismically active regions detected conductors under the seismogenic zones. The high seismicity clusters in the resistive region near the resistivity boundary or in the resistive region underlain by conductor (Ogawa et al., 2001, Mitsuhashi et al., 2001).

Ogawa et al. (2001) had a 90km long MT profile of 34 stations in the back arc of the Northeast Japan. The current high seismicity is regarded as aftershocks of two historically known large intraplate earthquakes, Senboku earthquake (M 7.1 in 1914) and Rikuu earthquake (M7.2 in 1896). The MT data showed strong two-dimensionality and anisotropic responses at the periods around 100s. The electric current flowing along-arc direction detects conductors, but the one flowing across-arc direction is insensitive to the conductors. The resistivity model to account for the anisotropic responses required three mid-crustal conductive blocks that were horizontally disconnected. The correlations of the conductors to the seismic scatterers and to the low velocity anomalies suggest that the conductors represent fluids. High seismicity clustering near the rims of conductors suggests that the intraplate seismicity results from the migration of the fluids to less permeable crust.

Mitsuhashi et al. (2001) had a detailed profiling around a seismically active region in the forearc of Northeastern Japan. The current seismicity is interpreted as aftershock of Northern Miyagi Earthquake (M6.5) in 1962. A two-dimensional inversion revealed the existence of a deep conductive zone and overlying resistive zone in the upper crust. They found that the micro-earthquakes occur just above the deep conductor and in the resistive zone, and that several S-wave reflectors are just above the deep conductor. Since the S-wave reflectors suggest the existence of fluid beneath them, the deep conductor was interpreted as a fluid-filled zone. They suggested that the seepage of the fluid from the conductive fluid-filled zone to the resistive granitoid pluton can become a trigger of the earthquakes.

These previous studies found consistent electromagnetic images of the high seismicity region, which are aftershock region of historically known large intraplate earthquakes. Namely, the high seismicity corresponds to the resistive area underlain by the conductor, or the one near the conductor. This suggests the fluid involvement in generating the aftershocks.

S2-9

**Seismic Properties of a Major Fault Zone at 7-8.5 km Depth:
Results from Vertical Seismic Profiling
at the Superdeep Continental Drillhole KTB (South Germany)**

W. Rabbel¹, Th. Beilecke¹, G. Borm³, K. Bram⁴, D. Fischer¹, A. Frank¹, H. Gebrande², J. Kück³, E. Lüschen², D. Okaya⁵, S. Smithson⁶

1. Institute of Geosciences, University of Kiel, Otto-Hahn-Platz 1, D-24098 Kiel; Germany; email: wrabbel@geophysik.uni-kiel.de
2. Institute of Geophysics, University of Munich, Munich, Germany
3. GeoForschungsZentrum Potsdam, Potsdam, Germany
4. Geowissenschaftliche Gemeinschaftsaufgaben, Hannover, Germany
5. Department of Earth Sciences, University of Southern California, Los Angeles, USA
6. Department of Geophysics, University of Wyoming, Laramie, USA

In its lowermost part, between 7 and 8.5 km depth, the Continental Deep Drillhole KTB (Oberpfalz, S Germany), intersects a major cataclastic fault zone which can be traced back to the earth surface where it forms a lineament of regional importance, the so-called Franconian Line. At depth this fault zone seems to be split into several branches one of which, known as "SE1-reflection", had already been detected by 2D and 3D reflection seismics prior to drilling. To determine the seismic properties of the SE1-zone in situ was one of the major goals of the Vertical Seismic Profiling (VSP) performed recently in the bottom part of the borehole. For the measurements a newly developed HP/HT borehole geophone was applied capable to withstand temperature and pressure up to 250 deg C and 140 MPa, respectively. Seismic signals of 10 to 300 Hz were generated by explosive charges of 0.5 to 2 kg fired in 15 to 30 m deep shotholes. The velocity- depth profiles and reflection images resulting from the VSP are of high spatial resolution due to a narrow geophone spacing of 12.5 m. High timing accuracy was achieved by using a reference geophone at a constant depth of 3.8 km in the KTB pilot hole situated 200 m north of the KTB main borehole.

Compared to the upper part of the borehole, we found more than 10% decrease of the P-wave velocity in the deep, fractured metamorphic rock formations. P-wave velocity is about 5.5 km/s at 8.5 km depth compared to 6.0-6.5 km/s at shallow levels above 7 km. In addition, seismic anisotropy was observed in terms of shear wave splitting. S-wave polarization anomalies were found at depths where the borehole intersects the deep fracture zones.

In order to quantify the effect of fractures on the seismic velocity in situ we computed a reference velocity-depth profile in comparison to which zones of anomalous velocity could be identified. This reference profile simulates P- and S-wave velocities to be expected if the rocks were isotropic and free of cracks. The reference velocities were computed as a function of depth on the basis of laboratory measurements and of the observed mineral composition (derived by X-ray diffraction from rock cuttings as a function of depth). The comparison of reference versus in situ velocities enabled us to identify fractured and solid rock sequences. It shows that the P-wave velocity is much stronger influenced by the fracturing than the S-wave velocities. In terms of a "penny-shaped-crack model" we need several percent crack porosity in order to explain the observed velocity reduction. These results are supported by additional investigations of the reflected and forward scattered wavefields, and by finite-difference wave field modelling. In particular the high resolution reflection images of the VSP show that the SE1 fault zone corresponds to a bundle of linear steeply dipping reflection elements the reflection strength of which can only be explained by open fractures. Also, the intensity of forward scattering, generating PS-converted arrivals along the VSP, correlates with zones of increased crack density as identified by velocity decrease compared to the reference profile.

S3-1

Numerical Modeling of Dynamic Rupture Propagation along a Fault: Which Parameters are Critical?

E. Fukuyama¹

1. National Research Institute for Earth Science and Disaster Prevention, Tsukuba, Ibaraki, 305-0006, Japan (Phone: +81-298-51-1611, Fax: +81-298-54-0629, E-mail: fuku@bosai.go.jp)

There are three important parameters in numerical modeling of dynamic faulting: 1) fault geometry, 2) constitutive relation (friction law), and 3) initial stress field. We demonstrate how these parameters affect a dynamic rupture simulation. To show that we use a boundary integral equation method (Fukuyama and Madariaga, 1998, BSSA) and apply it to a simple fault model.

For the fault geometry, aftershock distribution might be a good information source. However, we could obtain this information only after a big earthquake. Distribution of active fault traces is an alternative for shallow strike slip earthquakes. However, sometimes there are a lot of blind faults that appear during the earthquake (Fukuyama, Ellsworth, Waldhauser, and Kubo, 2002, submitted to BSSA). We will show how these fault geometry is included in the numerical simulation and discuss the effect on fault rupture dynamics (Fukuyama, Tada and Shibazaki, in preparation).

As for the constitutive relation, slip-weakening friction law is considered to play a major role during a high speed rupture (e.g. Ohkubo and Dieterich, 1989, JGR). In slip-weakening law, two parameters (critical strength drop $\Delta\sigma_b$ and critical slip-weakening distance D_c) control the rupture (Fukuyama and Madariaga, 2000, PAGEOPH). However, since the fracture energy, which is proportional to the product of $\Delta\sigma_b$ and D_c , controls the rupture velocity, it becomes difficult to estimate $\Delta\sigma_b$ and D_c separately from traditional waveform inversion using seismic waveform array data (Guatteri and Spudich, 2000, BSSA). However, if near-field waveforms (or waveforms on the fault) are available, it becomes possible to estimate D_c (Olsen, Fukuyama and Mikumo, 2002, submitted to Nature).

The most difficult parameters to estimate at this moment is the stress field. From the stress tensor inversion of earthquake focal mechanisms, it becomes possible to estimate the direction of stress tensors and the ratio of its principal components (Kubo, Fukuyama, Kawai and Nonomura, 2002, submitted to Tectonophys.). The result suggests a rather homogeneous stress field. It is also possible to estimate the relative stress drop during the earthquake (e.g. Ide and Takeo, 1997, JGR), which is quite heterogeneous in space. The shear stress distribution on the fault is closely related to the fault geometry. Thus we can propose the hypothesis that stress field is relatively homogeneous and local stress variation is caused by the geometry of the fault. Of course there should exist a locally heterogeneous stress field, however, this assumption seems to work for some earthquakes (eg. Aochi and Fukuyama, 2002, JGR in press). In this case, it would be important to calibrate the stress by using the result of *in-situ* downhole measurements.

S3-2

Fault Geometry in Numerical Simulation of Earthquake Rupture: Implication to a Complex Fault Jog

Hideo Aochi and Raul Madariaga

Laboratoire de Géologie, École Normale Supérieure, 24 rue Lhomond, 75231 Paris Cedex 05, France (Tel: +33.1.44.32.22.04; Fax: +33.1.44.32.22.00; E-mail: aochi@geologie.ens.fr, madariag@geologie.ens.fr)

We are now able to treat non-planar fault geometries in dynamic rupture modeling of earthquakes, and it becomes very important to introduce tectonic and geological information into model parameters; fault geometry, stress field and friction law. Although we still have to simplify some of these information due to numerical limitations, it should be very important to consider how to define model parameters reasonably.

For the 1999 Izmit earthquake ($M=7.4$), we considered how to introduce fault geometry in the numerical simulation in the presence of insufficient observed fault traces [Aochi and Madariaga, *AGU Fall Meeting*, 2001]. We observed that small differences of fault geometry make a significant difference in the rupture process and seismic wave propagation. The main problem is fault jog. Under the Sapanca lake, it was better to model a continuous fault with a small bend to explain the near-field ground motion data, although observed fault traces also allow us to interpret this portion as a jog (disconnected parallel faults). In this earthquake, the use of a continuous fault is reasonable, because this event occurred on a segment of a large plate boundary (North Anatolian fault).

However, this kind of question appears very often, because observed fault traces are not always clear. We can treat a continuous fault in some cases, whereas we can also regard them as a disconnected system in other cases. We also have to consider the depth variation of fault geometry as shown in Figure 1. We examine how important is a partial discontinuity of fault geometry, changing the geometry, initial situation and frictional parameters. Figure 1 shows an example of a numerical simulation using a boundary integral equation method [Aochi et al., *Pageoph*, 2000]. Continuity of the fault is essentially important. Rupture directivity, position of hypocenter, plays a significant role on rupture history. In real field, anelastic deformation or formation of new faults would be possible between the discontinuity, so that the whole process should be more complex. However these simulations point out the importance of fault geometry for the estimation of seismic wave generation.

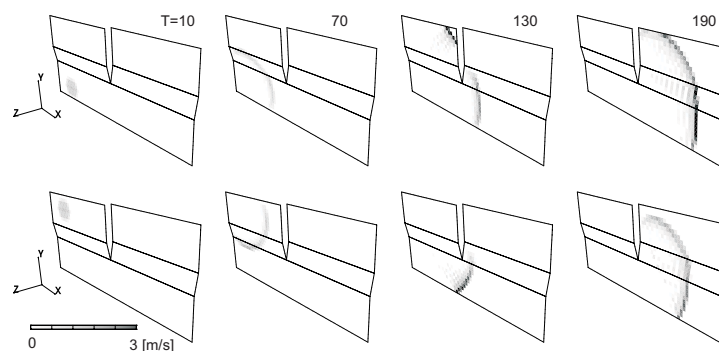


Figure 1: An example of dynamic simulation over a complex jog as an analogy of strike-slip fault. Fault slip is toward x -axis.

S3-3

Traction behavior within the cohesive zone during a dynamic crack propagation: absorbed fracture energy and fault constitutive properties.

Massimo Cocco and Andrea Bizzarri

Istituto Nazionale di Geofisica e Vulcanologia, Via di Vigna Murata, 605, 00143, Rome, Italy
[ph:+39 06 51860401; fax: +39 06 51860507; email: cocco@ingv.it bizzarri@ibogfs.df.unibo.it]

We study the dynamic traction behavior within the cohesive zone during the propagation of a 2-D in-plane crack obeying to rate- and state-dependent constitutive laws. We refer to the cohesive zone (or breakdown zone) as the zone of shear stress degradation near the crack tip of a propagating dynamic rupture front. Slip weakening behavior is a characteristic feature common to many constitutive formulations as resulting from theoretical studies and laboratory experiments. The resulting slip-weakening curve displays an equivalent slip-weakening distance (D_0^{eq} , i.e. the slip required for stress to drop), which is different from the length-scale parameter L , which controls the state variable evolution. The adopted constitutive parameters (A , B , L) control the slip-weakening behavior and the absorbed fracture energy. In this constitutive formulation, the dimension of the nucleation patch scales with L and not with D_0^{eq} . However, our simulations point out that slip-weakening occurs when the acceleration stage is already started. It is the evolution of the state variable within the cohesive zone from its initial value to the final one that drives the slip acceleration and the fast approaching to the peak slip velocity. We propose a scaling relation between these two length parameters which prescribes that $D_0^{eq}/L \sim 15$. In our simulations we have used values of the L parameter derived from laboratory experiments ($L \approx 1 \div 10$ mm), which yield D_0^{eq} values of the order of $0.02 \div 0.2$ mm. These values are much smaller than those obtained by waveform inversions which suggest $D_0^{eq} \approx 0.2 \div 0.5$ m. Estimates of the L parameter from strong motion recordings for the 1995 Kobe earthquake ranges between 1 to 5 cm assuming a SW distance of 0.5 m. According to our numerical simulations if D_0^{eq}/L is nearly equal to 15 and assuming $L \approx 1$ cm for actual fault dimensions, the proposed scaling law yields D_0^{eq} values very close to 0.2 m. If $D_0^{eq} \approx 0.2$ m is a believable result, the problem is therefore to scale the parameter L from laboratory to actual fault dimensions. If the lengthscale L of rate and state effects has the multi-micron scale of contacting asperities along surfaces, it can hardly be related to D_0^{eq} . The latter may be associated to different weakening processes (such as thermal weakening) occurring at high slip rates. On the contrary, we may assume that reasonable values of L for actual faults are close to the centimeter scale due to the presence of fault gouge responding to high slip velocities. In this latter case, we are allowed to scale our simulations to actual fault dimensions and the proposed scaling law may explain the inferred D_0^{eq} values. Because the nucleation patch scales with L and not with D_0^{eq} , we should expect a much reasonable dimension of the nucleation patch with respect to the whole fault length even for $D_0^{eq} = 0.2$ m. Our results could also be interpreted in the perspective of a unified constitutive formulation, at least for the dynamic slip episodes. While this can be a likely expectation for the dynamic rupture growth, this is certainly not true for the nucleation process.

S3-4

Nucleation process, and the associated convection current, in a fault model with dilatancy and fluid movements

B. Shibazaki¹, C. Marone², S. Yoshida³

1. International Institute of Seismology and Earthquake Engineering, BRI, Tsukuba, 305-0802, Japan (Phone:+81-298-64-6757, Fax: +81-298-64-6777, E-mail: bshiba@kenken.go.jp)

2. Dept. of Geosciences, Pennsylvania State Univ. University Park, PA 16802, United States (Phone: +1-814-865-7964, E-mail: cjm38@psu.edu)

3. ERI, Tokyo Univ., Yayoi, Bunkyo-ku, Tokyo 113-0032, Japan (Phone:+81-3-5841-5814, E-mail: shingo@eri.u-tokyo.ac.jp)

Dilatancy and fluid movements in a fault zone affect the mode of the nucleation process significantly and are keys for understanding physical mechanisms of some short-term precursory phenomena, e.g. foreshock activities and electromagnetic precursors. To understand the mode of nucleation processes, and the associated electric current, we investigate the model for earthquake generation processes on a vertical fluid infiltrated strike-slip fault in a 3-D elastic half space using a rate- and state-dependent friction law and the evolution equation of the porosity. The porosity change during the nucleation process is controlled by the dilatancy coefficients significantly. We assume the values of dilatancy coefficients to be 2×10^{-4} on the basis of the experimental results (Marone, 1990; Mair and Marone, 1999). During the nucleation process, porosity increases of 10-20 % are observed which lead pore fluid pressure decreases of 10-20 MPa. Permeability is also enhanced by the porosity increases during the nucleation process. As a result, fluid movements are enhanced and convection current due to a electrokinetic effect flows. The electric current density is in proportion to the gradient of pore fluid pressure. Yoshida (2000) has found that the streaming current coefficient is in proportion to the square root of permeability. Using his experimental results we calculate the electric current density in the fault.

The results of our numerical simulations show that, in some cases, dilatancy and the reduction in pore fluid pressure cause dilatant hardening and a slow growth of the nucleation zone. The magnitude of the electric currents is 10^{-4} - 10^{-3} mA/m² in the nucleation zone. During the nucleation process, at the stable region near the surface, slip velocity is increased and as a result fluid movement and electric current are enhanced. The magnitude of change in the electric current in the vertical direction near the surface reaches 10^{-3} - 10^{-2} mA/m² during the nucleation process. The changes in the electric current, which occurs before earthquakes, might be large enough to observe.

S3-5

Mechanical Effects of Fluid Migration in a Fault Zone on Seismic Activity

T. Yamashita

Earthquake Research Institute, University of Tokyo, 1-1-1 Yayoi, Bunkyo-ku, Tokyo 113-0032, Japan

(Phone : +81-3-5841-5660, Fax; +81-3-5841-5806, Email: tyama@eri.u-tokyo.ac.jp)

Spatio-temporal variation of rupture activity is modeled assuming fluid migration in a narrow, porous fault zone formed along a vertical strike-slip fault in a semi-infinite elastic medium. The principle of the effective stress coupled to the Coulomb failure criterion introduces mechanical coupling between fault slip and pore fluid. The fluid is assumed to flow out of a localized high-pressure fluid compartment in the fault at the onset of earthquake rupture. Our simulations show that the model can explain a foreshock-mainshock-aftershock sequence and earthquake swarm in a unified way.

If the rate of pore creation is large enough, rupture sequences with features of earthquake swarms are simulated. Such sequences generally start and end gradually with no single event dominating in the sequence. The b-value of the Gutenberg-Richter (GR) relation is shown to be unusually large. These are consistent with seismological observations on earthquake swarms.

If the rate of pore creation is relatively small, the occurrence of ruptures culminates in a large-size event regarded as the main-shock. The frequency-magnitude statistics of these events obey the GR relation; the b-value is close to unity.

Aftershocks can be simulated if the cohesive strength is assumed to drop at the instant of the earliest slip at each fault segment in a sequence of slips. It is actually observed that simulated aftershocks satisfy the Omori law of aftershock activity, the GR relation, the occurrence of secondary aftershock sequences, and the migration of aftershock activity. A large majority of simulated aftershocks consist of repeated slips, that is, slips on fault segments that have experienced slips earlier in the sequence. The emergence of the GR relation is shown to be closely related to the occurrence of these repeated slips.

S4-1

Elastic Property of Damaged Zone Inferred from *In-situ* Stresses near Fault: The Changes in Seismic Wave Velocities Caused by Faulting

Kiyohiko Yamamoto, Namiko Sato, and Yasuo Yabe
Graduate School of Science, Tohoku University, Sendai 980-8578, Japan
¹⁾e-mail: yama@aob.geophys.tohoku.ac.jp

SUMMARY

The Nojima fault in Awaji Is., Hyogo prefecture, Japan, ruptured during the 1995 Hyogo-ken Nanbu earthquake ($M_{JMA}=7.3$). The stresses at sites close to the fault were measured by deformation rate analysis (DRA) and the hydraulic fracturing technique (HF) after the earthquake. DRA is a method to estimate *in-situ* stresses from core samples by making use of the rock property of stress memory. The stresses measured by DRA are expected thus to be those before the earthquake, while the stresses by HF are those after the earthquake.

These measurements revealed as follows: 1) The direction of the largest horizontal stress is almost perpendicular to the strike of this nearly vertical fault at all of the sites except for shallow depths at a site. 2) In the zone within about 100 m from the fault core axis, the shear stress is small compared with those at a distance from the zone. 3) The shear stresses determined for the zone by DRA are slightly larger than those by HF. The results (1) and (2) have been interpreted as the reflections of the small fracture strength of the damaged zone that is in the post-failure state. The zone of small shear stress near the fault core axis is referred to as the damaged zone in the present paper.

There is a model proposed in order to correlate the fracture density and the crack density of damaged rocks with the applied stresses to the rocks. The seismic wave velocities of damaged zone were estimated from the shear stress obtained near the Nojima fault by using this model together with the theory of effective elastic constants. The velocities thus estimated were compared with the observed ones on the two assumptions as follows: The fracture density is constant throughout the damaged zone and invariable for any fault. The observed seismic wave velocity can be regarded as the velocity averaged over the propagation and motion directions, that is, the velocity of the zone that is elastically isotropic. The followings were the results of this comparison: a) The estimated velocity of P-waves is nearly equal to the observed one to the depth of about 15 km at greatest for the San Andreas Fault. b) The estimated velocity of S-waves is roughly equal to the velocities estimated from the trapped waves for some faults. c) Sealed or pressurized fluid is not required to explain the velocities of the damaged zone.

The difference in the measured stress between DRA and HF in (3) might not exactly mean the change in the shear stress caused by the faulting because of noises. However, if the faulting causes the stress in the damaged zone to drop, the difference may be regarded as the upper bound of the stress drops. The change in the velocity estimated from this upper bound is about 1.1 % of the host rock velocity for P-waves and about 2.7 % of the host rock velocity for S-waves. Some authors reported the arrival time delay for some phases in seismic coda waves after an earthquake. Although the ray paths for the phases have not been specified, the velocity changes inferred from the delay appear to be smaller than the changes estimated above. It may be thus one of the possible interpretations that the phases are the trapped waves scattered from damaged zone and the delay results from the velocity of damaged zone decreased by faulting.

Anisotropy of seismic wave velocities is calculated on the assumption that the crack surfaces lie parallel to the direction of the largest principal stress and orient symmetrically around the direction. At the depth of 10 km, the velocity of the S-waves, whose motion direction is oblique to the principal direction, varies in the range from about 43 to 85 % of the host rock velocity with the change in the propagation direction, while the velocity of P-waves does in the range from about 99 to 75 % of the host rock velocity. The largest and the smallest velocity respectively are attained at the propagation directions of about 50° and 0° or 90° from the principal direction for the S-waves and at the propagation directions of 0° and about 60° for P-waves. The decrease in the crack density of the damaged zone advances the arrival times of the direct P- and S-waves. The ratio of the advance of P-waves to that of S-waves varies in the range from near zero to 1.25 depending on the propagation direction and the largest advance is given at the direction of about 55° from the principal direction, if it is assumed that the ray paths for both the waves are identical.

S4-2

**Effects of Water, Strain-Rate, and Heterogeneity on Rock Strength:
Experimental Study on Strength of Fault Zone Materials**

Koji Masuda and Koichiro Fujimoto

Institute of Geoscience, National Institute of Advanced Industrial Science and Technology,

AIST Tsukuba Central 7, Tsukuba 305-8567, Japan

(Phone:+81-298-61-3994, Fax:+81-298-61-3682, E-mail: koji.masuda@aist.go.jp)

Fault zones are formed from fault materials of which properties are different from those of the rocks distributed around the fault zones. In order to evaluate the stress and strength of active fault, we need to understand the physical properties of fault materials under the high-pressure and high-temperature conditions. Although its importance is well recognized, only limited amounts of data on the deformation process and the physical properties of fault materials are available. Because the physico-chemical effect seems to play an important role, the weakening of the fracture strength may be greater, especially at greater depth and in fault zones, than current strength model of the lithosphere. We carried out a series of systematic experiments on time-dependent rock strength. Failure strengths of granite and andesite have been measured under various conditions of strain rate and confining pressure both in the dry and wet states. The strain rate varied from 10^{-4} to 10^{-7} s⁻¹ and effective confining pressures from 0 to 200 MPa (for granite) and to 50 MPa (for andesite). In order to test the effects of heterogeneity of the fault zone rocks, mylonite samples taken from the exposed brittle-ductile transition zone, are also tested under the confining pressure of 50 MPa and temperatures up to 500C. The failure strength decreased linearly as the logarithm of the strain rate decreased. The strain rate dependence of the failure strength is increased at higher confining pressures. The strain rate effect is more apparent on the failure strengths of wet samples than dry samples in lower confining pressure ranges. Mylonite samples showed the similar deformation curves to those of granitic rocks. However, compared with the granite data, the peak shear stress needed to cause the fracture/sliding along the foliation structure is smaller. The foliation structure of mylonite rocks dramatically affects the value of the peak shear stress. The mylonite sample under the temperature of 500 C can deform more than that under 300 C before the fault surface formation. The shear stress values that initiate the fault movement along the fault surfaces may be small under the high-pressure and high-temperature conditions in the seismogenic region.

S4-3

Permeability and Strength of Borehole Core Samples from the Nojima Fault

David Lockner*
Diane Moore*
Hidemi Tanaka**
Riuji Ikeda***
Hisao Ito****

*U.S. Geological Survey
345 Middlefield Road
Menlo Park, CA 94025
USA
email: dlockner@usgs.gov

**University of Tokyo, Tokyo, Japan

***National Research Institute for Earth Science and Disaster Prevention, Tsukuba, Japan

****Geological Survey of Japan, Tsukuba, Japan

Following the M=7.2 1995 Hyogoken-Nanbu (Kobe) earthquake on the Nojima fault, a number of scientific drillholes were completed in the epicentral region. Four of these drillholes, located on Awaji island, were designed to penetrate the Nojima fault and provide cores of the fault zone material. These unique samples show the condition of an active fault, at depth, following a damaging earthquake. We have completed permeability and strength tests on representative core samples from all four drillholes: the two holes completed by a consortium of Japanese universities, the National Research Institute for Earth Science and Disaster Prevention (NIED) drillhole and the Geological Survey of Japan (GSJ) drillhole. Permeabilities were tested at pressures spanning the range of *in situ* overburden pressures as well as under deviatoric stress conditions. The shallow university hole showed the simplest fault geometry with granodiorite abutting a conglomerate and sandstone sedimentary sequence across the fault at a depth of 389.4 m. Peak strength of core samples from the granodiorite side are a minimum at the contact, consistent with observations of localized shear along this interface. Strength within the poorly indurated sandstone remains equal to or slightly above the fault zone strength. Permeability measurements indicate a damage zone of enhanced permeability and microcrack damage extending about 30 m into the granitic protolith on the southwest side of the fault shear axis.

The GSJ hole also shows a simple geometry composed of a gouge-bearing fault (presumably the trace of the Nojima fault) at a depth of 624 m. Strength measurements again are at a minimum at the shear zone axis. The axial zone is surrounded by a 20 to 40 meter zone of enhanced permeability related to intense microcrack damage. Thin section examination reveals evidence of significant fluid flow and multiple episodes of fracture and re-healing in this broad damage zone. The NIED drillhole encountered three fault strands. Based on strength, permeability and petrographic evidence, the upper two strands, at depths of 1140 and 1320 m, appeared to be activated by the 1995 earthquake. Each of these shear zones has a minimum in strength in the highly crushed material, suggesting localized deformation. Permeability is again enhanced in a 20 to 30 meter wide zone surrounding each fault strand. In contrast to these shallower fault crossings, the 1800-m university drillhole did not cross any obvious zone of localized shear. Instead, a relatively diffuse fault zone was encountered in the granodiorite beginning at about 1670 meters and continuing to the bottom of the hole. As described above, the shallower fault crossings contain a central narrow gouge-filled shear zone that is relatively weak and which accommodates intense shearing. This sheared core region is surrounded by a zone of highly damaged rock which, despite the intense microcrack damage, has undergone little net shearing. Following an earthquake, this broad damage zone will provide a conduit for fluid flow in the plane of the fault. The rate at which this damaged region will resealed remains an open question. It is interesting that the four drillholes studied here show a steady increase in complexity with depth of fault zone crossing. As additional deep fault zone drilling projects are completed, we will learn how general this type of fault structure is.

S4-4

Frictional heating and high-velocity frictional properties of faults

**Toshihiko Shimamoto⁽¹⁾, Takehiro Hirose⁽¹⁾, Kazuo Mizoguchi⁽¹⁾
and Tatsuro Fukuchi⁽²⁾**

⁽¹⁾ Division of Earth and Planetary Sciences, Graduate School of Science,
Kyoto University, Kyoto 606-8502, Japan,

⁽²⁾ Department of Earth Sciences, Faculty of Science, Yamaguchi University,
Yamaguchi 753-8512, Japan

Presence of pseudotachylyte indicates that temperature rise can be high enough to melt rocks at least for some natural faults. This rock, however, is rare and an important question is whether frictional heating is universal or not along faults. The famous heat flow paradox along the San Andreas fault has been discussed over 30 years, but the data on heat flow anomaly have not yet provided a clear answer to the question. Petrological analyses of fault rocks have not revealed the degree of frictional heating either probably because of slow reaction rate. We have thus started “heat-detection project” seeking for new methods to detect temperature rise within fault zones, particularly in the slipping zones. One of the exciting outcomes from the Nojima drilling project is that fault gouge of several millimeters in width, out of about 100 mm wide gouge zone, exhibits reduction in ESR (electron spin resonance) signals of quartz and clay minerals (Fukuchi and Imai, 2001; Matsumoto *et al.*, 2001). Fukuchi recognized even more dramatic changes in ESR signal from Fe³⁺ ions from adjacent fault gouge into pseudotachylyte-bearing gouge at an outcrop of the Nojima fault at Hirabayashi. The same change was reproduced by heating the gouge in an oven for one minute and by our high-velocity friction experiments on the gouge. A preliminary analysis of the data by T. Fukuchi shows that the signal changes correspond to temperature rise of several degrees. ESR measurements may provide much more direct data on the frictional heating than the heat flow anomaly on the slipping zones within fault zones. Frictional heating seems to be universal and high-velocity frictional properties of faults must be studied systematically to understand earthquake initiating processes. Detection of temperature rise can be a possible link between laboratory experiments and natural fault zones.

We would like to present highlights of ongoing high-velocity friction projects in Kyoto. Experiments by Hirose consistently reveal two stages of slip weakening; i.e., the first immediately after the onset of slip due to flash temperature at asperity contacts, and the second after the second peak frictional due to the growth of molten layer. The weakening distance during the first weakening is much larger than that measured conventional frictional experiments. The first weakening is likely to be associated many natural earthquakes. Melt patches begin to form after the first weakening and the onset of melting induces marked strengthening of faults possibly due to viscous drag of very thin melt patches. This high-velocity barrier may act as a break to dynamic fault motion. The second slip weakening occurs after a continuous molten layer forms and Hirose’s detailed analyses reveal how the growth of molten layer causes the weakening fault. Abundant data show that the weakening distance, D_c varies dramatically with the rate of frictional heating and is not a material constant. It can vary with depth and along faults. We propose a physical model to solve the highly nonlinear problem involved with viscous flow, heat dissipation and melting. The rate of melting is probably the most critical process to determine D_c during frictional melting.

A controversy in the last 15 years or so is the difference in D_c of several orders between seismically determined values and those measured in conventional friction experiments. D_c for natural faults is very difficult to determine for natural faults. Hirose has shown that fractal dimension of melting surface and the growth of molten layer can be correlated with the weakening behavior. The thickness-displacement data on pseudotachylytes in the Outer Hebrides indicates D_c of the order of several decimeters, the same order to the seismically determined values. The controversy may be solved taking into account of the frictional heating, although the effect of scaling still remain difficult problem to evaluate.

S4-5

Comminution and Fluidization of fault gouge: their implications to fault slip behavior

Kenshiro Otsuki and Nobuaki Monzawa

Department of Geoenvironmental Sciences, Graduate School of Science, Tohoku University, Japan

A part of elastic strain energy in the earth crust is dissipated as comminution energy. Comminuted fault gouge have serious effects on the dynamic frictional properties during seismic slip. According to the knowledge of granular material technology, mechanical properties (strength, viscosity) of granular materials are a function of grain size distribution function, volume fraction of grains, viscosity of interstitial fluid and shear velocity. A noteworthy phenomenon is the phase transition from grain friction regime to the fluidization, and the problems are how we can distinguish the fluidized fault gouges from the gouges that have not experienced fluidization, what are the appropriate conditions for the phase transition, and what is the frictional properties of fault gouge during fluidization. In order to clarify these issues, we at first analyzed the grain size distribution of selected four gouge samples, and will propose a new evolutionary comminution law of fault gouge. Next, we have developed a new method to identify the fluidized and non-fluidized gouges. Thirdly, the dynamic property of fault gouge was synthesized based on the articles of granular material technology. Fourthly, the appropriate condition for the phase transition from the grain friction regime to fluidization and their implications to seismic slip behavior will be discussed.

1) *Size frequency function of fault gouge and its evolutionary trend*

Cumulative size frequency of fault gouge shows a fractal nature as noted already by previous workers. The data of 2-D measurement are fitted well to the modified power function

$$P \equiv N(> D)/N_t = [1 + (D/D_c)^\alpha]^{-\beta/\alpha} \quad \text{----- (1)}$$

where N is the number of grains larger than diameter D among total grain number N_t , D_c is the grain size characterizing cut-off at small grain sizes, α is the parameter of cut-off sharpness, and β is fractal dimension. The evolutionary trend of β can be expressed as

$$\beta = 2.814 D_c \sum D_i^{-1} + 1.448, \quad R^2 = 0.9808 \quad \text{----- (2)}$$

irrespective of rock species (Fig.1), where $\sum D_i^{-1}$ is the reciprocal sum of grain diameters. When we take our measurement precision into the consideration, it is noteworthy that comminution starts likely at β equal to golden ratio 1.618..., and β increases as comminution proceeds. When β =golden ratio, 2-D space can be filled by grains and a given grain can be surrounded by most grains attainable, and hence the bulk granular material is the strongest. Therefore, comminution itself is a slip weakening process.

2) *A new method how to identify fluidized/non-fluidized fault gouges*

When closely packed granular material is shared, grains tend to be fracture by stresses concentrated at points of contact, while grain fracturing occurs by collision of flying grains when fluidized. Based on the knowledge of granular material technology, the critical velocity v_c at which quartz grains of $D=1$ mm can be fractured by head-on collision is estimated at 10 m/s, and v_c for $D=0.1$ mm is 30 m/s. Therefore, it is expected that the fragmentation probability is much smaller in fluidized gouge than in non-fluidized (grain friction) regime. Moreover, fragmented counterparts in fluidized gouge go away at a high velocity from each other, and they cannot be identified as counterparts even just after the fragmentation, while fragmented counterparts in the grain friction regime will stay aside. Therefore, the key parameter of our new method is the identification probability P_d of fragmented counterparts in gouge samples.

We measured P_d for four samples, and it is given in Fig.2 as a function of D . The results support our expectation; P_d decrease as D becomes smaller, reflecting size dependency of grain strength, two samples have large P_d , while other two show much smaller P_d , and there is a distinct gap between these two groups. The former two samples and the latter two samples can be safely regarded as non-fluidized

and fluidized gouges, respectively.

3) Dynamic frictional property of fluidized gouge

The viscosity η_g of spherical equi-granular materials is a function of the viscosity η_f of interstitial fluid, volume fraction ϕ of grains as

$$\eta_g = \eta_f [1 - (\phi/\phi^*)]^K, K=3.12, \phi^*=0.647 \quad \text{----- (3)}$$

(Krieger, 1972), where ϕ^* is maximum volume fraction of grains attainable. η_g is dependent also on shear strain rate $\dot{\gamma}$. We synthesized the experimental data by various authors for η_g/η_f as a function of ϕ and $\dot{\gamma}$. Attention should be paid on the fact that η_g/η_f drastically decreases (more than 2 order of magnitude) when ϕ become only 0.02 smaller than ϕ^* , namely the phase transition from grain friction regime to fluidization. This predicts sudden and nearly complete stress drop when fault gouge is fluidized during seismic slip.

4) A plausible mechanism of the phase transition during seismic slip

As known already, ϕ/ϕ^* is a key parameter of the phase transition from the grain friction regime to fluidization, but it never realized by the comminution only, because as noted in (1), ϕ^* decreases inevitably as comminution proceeds. The validity of acoustic fluidization by Melosh (1996) was recently doubted by Sornette and Sornette (2000). We need the widening of the gap between fault wall rocks, but the interstitial fluid pressurized by shear heating (Mase and Smith, 1987) is not effective for it, because the fluid pressure never reach the lithostatic pressure acting on the fault plane. We think for the present that the normal interface vibration by Brune et al. (1993) and Bouissou et al. (1998) is most appropriate for fluidization. We have some lines of the geologic evidence suggesting coseismic fault plane separation.

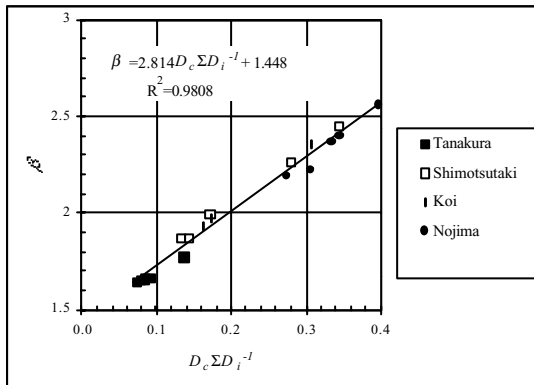


Fig.1 Evolutional trend of fault gouge size frequency through comminution.

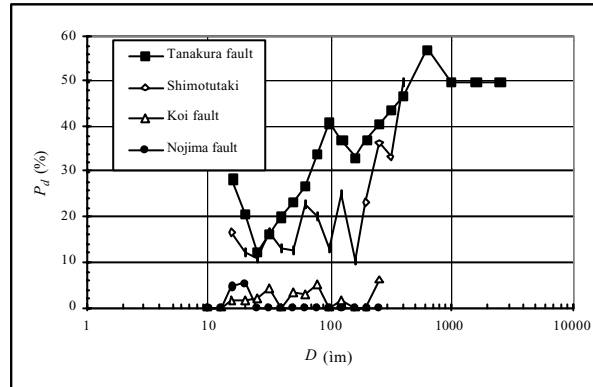


Fig.2 Identification probability of fragmented counterparts in four fault gouge samples.

References

Bouissou, S., J. P. Petit, and M. Barquins, 1998, Experimental evidence of contact loss during stick-slip: possible implications for seismic behavior, *Tectonophysics*, **295**, 341-350.
 Brune, J. N., S. Brown, and P. A. Johnson, 1993, Rupture mechanism and interface separation in foam rubber models of earthquakes: a possible solution to the heat flow paradox and the paradox of large overthrusts, *Tectonophysics*, **218**, 59-67.
 Krieger, I. M., 1972, Rheology of monodisperse lattice, *Adv. Colloid Interface Sci.*, **46**,491-506.
 Melosh, H. J., 1996, Dynamical weakening of faults by acoustic fluidization, *Nature*, **379**, 601-606.
 Sornette, D. and A. Sonette, 2000, Acoustic fluidization for earthquakes?, *Bull. Seism. Soc. Am.*, **90**, 781-785.
 Mase, C. W., and L. Smith, 1987, Effect of frictiona, heating on the thermal, hydrologic, and mechanical response of a fault, *J. Geophy. Res.* **92**, 6249-6272.

S4-6

Fault rocks distribution and physical properties of the Nojima fault fracture zone - Analysis of core samples and well logging in the Hirabayashi NIED borehole -

Kentaro OMURA¹⁾, Hidemi TANAKA²⁾, Kenta KOBAYASHI³⁾, Takashi ARAI²⁾, Satoshi HIRANO⁴⁾,
Ryuji IKEDA¹⁾, Tatsuo MATSUDA¹⁾, Koji SHIMADA⁵⁾, Tomoaki TOMITA⁶⁾

1) Nat'l Res. Inst. Earth Sci. Disast. Prev. (NIED), 3-1, Tennodai, Tsukuba, Ibaraki, 305-0006, Japan, (omura@bosai.go.jp), 2) Tokyo University, 3) Niigata University, 4) Japan Marine Sci. Tech. Cent., 5) Waseda University, 6) University of Tsukuba

The Hyogo-ken Nanbu earthquake (1995) activated the Nojima fault in the northern part of Awaji Island, southwest Japan and a surface rupture appeared more than 10km long. Within a year after the earthquake, the Hirabayashi NIED borehole was drilled penetrating through the fault zone to a depth of 1838m from a point about 302m SE from the surface trace of the Nojima fault.

In the borehole, in-situ experiment and physical well logging was done from a depth of 251m down to the bottom. At the same time, drilling cores were collected continuously from 1000m to 1838m depth with a nearly 100% recovery rate. The features of fault rocks distribution and physical properties in the fault zone were investigated based on mesoscopic (by naked eyes) and microscopic (by optical microscope) observations and logging data analysis.

Cores are all granitic rocks including porphyritic intrusive rocks in spots. Three remarkably fracture zones are found in the cores consisting of cataclastic rocks at depths around 1140m, 1300m and 1800m. Each fracture zone consists of several thin shear zones including three types of fault related rocks, fault breccia, fault gouge and cataclasite, and calcite veins intruding cemented fragments and matrix. These shear zones are generally surrounded by fault related rocks that are weakly pulverized and altered rock (WPAR). Shear zones appears to evolve from the WPAR, indicating that pulverization and alteration of recent activity are more diffused at the initial stage of faulting, becoming gradually localized to individual shear zones. The hanging wall and footwall of each shear zone typically shows explosion brecciation texture with carbonate and zeolite matrices, respectively, which are also regarded as dilatant co-seismic shear zones. Some specimens indicate textural changes resultant of the reaction weakening deduced from the alteration of feldspar grains to clay minerals.

The over all extent of pulverization and alteration seems to a little different among the three fracture zones. A fracture zone around a depth of 1140m is characterizes by the dark gray ultracataclasite zone and the existence of pseudotachylyte. The fracture zone around a depth of 1300m is likely less altered than other two fracture zones. The extent of alteration seems to be harder and denser in the fracture zone around a depth of 1800m. These features are considered to reflect of the history of fault zone activity.

Results of well logging show that, in the depth intervals of host rocks, normal resistivity is from several hundreds to several thousands $\text{ohm}\cdot\text{m}$, micro resistivity is several tens $\text{ohm}\cdot\text{m}$, P wave velocity is 5 - 6km/sec, density is about $2.6\text{g}/\text{cm}^3$ and neutron porosity is several %. On the other hand, in the depth intervals of fracture zones, those properties decrease down to several tens $\text{ohm}\cdot\text{m}$, several $\text{ohm}\cdot\text{m}$, 2-4km/sec, $1.5-2.0\text{g}/\text{cm}^3$ and increase up to several tens %, respectively.

Investigating correlations between physical properties measured by well logging, three fracture zones are characterized. In fracture zones, neutron porosity is beyond 10%, P wave velocity is less than 5 km/sec. The correlation between neutron porosity and P wave velocity is not clear and normal resistivity does not obey the Archie's relation in the fracture zones. The fracture zone at a depth of 1800m indicates some different characters from other two fracture zones; P wave velocity, density and neutron porosity appear to change gently contrasting to a remarkable decrease of normal resistivity. In shear zones distributing in the fracture zone, physical properties changes steeply. Caliper log indicates the diameter of well is elongates at the shear zones that are weak due to strong pulverization and alteration. Other physical properties recognized by logging seem to close relation to the extent of pulverization and alteration of fault related rocks in fracture zones.

S4-7

**Fracture-zone conditions on an active fault that has just moved:
Analyses of the Hirabayashi NIED drill core on the Nojima fault that ruptured
in the 1995 Kobe Earthquake, southwest Japan**

T. Matsuda, R. Ikeda, and K. Omura

National Research Institute for Earth Science and Disaster Prevention

3-1 Tennoudai, Tsukuba, Ibaraki, 305-0006, Japan

Phone: +81-298-51-1611, Fax: +81-298-54-0629

E-mail: mtatsuo@bosai.go.jp, ikeda@bosai.go.jp, omura@bosai.go.jp

A 1800-m-deep borehole was drilled at Nojima Hirabayashi and penetrated the Nojima fault that was activated at the time of the 1995 Hyogo-ken Nanbu Earthquake (Kobe Earthquake) in Japan. Three possible fracture zones were detected at depths of about 1140 m, 1300 m, and 1800 m. In order to assess these fracture zones in a fault that had just moved, we analyzed the mode of distribution of rocks, minerals and chemical elements in them. One remarkable feature we encountered is foliated blue-gray gouge at a depth of 1140 m. We infer that this is the central fault plane, and began our fracture zone analysis there, as follows. The degree of fracturing is evidently greater in the hanging wall than in the footwall. We estimated the relative amounts of minerals qualitatively, and we detected not only quartz, orthoclase, plagioclase, biotite and hornblende in the parent rock (granodiorite), but also kaolinite, smectite, laumontite, stilbite, calcite, ankerite and siderite, which are related to hydrothermal alteration. Biotite notably disappears in both the hanging wall and footwall across the central fault plane, although it disappears over a significantly greater distance in the hanging wall than in the footwall. We estimated the amounts of major chemical elements quantitatively. Al_2O_3 , Fe_2O_3 , MnO , TiO_2 , and P_2O_5 all decrease throughout this interval, except at a few points. H_2O^+ and CO_2 increase throughout the interval. Na_2O increases in the region adjacent to the central fault plane, while MgO and CaO increase in the hanging wall and decrease in the footwall. SiO_2 and K_2O decrease in the hanging wall and increase in the footwall. In short, hydrothermal alteration minerals (such as kaolinite and smectite) occur across the central fault plane for a greater distance in the hanging wall than in the footwall. Similarly, H_2O^+ and CO_2 had higher concentrations in the hanging wall than in the footwall. This is probably due to the greater degree of wall-rock fracturing observed in the hanging wall. We infer that these characteristics are associated with fault activity and the nature of fluid-rock interactions in the fracture zone. We analyzed the other fracture zones along this fault in the same way. Based on our analyses, the fracture zone at 1140 m depth is very similar to the fracture zone at 1800 m depth and differs significantly from the fracture zone at 1300 m depth. From this, we infer that the fracture zones at depths of 1140 m and 1800 m were activated at the time of the 1995 Hyogo-ken Nanbu Earthquake.

S4-8

Textural evidences for ancient and recent earthquakes on the Nojima fault.

Anne-Marie Boullier¹, Koichiro Fujimoto², Tomoyuki Ohtani², Hisao Ito², Philippe Pezard³, Michel Dubois⁴, Benoît Ildefonse³

1 - C.N.R.S. – L.G.I.T., BP 53X, 38041 GRENOBLE CEDEX 9, France

2 - Geological Survey of Japan, A.I.S.T., 1-1-1 AIST Tsukuba Central 7, Tsukuba, Ibaraki, 305-8567

3 - Laboratoire de Tectonophysique, ISTEEM, Université Montpellier II, 34095 Montpellier cedex 05, France

4 - Université des Sciences et Technologies de Lille, Sédimentologie et Géodynamique, 59655 Villeneuve d'Ascq Cedex, France

The GSJ Hirabayashi borehole allows to study the complete sequence of deformation near the Nojima fault from the undeformed granodiorite to the fault gouge. In the fault core, different types of gouges have been previously described among which it is possible to recognize the products of ancient and recent earthquakes.

Pseudotachylytes are present in the center of the fault core and are the oldest structures recognized in the fault zone at the scale of the thin sections. Petrographical studies have been performed on these rocks. They indicate that friction melting has occurred on millimeter thick layers at 1200°C minimum. Volatile content of the glass (8 ± 3 %) suggests that the fault zone was already altered before melting. Aquo-carbonic fluid inclusions trapped in the glass during quenching allow to determine a depth of 15 km for their formation, assuming a 24°C/km geothermal gradient. This depth corresponds to the base of the seismogenic zone where such rocks are supposed to form during large earthquakes. Very fast quenching of the glass indicates also a very fast healing of the fault plane after the slip. The 15 km depth estimation has important implications on the minimum age of these pseudotachylytes which are probably older than the basal unconformity of the Miocene Kobe Group.

Above 624.15m, foliated cataclasites and gouges are observed and are cross-cut by fractures which are filled by small carbonates (siderite and dolomite). The small size of these crystals (less than 10µm) suggests a fast nucleation in a saturated fluid. The fact that the fractures cross-cut all the visible structures at the scale of the thin sections, the euhedral shape of the small crystals, their zonation, the absence of any deformation (no compaction) and the high apparent porosity, suggest that they are very late in the evolution of the fault zone. These carbonate-filled fractures have been observed on thin sections within a 624-570 m depth interval, that is on a 5.5m wide zone above the fault zone. They are interpreted as being the result of a coseismic fracturation and circulation of fluids in the hanging-wall of the fault. Fast nucleation is attributed to a sudden fluid pressure drop due to fracturing. It is suggested that these non-compacted carbonate-filled veins correspond to a recent earthquake (1995 Hyogo-ken Nanbu earthquake?) and that similar but compacted carbonate veins could represent previous seismic events. Whatever the age of these carbonate-filled fractures, the healing of such a fractured fault zone should involve mechanical (compaction) and chemical (dissolution-crystallisation) processes and, therefore, should be much slower than the healing of a fault smeared by pseudotachylytes.

S4-9

Geochemical characteristics of fault rocks along the Nojima fault: Implications for the fluid in the fault zone

K.Fujimoto¹, A.Ueda², T.Ohtani¹, H.Ito¹ and H.Tanaka³

1. Geological Survey of Japan/ AIST, Tsukuba, Ibaraki 305-8567, Japan (Phone: +81-298-61-3985, Fax: +81-298-61-3682, E-mail: k-fujimoto@aist.go.jp, tomo-ohtani@aist.go.jp, hisao.itou@aist.go.jp)
2. Central Research Institute, Mitsubishi Materials Corporation, 1-297 Kitabukuro, Omiya, Saitama 330-8508, Japan (E-mail: A-UEDA@mmc.co.jp)
3. Department of Earth and Planetary Sciences, University of Tokyo, Bunkyo-ku, Tokyo 113-0033, Japan (E-mail: tanaka@eps.s.u-tokyo.ac.jp)

The active fault drilling at Nojima Hirabayashi after the 1995 Hyogoken-nanbu (Kobe) earthquake provides us a unique opportunity to investigate subsurface fault structure and in-situ properties of the fault. The borehole (746m deep) is situated at Nojima Hirabayashi, on the northwestern coast of the Awaji Island, Japan, where the surface displacement at the 1995 Kobe earthquake was at maximum. We identified the fault core at about 623m to 625m depth interval based on both geophysical logging data and core lithology. The core lithology is mostly Cretaceous granodiorite with some porphyry dikes. The rocks above 426m depth are nearly intact granodiorite. The borehole enters into the fault zone at 426m depth and the rocks are affected by the fault even at the bottom of the borehole. Characteristic alteration minerals in the fault zone are smectite, zeolites (laumontite, stilbite) and carbonate minerals (calcite, siderite, and dolomite). Carbonate minerals are important as sealing material in the shallow level of the Nojima fault.

Carbon and oxygen isotope ratios of carbonates were analyzed. The samples were taken from 41 bulk samples and 8 carbonate vein samples from various depth. The analytical results and preliminary interpretations are as follows.

- (1) As a whole, $\delta^{13}\text{C}$ (PDB) and $\delta^{18}\text{O}$ (SMOW) values cover -12.2 to -0.6% and 14.4 to 30.4% , respectively. The two ratios do not show good correlation.
- (2) Carbonates at the fault core (623 ~ 625m depth) is characterized by low $\delta^{18}\text{O}$ ($\sim 15\%$) and relatively high $\delta^{13}\text{C}$ ($-3.5 \sim -1.9\%$). This implies two possibilities of the origin of the fluid. One is that connate sea water precipitates carbonates at relatively higher temperatures ($100 \sim 200^\circ\text{C}$) and the other is that meteoric water precipitates them at relatively lower temperature ($<50^\circ\text{C}$).
- (3) Carbonates in the intact zone (above 426m depth) are characterized by low $\delta^{13}\text{C}$ ($< -5.8\%$). In particular, vein calcite is characterized by low $\delta^{18}\text{O}$ ($14.4 \sim 22.9\%$) and is considered to be precipitated from connate sea water at the relatively higher temperatures ($100 \sim 200^\circ\text{C}$).
- (4) Carbonates in the hangingwall (426 ~ 623m depth) and footwall (625 ~ 746m depth) are different in $\delta^{13}\text{C}$ values, in contrast, $\delta^{18}\text{O}$ values are nearly in the same range. $\delta^{13}\text{C}$ value is $-1.3 \sim -6.0\%$ in the hangingwall and it is $-0.5 \sim -2.4\%$. This difference results from difference in original fluid and/or precipitation environment.

Preliminary interpretations suggest the possibility of localized meteoric water flow at the fault core. Isotopic study of carbonate minerals has a potential for elucidate the characteristics of fluid in the fault zone.

S4-10

Fault Rocks and Hydrothermal Alteration of the Nojima Fault, southwest Japan

T. Ohtani¹, H. Tanaka², K. Fujimoto¹, and H. Ito¹

1. Geological Survey of Japan, AIST, Tsukuba, Ibaraki, 305-8567, Japan (Phone: +81-298-61-3851, Fax: +81-298-61-3717, E-mail: tomo-ohtani@aist.go.jp, k-fujimoto@aist.go.jp, hisao.itou@aist.go.jp)

2. Dept. Earth and Planetary Sciences, Univ. Tokyo, Hongo, Bunkyo, Tokyo, 113-0033, Japan (Phone: +81-3-5841-4525, Fax: +81-3-5841-4569, E-mail: tanaka@eps.s.u-tokyo.ac.jp)

The mineralogy, fluid inclusions, and distribution of fault rocks of the Nojima fault were examined in the core recovered from a borehole drilled by the Geological Survey of Japan (GSJ) one year after the 1995 Kobe (Hyogo-ken Nanbu) earthquake (MJMA=7.2), southwest Japan. The borehole was drilled across a slipped portion of the fault to a depth of 746.7 m. Nearly continuous coring between 152.2 m and 746.7 m recovered granodiorite protolith, porphyry dikes and fault-related rocks. The fault zone was intersected at 426.2 m and is characterized by a greater intensity of brittle deformation and/or hydrothermal alteration than typical host granodiorite. The fault core consists of three types of fault gouge, and occurs at the depth range of 623.1 m to 625.3 m. The fault-normal thickness of the fault core and the fault zone is 0.3 m and > 46.5 m, respectively.

The rocks obtained from the borehole were divided into five types based on the intensities of deformation and alteration: host rock, weakly deformed and altered granodiorite, fault breccia, cataclasite, and fault gouge. Weakly deformed and altered granodiorite is distributed widely in the fault zone. Fault breccia appears mostly just above the fault core. Cataclasite is distributed mainly in a narrow zone in between the fault core and a smaller gouge zone encountered lower down from the borehole. Fault gouge in the fault core is divided into three types based on their color and textures. From their cross-cutting relationships and vein development, the lowest fault gouge in the fault core is judged to be newer than the other two. The fault rocks in the hanging wall (above the fault core) are deformed and altered more intensely than those in the footwall (below the fault core). Furthermore, the intensities of deformation and alteration increase progressively towards the fault core in the hanging wall, but not in the footwall. The difference in the fault rock distribution between the hanging wall and the footwall might be related to the offset of the Nojima Fault and/or the asymmetrical ground motion during earthquakes.

Three types of hydrothermal alteration are recorded by mineral assemblages and fluid inclusions. The first type is characterized by chloritization of mafic minerals at more than 200° C, and occurred prior to the fault activity during the intrusion and cooling of the granodiorite. The second type occurred during faulting, and is recorded by zeolite mineralization at less than 200° C. The third type is recorded by carbonate mineralization related to recent fluid flow. Although most of the second type alteration occurred prior to the third type, repeated mineralization is recorded by mutually cross-cutting relationships between zeolite and carbonate veins and between zeolite vein and carbonate-precipitated fault gouge. This may record repeated changes in fluid chemistry within the fault zone in connection with the seismic cycle. Although the Nojima fault slipped in the 1995 earthquake, ancient fault-related textures and mineral alteration are well preserved in the fault rocks.

S4-11

Paleostress and Slip Distribution in Large-Displacement Faults of the San Andreas System, California

F. M. Chester¹, J. S. Chester¹, J. E. Wilson^{1,2}, D. L. Kirschner³

1. Center for Tectonophysics, Dept. Geol. & Geop., Texas A&M Univ., College Station, TX 77843, USA

2. Now at: Department of Earth and Environmental Science, New Mexico Tech., Socorro, NM, USA.

3. Department of Earth & Atmospheric Sciences, Saint Louis University, St. Louis, MO, USA.

Deep drilling across active faults provides unique observations of the structure, petrology, fluid chemistry, distribution of slip, and stress states around active faults that are necessary to better understand the processes responsible for fault-strength reduction over long (geologic) and short (earthquake) time periods. Unfortunately, core recovery and down-hole measurements only sample a relatively small portion of the fault zone over short time periods. We need to continue to develop strategies to better characterize the spatial and temporal variation in fault zone properties and to understand the significance of heterogeneity to fault mechanics. Field study of exhumed faults may provide information useful to designing drilling programs and data analysis.

We have characterized the distribution and fabric of fault-rocks in exhumed faults to test current hypotheses of the origin of damage in fault zones and the processes of seismic slip. Detailed mapping of the Punchbowl and San Gabriel faults reveals that the structure of ultracataclasite layers records extreme localization of displacement to slip-surfaces. These surfaces may exist over many earthquake cycles and accommodate kilometers of displacement. Extreme localization is consistent with long-term fault weakness, and with several dynamic weakening mechanisms hypothesized for earthquake slip. The damaged host-rock adjacent to zones of localized slip display relatively small magnitude of strain, and thus fabric elements in the damage zone may be used to infer paleostress directions. The microfracture fabric of samples from 0.075 m to 1 km from the ultracataclasite layer of the Punchbowl fault define several distinct fabric domains. Fault-related microfracture damage occurs up to 100 m from the ultracataclasite. Healed (older) and open (younger) microfracture fabrics provide a record of paleostress at different periods of fault activity. Microfracture orientations in the outermost damage zone may provide the best record of stress directions during fault formation and subsequent fault weakening. A distinct microfracture set that is perpendicular to the slip direction of the fault is present throughout the damage zone. This fabric implies that the average orientation of the maximum principal compressive stress within the damage zone was nearly normal to the fault surface, and is most consistent with local damage accumulation from stress cycling associated with slip on a geometrically irregular, relatively weak fault surface. An additional microfracture set that is only present adjacent to the ultracataclasite layer may reflect paleostress associated with earthquake slip.

S4-12

Geological and geophysical logging results of shallow drilling penetrating into Chelungpu fault zone, ROC, Taiwan

H. Tanaka¹, Arito Sakaguchi², Kotaro Ujiie², C. Y. Wang³, W. M. Chen³, Hisao Ito⁴ and Masataka Ando⁵

1. Department of Earth Science, University of Tokyo, Tokyo, 103-1133, Japan (Phone: +81-3-5841-4525, Fax: +81-3-5841-4569, E-mail: tanaka@eps.s.u-tokyo.ac.jp)

2. IFREE / Japan Marine Science and Technology Center, Yokosuka, 237-0061, Japan (Phone: +81-468-67-9787, Fax: +81-468-67-9775, E-mail: arito@jamstec.go.jp, ujiiek@jamstec.go.jp)

3. Institute of Geophysics, National Central University, Chung-Li 32054, Taiwan (Phone: +81-886-3-426-2305, Fax: +81-886-3-422-2044, E-mail: wangcy@cc.ncu.edu.tw, wmchen@cc.ncu.edu.tw)

4. Geological Survey of Japan, AIST, Tsukuba, 305-8567, Japan (Phone: +81-298-61-3757, Fax: +81-298-61-3682, E-mail: hisao.itou@aist.go.jp)

5. Research Center for Seismology and Volcanology, Nagoya University, Nagoya, 464-8602, Japan (Phone: +81-52-789-5390, Fax: +81-52-789-3047, E-mail: ando@seis.nagoya-u.ac.jp)

The Chelungpu fault is a reverse fault with left lateral component dipping moderate to the east, which was activated in 21, September, 1999 Chichi earthquake ($M_w = 7.6$), with maximum vertical and lateral offsets of 5.6 m and 9.8 m. Characteristics of earthquake and related phenomena are contrasting between northern and southern regions along the Chelungpu fault. In the northern region, (1) larger displacements (4 to 9 m), (2) low frequency seismic waves with higher velocity of slip surface, and (3) less disasters except for the northern most area were observed in contrary to the southern region. The drilling penetrating into the Chelungpu fault was thus conducted at northern (Fengyan) and southern (Nantou) regions, and successfully completed in March 2001. Meso- and microstructural examinations as well as measurements of static/dynamic physical properties have been conducted for each drilled core. The analyses are on the way half and producing interesting results, including (1) possible rupture zones activated at 1999 earthquake can be listed up by combining geological, geophysical logging and reflection seismic data, which are the fracture zones of 225 m and 330 m depths in the core from northern well and 177 m and 180 m fracture zones from southern well, (2) water contents of the core of the 225 m fracture zone in the northern well attains up to 45 vol.%, (3) fault rocks is mainly composed of random fabric fault breccia in the northern rupture zones at depth, whereas in the southern well, foliated fault breccia is dominated associated with ultracataclasite and pseudotachylite in the centralized layer along the 177 m fracture zone. (4) Some temperature rises are detected at 330 m fracture zone in the northern well and 180 m fracture zone in the southern well by temperature logging that was performed after drilling.

P1-1

A Preliminary Report on Continuous 24-bit 25-Hz Strain Monitoring on Seismogenic Faults of $M \sim 3$ in Deep Gold Mines

H. Ogasawara¹, H. Ishii², S. Moriyama¹, Y. Iio³, SA Group⁴

1. Fac. Sci. Engr, Ritsumeikan Univ., Kuwatsu, 525-8577, Japan (Phone: +81-77-561-2660, Fax: +81-77-561-2661, E-mail: ogasawar@se.ritsumei.ac.jp)

2. Tono Geoscience Center, JNC Devel. Inst., 959-31, Jorinji, Izumi, Tokishi, Gifu, 509-5102 Japan (Phone: +81-572-67-3105, Fax: +81-572-67-3108, E-mail: ishii@tries.gr.jp)

3. Earthquake Research Institute, Univ. Tokyo, Yayoi, Bunkyo, Tokyo, 113-0033, Japan (Phone: +81-3-5841-5787, Fax: +81-3-5689-7234, E-mail: iio@eri.u-tokyo.ac.jp)

4. The Research Group for Semi-controlled Earthquake Generation Experiments in South African Deep Gold Mines. Except for the above authors, the group consists of colleagues from Japanese universities (Tokyo, Nagoya, Kyoto, Kobe Gakuin), Geological Survey, Japan, ISS International, Welkom and Wits Univ., Johannesburg.

In South African deep gold mines, earthquakes are induced in proximate front of excavation. So, we can *a priori* install instruments to monitor seismogenic process. To monitor strain buildup larger than 10^{-4} , strain transient as subtle as 10^{-8} and dynamic response of remote triggering faster than several Hz on seismogenic fault, we installed Ishii's borehole multi-component strain meters several m from the faults where $M \sim 3$ events are expected, associated with mining. The strain meter accommodates normal and shear strains on seismogenic faults larger than 10^{-4} continuously with a 24-bit, 25-Hz resolution. In addition, unclipped 120-dB seismic data of these mines are available to discuss stress change. We have had two experimental fields: ~ 2400 m deep in Bambanani mine since 1998 and ~ 2850 m deep in Mponeng mine, Carletonville since 2001. In the poster, we introduce the details about these two experimental fields. Secular strain buildup of $\sim 5 \times 10^{-5}$ / 6 months is successfully recorded, with the earth tide clearly recorded. Associated with a few $M2$ events at distances of a few hundred meters, significant postseismic drifts are observed. However, significant precursory strain transient has not yet observed because our strain meters are still located outside seismogenic area, being farther than the dilatometers that McGarr et al attempted without success decades ago. In Bambanani mine, the mining in the proximity of the strain meter begins at the end of 2001. In Mponeng mine, the strain meter was installed in November 2001. We hope we can obtain the newest data by the workshop to show interesting phenomena.

ACKNOWLEDGEMENTS: We thank Bambanani mine and Mponeng mine for the permission of our attempt and use of mine's seismic data. These mines also covered the cost of drilling and cabling and helped installation. Tony Wald, Artur Cichowicz and Patrick Lenegan helped coordination and installation. Ishii supplied the strainmeters. He and Ritsumeikan University fund this work.

P1-2

A Key Point of Potential Future Hypocenter Fault Studies in Deep Mines: A Report on a Scientific Tour of RaSim5

H. Ogasawara

Fac. Sci. Engr, Ritsumeikan Univ., Kusatsu, 525-8577, Japan (Phone:+81-77-561-2660, Fax: +81-77-561-2661, E-mail: ogasawar@se.ritsumei.ac.jp)

In the last September, the 5th International Symposium of Rockburst and Seismicity in Mines (RaSim5) was held in South Africa. As a participant of one of scientific tours of the symposium, I visited the hypocenter of an M 4.2 earthquake at No. 5 shaft fault in African Rainbow Minerals Mine. Ze'ev Reches and his colleagues carried out excellent post-seismic survey of the fault movements for the event, who guided the tour together with Gerrie van Aswegen. Some of their works will be probably talked in the present workshop.

The purpose of the poster is to discuss a key point of potential future study in such fields, based on our experience of the multidisciplinary monitoring in South African deep gold mines and my report of the tour with photos.

Fracture pattern is complicated, as documented by e.g. Ortlepp (1997). However, it was interesting to see the contrast in damage regardless of similar magnitude of fault slip, probably suggesting difference in slip manner. We should compare *in situ* source observation in detail with what we can learn from seismograms or strain recordings. The Research Group for Semi-Controlled Earthquake Generation Experiments in South African Gold mines installed only a single strain meter on a fault. However, if an event takes place where we install Ishii's borehole strain meter and we can *in situ* pre-/post-seismically observe what is going on, we will be able to learn more about the meaning of the strain recordings. It was my strong impression that, if possible, we have to drill multiple holes with redundant array of Ishii's strain meters and accelerometers to cover an entire seismogenic fault, in conjunction with pre- and post-seismic *in situ* surveys of fault, fault movement and damage. Such attempts in deep mines should be strongly encouraged.

Interestingly, I also found that South African gold mine is a field where we can collect samples of pseudotachylite though it is, of course, not associated with the recent M4.2 event. In front of my poster, I will also present a sample that I was given as a souvenir of the tour.

P1-3

Deep Structure of the Nojima Fault Estimated by a Borehole Observation of Trapped-Waves

Takashi Mizuno and Kin`ya Nishigami

(DPRI, Kyoto University)

(E-mail: tmizuno@rcep.dpri.kyoto-u.ac.jp, Web: <http://www.rcep.dpri.kyoto-u.ac.jp/~tmizuno/>)

Analyses of the fault-zone trapped-wave are expected to be one of the effective approaches for imaging a deep fault structure. In this study, we used high signal-to-noise ratio seismograms recorded in the DPRI, 1800-m-deep borehole at Toshima, southern end of the Nojima Fault. We analyzed 525 natural and induced earthquakes that occurred from January 1, 1999 to May 31, 2000. Natural events were distributed along the Nojima and Rokko fault system (about 40-km-long) at depths ranging from 3 to 15 km. Induced earthquakes were located near the Toshima borehole site.

To detect the trapped-waves with Love wave type, we analyzed dispersion, polarization, and amplitude spectrum of S-wave part in each seismogram. To obtain the dispersion curve of the group velocity, we calculated envelopes for several frequency bands. In this study, we calculated synthetic dispersion curve for trapped-waves propagating along a vertical low velocity layer sandwiched between two half-spaces. We assumed the S-wave velocity of the surrounding rock to be 3.5 km/s in this study. The S-wave velocity and the width of the low velocity fault-zone were estimated by comparing observed and synthetic dispersion curves. We obtained the following results.

- (1) We found 84 seismograms (16 percent) whose S-wave parts contain dispersive wave trains. This result suggests that, at least, 84 percent earthquakes are located outside of the low velocity fault zone.
- (2) We found 11 seismograms whose S-wave parts contain dispersive wave trains with fault parallel polarization. We divided these 11 earthquakes into two groups, group 1 and group 2. Group 1 consists of four induced earthquakes and one natural event located north to north - east of the borehole at hypocentral distances of 2 to 3 km. Group 2 consists of 6 natural events located north-east of the borehole at hypocentral distances of 6 to 10 km. However, we cannot observe trapped-waves in 32 induced earthquakes. This result suggests that induced earthquakes were located not only in the fault zone but also outside of the fault zone.
- (3) Dominant frequency of the trapped-waves were 10 Hz for group 2 and 30 Hz for group 1. We estimated that fault-zone trapped-waves of first higher mode were dominant at shorter hypocentral distances and fundamental mode dominated at larger hypocentral distances.
- (4) We estimated the S-wave velocity and the width of the low-velocity fault-zone as 2.5 km/s and 130 m. Tanaka et al. (2001) discussed the fault zone structure by petrological method, and showed that the width of the damage zone of the Nojima fault was about 100 m. The seismological fault zone may consist with the damage zone.

P1-4

Permeability evaluation at the GSJ Hirabayashi borehole in the Nojima fault from VSP experiment and sonic logging

Tsutomu Kiguchi, Hisao Ito and Yasuto Kuwahara

Geological Survey of Japan, AIST, Central 7, Higashi 1-1-1, Tsukuba, Ibaraki 305-8567 Japan

E-mail : kiguchi.t@aist.go.jp

We analyzed hydrophone vertical seismic profiling (VSP) experiment data and sonic logging (DSI : Dipole Shear Sonic Imager) from GSJ Hirabayashi borehole in order to estimate the permeability of the Nojima fault. The borehole was drilled to penetrate the Nojima fault, which was active in the 1995 Hyogo-ken Nanbu earthquake.

The analysis of hydrophone VSP data is based on a model by which tube waves are generated when incident P-waves compress the permeable fractures (or permeable zones) intersecting the borehole and fluid in the fracture is injected into the borehole. Permeable fractures (or permeable zones) are detected at the depths of tube wave generation, and permeability is calculated from the amplitude ratio of tube wave to incident P-wave. Distinct tube waves were generated at depths of the fault zone that are characterized by altered and deformed granodiorite with a fault gouge, suggesting that permeable fractures and permeable zones exist in the fault zone.

We also evaluated the permeability structure in the fault zone from acoustic waveforms obtained by sonic logging. The analysis is based on the fact the Stoneley wave, which is a type of a boundary wave in a borehole, is sensitive to fractures and formation pore fluid mobility. Stoneley wave reflections, Stoneley attenuation and slowness increase were observed at several depths of the fault zone. These effects on Stoneley waves suggest that permeable zones exist in the fault zone. The regions of permeable zones detected by the Stoneley wave analysis correspond to the depths of tube wave generation obtained from the VSP data.

We estimated the permeability of the narrow zone of the fault gouge (623.3-625.1 m) in the coaxial zone by means of comparing the ratios of the tube wave to P-wave amplitudes obtained from the VSP data with the theoretical curves. The width of this permeable zone, which is a necessary parameter for quantitative permeability analysis, is determined to be 1.0 m from the Stoneley wave attenuation. The estimated value of permeability of the fault gouge is remarkably high to be about 40 darcy.

As a results of analysis of hydrophone VSP data and sonic logging, we have conclude that only the specific regions of the fault zone, such as fault gouge and cataclasite, are permeable. It is important that only restricted parts of the fault zone are permeable, which suggests that whole fault zone was not uniformly damaged in the 1995 Hyogo-ken Nanbu earthquake and only the limited narrow zone was damaged.

P1-5

Nankai Trough Seismogenic Zone Drilling and Observatory

Nankai Trough Seismogenic Zone Research Group
(presented by R. Hino¹)

1. Research Center for Prediction of Earthquakes and Volcanic Eruptions, Graduate School of Science, Tohoku University, Sendai, 980-8578, Japan (Phone: +81-225-1950, Fax: +81-22-264-3292, E-mail: hino@aob.geophys.tohoku.ac.jp)

Drilling and installation of a deep borehole observatory into a fault zone is one of the most powerful approaches to understand fault mechanics and physics of earthquake generation, and many scientific drilling projects have been made or are on-going all over the world. A subduction megathrust, where large interplate earthquakes occur frequently and regularly, is of course an important target of such borehole-oriented researches. We selected the Nankai subduction zone as the most suitable location to carry out the first riser drilling program of IODP because seismic images show clear drilling targets, the subduction zone is well characterized geophysically, and monitoring systems can be supported from the nearby Japanese Islands. A new riser drilling vessel, the flagship of IODP starting from 2006, has enough capability to penetrate to the shallowmost part of the Nankai seismogenic plate interfaces, supposed to be at ~ 6 km below seafloor of ~ 2.5 km water depth. Subduction megathrust systems present clear advantages in the analysis of seismogenesis because they are shallowly dipping, amenable to imaging and drilling, and can be sampled in multiple locations from the incoming plate to depths where earthquakes occur, in order to document evolution of fault properties. Taking this advantage into account, we have proposed to drill down to the Nankai seismogenic zone for studying what control seismic and aseismic nature of the plate interface. The program we proposed is composed of 1) a non-riser drilling at reference site, 2) riser drilling at shallow out-of-sequence-thrust or spray fault sites, 3) deep drilling to penetrate into the interplate boundary at the up-dip limit of the seismogenic zone, and 4) the installation of borehole observatories to monitor geophysical/geochemical properties in the course of megathrust earthquake cycle. Core samples and logging data obtained by these sites will enable us to understand what changes in material composition and in-situ properties of the fault zone are subject to the aseismic-seismic transition at the up-dip limit. Downhole seismic, geodetic, hydrologic, and electromagnetic observatories will not only depict how slip and deformation progress through the seismic cycle but also clarify detailed structure of the megathrust zone, which also affects frictional properties of the fault in macro scale.

P2-1

Multiple-Fault Rupture of the *M*7.1 Hector Mine, California, Earthquake from Fault-Zone Trapped Waves

Yong-Gang Li¹, John E. Vidale², Steven M. Day³, and David D. Oglesby⁴

1. Department of Earth Sciences, University of Southern California, Los Angeles, CA 90089, USA (Phone: 213-740-3556, Fax: 213-740-8801, E-mail: ygli@terra.usc.edu)

2. Department of Earth & Space Sciences, University of California at Los Angeles, Los Angeles, CA 90095, USA

3. Department of Geological Sciences, San Diego State University, San Diego, 92182, USA

4. Department of Earth Sciences, University of California at Riverside, Riverside, CA 92521, USA

We studied the complex multiple-faulting pattern of the 40-km-long rupture zone of the 1999 *M*7.1 Hector Mine earthquake with fault-zone trapped waves generated by near-surface explosions and aftershocks, and recorded by linear seismic arrays deployed across the surface rupture. The explosion excited trapped waves, with relatively large amplitudes at 3-5 Hz and a long duration of *S* coda waves, are similar to those observed for aftershocks, but have lower frequencies and travel more slowly. 3-D finite-difference simulations of fault-zone trapped waves indicate a 75 to 100-m-wide low-velocity and low-*Q* zone (waveguide) along the rupture surface on the Lavic Lake fault (LLF) in the Bullion Mountains. The *S* velocity within the waveguide varies from 1.0 to 2.5 km/s at depths of 0-10 km, reduced by ~40-50% from the wall-rock velocity, and *Q* is ~10-60. The pattern of aftershocks for which we observed trapped waves shows that this low-velocity waveguide has two branches in the northern and southern portions of the rupture zone, indicating a multiple-fault rupture at seismogenic depth. North of the Bullion Mountains, although only the rupture segment on the northwest LLF broke to the surface, a rupture segment on a buried fault also extended ~15 km in the more northerly direction from the mainshock epicenter. To south, the rupture on the LLF intersected the Bullion fault (BF) and bifurcated. The rupture on the south LLF extended ~10 km from the intersection and diminished while there was minor rupture on the southeast BF, which dips to northeast and disconnects from the LLF at depth. Thus, the analysis of fault-zone trapped waves helps delineate a more complex set of rupture planes than the surface breakage, in accord with the complex pattern of aftershock distribution [*Hauksson et al.*, 2001] and geodetic evidence that the Hector Mine event involved several faults which may also rupture individually [*Ji et al.*, 2001; *Simons et al.*, 2001]. Our simulations of dynamic rupture using a finite-element code show that generic models are able to produce the general features of the northern part of the rupture, including slips on sub-parallel fault segments [*Oglesby et al.*, 2001]. The models indicate that such a faulting pattern is physically plausible and consistent with observations. Repeat experiments using explosions at the Hector Mine rupture zone show that shear velocities within the rupture zone increased by 0.7-1.0% from wall-rock velocities between 2000 and 2001, indicating the Hector Mine rupture zone has been healing by strengthening after mainshock most likely due to the closure of cracks that opened during the 1999 earthquake.

P2-2

Stress Drop of Off-Fault aftershocks of the 1995 Hyogo-ken Nanbu, Japan earthquake

Sihua ZHENG

(Center for Analysis and Prediction, China Seismological Bureau, China)

Shigeki HORIUCHI

(National Research Institute for Earth Science and Disaster Prevention, Japan)

Masataka ANDO

(Research Center for Seismology and Volcanology, Nagoya University, Japan)

Abstract

Following the Hyogo-ken Nanbu, Japan earthquake of 17 January 1995 ($M=7.2$), a prompt increase in the seismicity was observed in the wide area of surrounding Kobe. The cumulative number of earthquakes shows a dramatic rate increase of seismicity within Inagawa, Tamba and Yamasaki regions following the Hyogo-ken Nanbu earthquake. Particularly, within the Inagawa region, the seismicity is rather low in the days preceding the Hyogo-ken Nanbu earthquake, however the seismicity increases rapidly immediately after the Hyogo-ken Nanbu earthquake. This earthquake swarm, so-called off-fault aftershocks (Das and Scholz, 1981), started from ten hours after the Hyogo-ken Nanbu earthquake and has been continued through June 1996.

The off-fault aftershock clusters or earthquake swarms after a large earthquake have been observed previously. Several investigations indicated that these aftershocks may be due to the increase of shear stress off the fault plane.

Seismic wave data recorded at the station ABU near the Inagawa region provided a good opportunity to systematically investigate the source parameters of these triggering off-fault aftershocks. In addition before the 1995 Hyogo-ken Nanbu earthquake several earthquake swarms have occurred in the Inagawa region. The seismic data recorded at the same station enable to compare the source parameters of the events before and after the Hyogo-ken Nanbu.

Single-station data obtained at station ABU are used in this study. We analyze 279 events that were recorded for the period from January 1994 to May 1995. The magnitudes of these events are ranging from 0.5 (31 January 1995) to 3.3 (30 March 1995), and the depths are ranging from 0 to 16.9 km.

For these relatively small earthquakes, we assume a circular fault source model and estimate the spectrum parameters, as well as seismic moment and stress drop.

The results do not indicate that the stress drops of these off-fault aftershocks were particularly higher than those of the earthquake swarms in the same area before Hyogo-ken Nanbu earthquake.

This result may suggest that before the Hyogo-ken Nanbu earthquake the rocks in the area were at a pre-stress level very close to that at which slip occurs, the small increase in the static stress caused by the Hyogo-ken Nanbu earthquake triggered these off-fault aftershocks, but did not have significant influence on the stress drop of these triggered off-fault aftershocks.

P2-3

Exploration of subsurface structure across the Atera fault zone

T. Tanaka¹, H. Aoki¹, M. Okubo¹, M. Onishi², and K. Oshita³

1. Tono Res. Inst. of Earthq. Sci., Yamanouchi1-63, 509-6132, Japan (Phone: +81-572-67-3107, Fax: +81-572-67-3108, E-mail: tanaka@tries.gr.jp, aoki@tries.gr.jp, okubo@tries.gr.jp)
2. JGI Inc., Meikei Bldg, 1-5-21, 112-0012, Japan (E-mail: oshita-kenichi@oyonet.oyo.co.jp)
3. OYO Corp., Nakashima102, Seko, 463-8541, Japan (E-mail: onishi@jgi.co.jp)

Introduction

We carried out seismic and gravity prospecting in Kashimo village (here in after, Northern area) and Sakashita town (here in after, Southern area) across the Atera fault zone (Fig. 1). In the seismic prospecting (Line-1~3&A), a general vibroseis method was used and horizontal tomography analysis (Northern area only) was tried, too. In the gravity prospecting, a microgravity method was used (one digit high-precise than what we call "1 mgal-aimed" survey). In the Northern area, a graven structure has been estimated geologically among a few parallel faults. We aimed to reveal the precise three-dimensional structure of the graven or fracture zone, and detect the structure which related to the tectonics of Central Honshu Island. In the Southern area, the Ueno basalt (or Ueno volcano) widely covers the southwest side of the Atera fault and must have been concerned in the faulting. We aimed to investigate the relationship between basalt distribution and fault.

Results

•Southern area

The deepest event is confirmed about 20km depth. In the southwest part of Line-1, a series of reflection events, which slightly tilts in the southwest direction, exits from 4 to 8 km depth. Near the center of Line-1 (about 600m interval of the fault crossing site), some reflection patterns peculiar to fault are found. A non-reflective zone is correspondent to the Ueno basalt layer from the comparison with a geological map. The basalt is high density (probably more than Naegi-Agematu granite), and the interpretation of the gravity anomaly is difficult. In future, referring to the drilling data of NIED, we want to try three-dimensional structure analyses.

•Northern area

The deepest event is confirmed about 11km depth. A reflection event obviously concerning the fault activity is found until 1.5km depth. Among the two or three parallel faults, the collapse structure is seen and the velocity structure changes suddenly. The low velocity zone detected by the horizontal tomography between Line-2 and Line-3 agrees with this collapse structure. Moreover, low gravity zone also corresponds the same position.

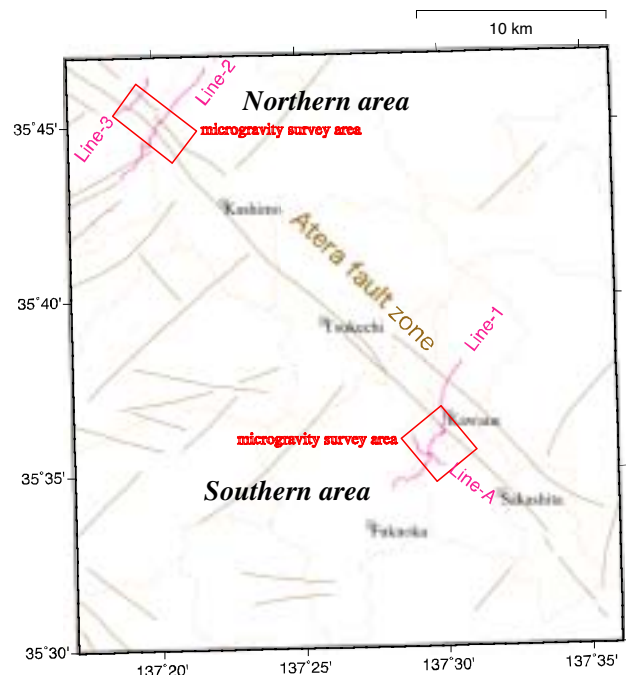


Fig. 1

The authors wish to express their grateful thanks to Dr. Ryuji Ikeda and Dr. Kentaro Omura, who provided the information of "Atera active fault zone drilling project" by NIED.

P2-4

Ground-Penetrating Radar Image of the 1999 Rupture in Chi-Chi Earthquake, Taiwan

T. Miyata¹, Y. Tanaka², R. Kayen², S. Takada³ and B.J. Shih⁴

1. Dept. of Earth & Planetary Sci., Fac. Sci., Kobe Univ., Nada-ku, Kobe, 657-8501, Japan (Phone: +81-78-803-5729, Fax: +81-78-803-5784, Email: miyata@kobe-u.ac.jp)
2. RCUSS, Kobe Univ., Nada-ku, Kobe, 657-8501, Japan (Phone: +81-78-803-6058, 6380, Fax: +81-78-803-6394, Email: ytgeotec@kobe-u.ac.jp, rkayen@usgs.gov)
3. Dept. Architecture & Civil Engin., Fac. Engin., Kobe Univ., Nada-ku, Kobe, 657-8501, Japan (Phone: +81-78-803-6037, Fax: +81-78-881-2812, Email: takada@kobe-u.ac.jp)
4. Dept. Civil Engin., Nat'l Taipei Univ. of Technology, Taipei, 10643, Taiwan (Phone: +886-2-2771-2171, Fax: +886-2-2781-4518, Email: bjshih@ntut.edu.tw)

The 1999 Chi-Chi (Mw7.6) earthquake produced 100 kilometers of surface ruptures along the Chelungpu fault (e.g., Chang *et al.*, 1998). This earthquake caused strong damages to the structures and infrastructures all along the rupture. We investigated the 1999 rupture of fault segments II and III (e.g., Rubin *et al.*, 2001) at eight selected sites using a GSSI ground-penetrating radar (GPR) unit and 100 MHz and 35 MHz antennas, in order to clarify the subsurface fault structures. Each GPR survey line across the surface rupture is 150- 300 m long. We have surveyed twice in July and again in December of 2001

We obtained the following interesting results: (1) Detection of an anomalous reflector was found all along the GPR survey lines across the 1999 rupture. The anomaly is characterized by discontinuity (fault) with monoclinical flexure (fold) of the reflected signal on the GPR profile. (2) We have clear GPR imagery showing a discontinuity with an eastward inclination of low angle at two sites (Takou and Tsanton). (3) The monoclinical flexure was formed in the hanging wall on the GPR profile at Fungyun. This flexure is consistent with the surface flexure of an asphalt road. The width of the flexure is in the range of 20-30 m. We can estimate a vertical offset of 2-8 m from the flexure.

These results suggest that the surface fault of the Chi-Chi earthquake dips clearly eastward, and that the surface flexure and the subsurface flexure on the hanging wall is thought to have been produced by a vertical component of the surface fault.

Judging from the GPR results and observation, we conclude that the discontinuity with flexural structures was caused by reverse faulting on the Chelungpu fault. Secondly, the flexure zone of the hanging wall is consistent with the 20-30m-wide rupture zone that had severe damages. We found GPR to be very useful in understanding the subsurface structures of a fault.

P2-5

Aftershocks triggered by released waters due to strong excitation of dynamic stress in the 1999 Chi-Chi earthquake of Taiwan

C.H. Lin^{1,2} and M. Ando²

1. Institute of Earth Sciences, Academia Sinica, P.O. Box 1-55, Nankang, Taipei, Taiwan (lin@earth.sinica.edu.tw).
2. Research Center for Seismology and Volcanology, Nagoya University, Furo, Chikusa, Nagoya City, 464-8602, Japan (Phone: +81-52-789-3036, Fax: +81-52-789-3047, E-mail: lin@seis.nagoya-u.ac.jp, ando@seis.nagoya-u.ac.jp).

A large number of aftershocks followed by the 1999 Taiwan Chi-Chi earthquake ($M_L=7.3$) provide some valuable observations to discuss characteristics of earthquake triggering along major faults. In particular, one group of aftershocks in the Central Range of Taiwan shows some anomalous characteristics. First of all, those aftershocks were surprisingly taken place in a very low-seismicity area of the Central Range, where the crust is often considered as a ductile-behavior due to higher temperature. Second, those aftershocks were clustered along a major geological boundary between the Slate belt and the Tananao Schist. Third, most of focal mechanisms are shown by normal faulting, which may not be usual in the strong convergence zone of Taiwan. Forth, the aftershock sequence didn't follow the Omori's law and instead a constant rate (~ 15 events/day) of aftershock occurrence was found during the first 6 months. Finally, the lower bound of focal depths gradually deceased with time at the rate of 30 m/day. Those phenomenons are hardly explained by general mechanisms such as changes of static stress, stress relaxation or directly dynamic stress. Alternatively, we suggest that water might play a large role on the aftershock triggering in the Central Range. Some water that had been accompanied with the subducted crust might be released after the strong shaking due to the dynamic stress generated by significantly seismic waves of the Chi-Chi earthquake. Those released water gradually ascent into the fault zone and generate clustered aftershocks.

P2-6

Magnetotelluric imaging of western part of the North Anatolian Fault Zone

S.B. Tank¹, Y. Honkura¹, Y. Ogawa², N. Oshiman², M.K.Tuncer⁴, C.Celik⁴, E.Tolak⁴

Department of Earth and Planetary Sciences, Tokyo Institute of Technology¹

Volcanic Fluid Research Center, Tokyo Institute of Technology, Tokyo, Japan²

Disaster Prevention Research Institute, Kyoto University³

Kandilli Obs. & E.R.I., Bogazici University⁴

(email: tank@geo.titech.ac.jp)

Abstract

Magnetotelluric (MT) surveys were carried out to investigate the deep resistivity structure in the western part of the North Anatolian Fault Zone (NAFZ), which was subject to a major rapture during the 17th August 1999, Izmit Earthquake. The geology of the study area is very complex since it is positioned between the two branches of the North Anatolian Fault. MT is preferred as a method for investigating the crustal structure of the fault zone, because it is an efficient method for detecting the presence of fluid in a media by monitoring the resistivity. Recent observations state that there is high correlation between the earthquakes and fluids.

Two-dimensional inversions were performed in four profiles by using the code developed by Ogawa and Uchida (1996). The frequency range for the inversions is between 240 Hz and 0.0005 Hz, which is enough to resolve upper-crust structures. The results show that the area is getting more conductive approaching west. The aftershocks tend to occur on the highly resistive areas around the mainshock hypocenter. On the western profiles, on the other hand, aftershocks are occurring in relatively conductive areas. This property of the fault may be related to the heterogeneity of the fault. Here, in this poster presentation we are showing two-dimensional inversion models of two profiles.

P2-7

Earthquake Scaling Down to M=0.9 Observed at the Western Nagano Deep Borehole, Central Japan.

A.L. Stork, K. Imanishi and H. Ito.

Institute of Geoscience, Central 7 AIST, Tsukuba, Ibaraki 305-8567

(Phone: +81-298-61-3757, Fax: +81-298-61-3682, Email: anna.stork@aist.go.jp)

The scaling of earthquake source parameters for small earthquakes has been the subject of much debate and is still unresolved. In this work the phenomenon has been investigated using data recorded at the borehole in western Nagano, central Japan. Recordings of shallow, nearby earthquakes by the three component seismometer, situated at a depth of 800m, show less attenuation and higher frequency components of the seismic waves than surface recordings. Therefore a more accurate investigation into the source parameters is possible. Waveform analysis was conducted in the frequency domain for events with magnitudes between 0.9 and 3.5. The objective was to determine the scaling relationships between stress, seismic moment and radiated seismic energy. The spectra were fitted to an \mathcal{O}^2 source model (Aki, 1967) to establish the corner frequency and quality factor, hence enabling the determination of source parameters.

So far, this investigation has shown that there is an almost constant stress drop with seismic moment. Almost all the earthquakes have stress drops between 0.01MPa and 10MPa with no discernible dependence of stress on seismic moment and no minimum source radius. The apparent stress decreases with the radiated seismic energy. The fall off in apparent stress with energy appears to occur below seismic moments of around 10^{11} Nm. This is the case even when the energy is corrected for the miscalculation due to finite bandwidth recording (Ide and Beroza, 2001). This result is in agreement with the conclusions of Abercrombie (1995) and Prejean and Ellsworth (2001). However these events are also mainly the events with hypocentral distances greater than 10km. The stress drop ($\Delta\sigma$) and apparent stress (σ_a) have a nearly constant relationship with $\sigma_a \approx 0.1 \Delta\sigma$. The stress drop and apparent stress both seem to fall off with hypocentral distance for events occurring further than 10km away giving results of smaller radiated seismic energies and smaller seismic moments.

These results indicate that the observed relationship between apparent stress and seismic moment is a consequence of the inclusion of data with hypocentral distances larger than 10km. Therefore I suggest that it may be necessary to consider path effects in this region, even for relatively clean borehole recordings, unless the hypocentral distances are very small. Studies conducted on data from other areas may also need to include such effects to obtain more accurate results. To determine the actual relationship between apparent stress and seismic moment it will be necessary to study more small earthquakes with hypocentres within 10km of the borehole.

Source parameters of small earthquakes estimated from an inversion method using stopping phases

K. Imanishi¹, M. Takeo², T. Matsuzawa²,
H. Ito¹, Y. Kuwahara¹, Y. Iio², S. Sekiguchi³, S. Horiuchi³ and S. Ohmi⁴
1. GSJ/AIST 2. ERI 3. NEID 4. DPRI
e-mail: imani@ni.aist.go.jp

The source parameters, most importantly the rupture velocity, of small earthquakes have been estimated by analyzing seismograms recorded by the dense seismic networks operated in the aftershock area of the 1984 western Nagano earthquake, central Japan. An inversion method using stopping phases (Imanishi and Takeo, 2001) was applied to these data. The outline of the method is as follows. We assume that rupture begins at one focus of an ellipse fault and spreads circularly with a constant rupture velocity, eventually terminating on the elliptical boundary. In this model, the difference of the arrival times between the two stopping phases is dependent on the average value of rupture velocity, the radius of major semi-axes of ellipse and its ellipticity. These parameters are estimated by a nonlinear least-square inversion method. To detect the stopping phases on seismograms, we use the relation of Hilbert transformation between the two stopping phases. Since we need high frequency components to identify the stopping phases, we used seismograms recorded by 800m deep borehole station in the detection of the stopping phases. We also used surface recordings to determine the differential time between the direct S wave and the peak of displacement pulse.

We analyzed earthquakes ranging in size from $M_w 1.0$ to $M_w 2.5$ which were observed at relatively short epicentral distances (mostly less than 5 km). Static stress drops range from approximately 0.1 to 10 MPa, where these static stress drops do not vary with seismic moment. The aspect ratio of fault geometry is greater than 0.8, suggesting that the assumption of circular crack model for small earthquakes is valid as a first order approximation. It should be noted that the average rupture velocities decrease with decreasing seismic moment.

It has been the subject of considerable controversy whether the dynamics of small and large earthquakes is different or not. This difference is reflected in the observed relation between radiated seismic energy and seismic moment. The observation shows that the seismic energy radiated from a unit fault area per unit slip for small earthquakes is 10 to 100 times smaller than that of large earthquakes. Kanamori and Heaton (2000) interpret this observation as a difference in frictional behavior during rupture between small and large earthquakes, while Ide and Beroza (2001) suggest that this arise from underestimation of energy due to limited recording bandwidth. Sato and Hirasawa (1973) derived a relationship between rupture velocity, stress drop and seismic energy for a circular crack model, where the seismic energy is dependent on square of rupture velocity. Using their equation and source parameters estimated in this study, we calculated the seismic energy. Although these estimations are dependent on the assumption of the circular crack model, they are not related with recording bandwidth. Note the estimated seismic energy is well consistent with the observed trend. We suggest that the dependency of rupture velocity on seismic moment is a cause of small energy radiation for smaller earthquakes in addition to underestimation due to limited recording bandwidth. It is necessary to study the mechanism why the rupture velocity varies with earthquake size. One possible mechanism is that small earthquakes stop before reaching the terminal velocity resulting in small average values of rupture velocity.

P2-9

Seismic Observation at the Nojima Fault with a PC-based High-speed Waveform Acquisition System

Y. Kano, K. Nishigami, and T. Yanagidani

Disaster Prevention Research Institute, Kyoto University, Gokasho, Uji, Kyoto, 611-0011,
Japan (E-mail: kano@rcep.dpri.kyoto-u.ac.jp)

Borehole seismometers were installed by a university group in two wells at Toshima in the Nojima fault zone, Japan. A set of seismometers is installed at three depth levels in the 1800-m-deep well: three-component seismometer at the bottom (1800 m) and two vertical component seismometers (1700 m and 1600 m). Another three-component seismometer is installed at the bottom of an 800-m-deep well. Seismic observations by borehole seismometers reduce the noise and site effects caused by near-surface layers. To take advantage of the observations in the deep boreholes, we developed a high-speed waveform acquisition system based on a personal computer. The system records the multi-channel (up to 16 channels) seismic waveform continuously to the hard disks with a sampling rate of 10 kHz and 16-bit resolution.

The waveforms recorded by the high-speed sampling system are useful for source studies of microearthquakes such as initial phase identification and earthquake scaling. Hiramatsu et al. (2001) analyzed the 1800-m-deep borehole seismograms acquired by an event-triggering recorder with a sampling rate of 10 kHz, and showed that microearthquakes ($M -1.3 - 1.3$) had corner frequencies at about 50 - 200 Hz. Water injection experiments were carried out at the observation site in 1997 (Tadokoro et al., 2001) and 2000 (Nishigami, presentation in this workshop) and induced earthquakes were observed. The waveforms will also be effective to detect differences of mechanism between natural earthquakes and injection-induced earthquakes.

Can we detect much smaller events that have a corner frequency above a few hundred Hz? There have been some observations under a special condition that have recorded such tiny events, such as in a deep mine. Ultra-microearthquakes ($M \sim -1.5$) occur along the Nojima fault and the focal depth of these events is relatively shallow (~ 2 km). It is possible that much smaller fracture occur at the same depth. Since the distance between the source region and the sensor is very close, the combination of the borehole seismometers and the high-speed and continuous waveform acquisition system may make it possible to observe tiny events that have energy in the high frequencies. The analyses of small fractures will contribute to the discussion about earthquake scaling relations in the range where the size of events approaches laboratory experiments.

We carried out observations with the same high-speed waveform acquisition system at the Kamioka mine and the Yamasaki fault. The results from these observations will be also discussed.

P2-10

Effect of crustal heterogeneities on deformation and stress change associated with faulting

Jason Zhao¹ and R. D. Müller²

1. Institute for Frontier Research on Earth Evolution, Japan Marine Science & Technology Center, 2-15 Natsushima, Yokosuka 237-0061, Japan (E-mail: zhao@jamstec.go.jp)
2. School of Geosciences, University of Sydney, NSW 2006, Australia (E-mail: dietmar@es.usyd.edu.au)

Abstract

Heterogeneities associated with geological structures are fairly common in the crust/lithosphere, such as sediment basins, fault belts, and cratons etc. However, the effects of the geological structures on stress modelling are often ignored, and their contribution to the pattern of a local or regional stress field has not yet been fully investigated. In this study, we use the finite element method (FEM) to investigate the effect of crustal heterogeneities on the pattern of deformation and stress change generated by strike-slip faulting. We define a lateral heterogeneity as a geological body of a lower or higher elastic strength than surrounding rocks, and assume that a strike-slip fault exists within the modelled structure. The deformation and stress change caused by strike-slip faulting in the presence of heterogeneities in the crust are computed and compared with those produced by a homogeneous model.

We find that the effect of the heterogeneities on the magnitude and pattern of the calculated deformation and stresses is significant. Compared with a homogeneous model, a geological structure of higher strength in the upper crust modifies the pattern of the deformation and leads to a belt of stress concentration inside its boundary, whereas a lower-strength structure reduces the magnitude of deformation and tends to keep the stress concentration outside its boundary. The orientations of the maximum horizontal stresses are also affected significantly by the presence of the heterogeneities in the crust. The combined effects of two geological structures with different strength in the crust on calculated stress orientations are dramatic, and significant changes (>30 deg) are observed at the points inside the structures and near their boundaries.

Our results indicate that, in the presence of heterogeneities in the crust, the magnitude and pattern of the stresses associated with fault motion will no longer be controlled by the active fault itself, i.e., the standard patterns of the deformation and stress changes associated with the fault motion disappear as perturbed by the effect of heterogeneities in the crust. Therefore, the heterogeneities in the crust will serve to control the pattern of a local stress field.

P2-11

Critical Slip-Weakening Distance Measured from Near-Fault Strong Motion Data

E. Fukuyama¹, K. B. Olsen², and T. Mikumo³

1. National Research Institute for Earth Science and Disaster Prevention, Tsukuba, Ibaraki, 305-0006, Japan (Phone: +81-298-51-1611, Fax: +81-298-54-0629, E-mail: fuku@bosai.go.jp)
2. Institute for Crustal Studies, University of California, Santa Barbara, Santa Barbara, CA 93106-1100, USA (E-mail: kbolsen@crustal.ucsb.edu)
3. Institute de Geofisica, Universidad Nacional Autonoma de Mexico, Mexico 04510 DF, Mexico (E-mail: mikumo@ollin.igeofcu.unam.mx)

We propose a new technique to measure one of the most important frictional parameters from near-fault seismic waveforms in the context of the slip-weakening friction law. The strategy is as follows: (1) The critical slip-weakening distance (D_c) is measured at the breakdown stress drop time (T_b) which is defined as the moment when the stress drops to the frictional level. (2) At around T_b , the maximum sliprate occurs. (3) D_c is measured from the slip at peak sliprate time (T_p).

First, we show some examples using numerical simulations. These experiments suggest that if the rupture propagates smoothly, T_b and T_p are very close to each other. Therefore D_c can be estimated with enough accuracy. However, if the rupture process is heterogeneous, these two times are significantly different. At the edge of the fault, for example, this feature is significantly enhanced due to the existence of stopping phases. However, these features can be calibrated by dynamic rupture modeling based on the slip history obtained by the waveform inversion.

Then we explain the theoretical background of this method. Fukuyama and Madariaga[1998, BSSA] derived the integral equation for a planar fault. This equation tells us that stress is composed of two terms: one is proportional to the sliprate and the other is an integration term of past slip history convolved with the stress Green's function. Thus, if this integration term is reasonably smooth compared with the abrupt change of sliprate at T_b , T_p is close to T_b . On the other hand, if this integration term significantly varies around T_b , T_p is quite different from T_b and it becomes difficult to estimate D_c from the slip at T_p . Since the integration term consists of the past history of sliprate, abrupt change of rupture significantly affects this integration term.

Finally, we applied this technique to a real earthquake. We assume that, close to the fault trace, the strike-parallel component of the ground velocity is an approximation of the slip velocity on the fault. For halfspace models we find values of D_c with an error of less than about 20% at distances up to approximately 1/2 the fault length in the direction perpendicular to the fault trace. If rupture terminates below the surface, D_c is underestimated. During the 2000 western Tottori earthquake (M_w 6.6), two near-fault waveforms (GSH and TTRH02) were recorded. We used the fault-parallel component of these waveforms corrected for their instrument responses to obtain ground displacement and velocity waveforms. Then we measured the displacement at the peak ground velocity (T_p) and we estimated that D_c at GSH and TTRH02 are 40cm and 25cm, respectively.

It should be emphasized that this method enables us to estimate D_c independently of fracture energy, which is proportional to the product of critical breakdown strength drop ($\Delta\sigma_b$) and D_c . From the estimates of spatio-temporal slip history obtained by waveform inversion, there exists a strong trade-off between D_c and $\Delta\sigma_b$ and only fracture energy can be estimated stably [e.g. Guatteri and Spudich, 2000, BSSA].

P2-12

Field Surveys and Trenching Surveys of Surface Ruptures Associated with 2000 Tottori-ken Seibu Earthquake, Japan

Yuichiro Fusejima¹, Kiyohide Mizuno¹, Ryusuke Imura², Yuichi Sugiyama¹,
Toshikazu Yoshioka¹, Shishikura Masanobu¹, Taku Komatsubara¹, Michio Morino¹,
Hideki Kurosawa³, Toshinori Sasaki⁴

1. Geological Survey of Japan, AIST, Tsukuba, Ibaraki, 305-8567, Japan (Phone: +81-298-61-3693, Fax: +81-298-61-3803, E-mail: fusejima.y@aist.go.jp, mizuno@, sugiyama-y@, yoshioka-t@, m.shishikura@, komatsubara-t@, morino-michio@)
2. Earth and Environmental Sci., Kagoshima Univ., Kagoshima, 890-0065, Japan (Phone: +81-99-285-8144, Fax: +81-99-259-4720, E-mail: imura@sci.kagoshima-u.ac.jp)
3. Oyo-chishitsu Inc., Saitama, Saitama 336-0015, Japan (Phone: +81-48-882-5374, Fax: +81-48-886-9681, E-mail: kurosawa-hideki@oyonet.oyo.co.jp)
4. INA Inc., Bunkyo, Tokyo, 112-8668, Japan (Phone: +81-3-5261-5761, Fax: +81-3-3268-8285, E-mail: ts-sasak@ina-eng.co.jp)

We found fractures of the ground surface and destructions of artificial structures in the epicentral area of the 2000 Tottori-ken Seibu earthquake ($M_w = 6.7$, $M_{JMA} = 7.3$). These surface fractures and destructions were found along five NW-SE-trending lines in the area 6 km long and about 1 km wide. The surface fractures strike $N40\pm 25^\circ W$ and have left-lateral strike displacements of 10 cm or more. Several to 40 cm left-lateral displacements toward $N40\pm 25^\circ W$ were estimated from analysis of the destructions and deformations of artificial structures.

In continuing, at the end of the last year, the trenching surveys were carried out for the surface fractures at Ryokusui-en and Mt. Kamakura. On the walls and floors of these trenches, fracture zones in granite were observed. At Ryokusui-en the fracture zones are accompanied by planar fabrics and fault gouges. The fracture zones have contacted with dikes, and a part of them are fractured. At Mt. Kamakura the sediments, covering the fracture zones have been cut by large number of minor faults showing cumulative displacements. These structures can be understood as structures made by multiple left-lateral faulting.

P2-13

Stress Field near the Fault: 2000 Western Tottori Earthquake and 2001 Northern Hyogo Swarm

A. Kubo and E. Fukuyama

National Research Institute for Earth Science and Disaster Prevention, 3-1
Tennodai, Tsukuba, Ibaraki, 305-0006, Japan (Phone: +81-298-51-1611, Fax: +81-
298-54-0629, E-mail: kubo@bosai.go.jp, fuku@bosai.go.jp)

It is quite important to estimate the stress field near the pre-existing active faults. Here we employ the seismic moment tensor solutions of earthquakes that occurred along the fault and inverted the fault plane solutions for the stress tensor in the fault area. Two examples in southwest Japan are shown: The 2000 western Tottori earthquake (M_w 6.6), which is a typical shallow strike-slip earthquake, and the 2001 swarm activity at northern Hyogo Prefecture ($M_{wmax} = 5.2$), which is an anomalous seismic swarm activity. In both cases, seismic activity occurred at shallow depth ($< 10\text{km}$) and strike slip type focal mechanisms are dominant. Stress tensors are estimated using *FMSI* code developed by Gephart (e.g. 1990, Tectonics). Using P- and T- axis directions, stress tensors are estimated by a grid-search technique. The optimum stress tensor directions are found by measuring the L1 norm of the misfit and by changing stress ratio $R = (\hat{\sigma}_1 - \hat{\sigma}_2) / (\hat{\sigma}_1 - \hat{\sigma}_3)$.

For the Tottori case, horizontal maximum shear stress direction ($\hat{\sigma}_{Hmax}$) was N107°E, which is consistent with that estimated based on the fault trace alignments of relocated aftershocks (N110°E). This direction is considered to be the tectonic loading applied to the western Tottori earthquake area. No positive reasons were found to introduce spatial variation of stress field because we divided whole dataset into two (northern and southern areas) and the solutions did not show any distinct difference. Although we observed some trade-offs between $\hat{\sigma}_1$ direction and R due to the insufficient number of dataset, the similar solutions can be found with the average misfits of less than 5°.

For the northern Hyogo swarm activity, there are two trends of earthquake distribution, directing to the west and northwest. We divided the region into three (along each trace and the junction at southeast of the swarm region). We conducted four analyses of the stress tensor inversion including the whole dataset. Except for the junction, the results show the similar $\hat{\sigma}_{Hmax}$ directions (N120°E) and at the junction, $\hat{\sigma}_{Hmax}$ directed to N310°E. It means that $\hat{\sigma}_{Hmax}$ is consistent with the formation of conjugate strike-slip fault system corresponding to two trends. However, some abnormal stress field should exist at the junction of two fault traces.

P3-1

3D Finite-Difference Simulation of Fault Zone Waves
-Application to the Fault Zone Structure of the
Mozumi-Sukenobu Fault, Central Japan-

Yutaka Mamada(y-mamada@aist.go.jp), Yasuto Kuwahara, Hisao Ito
National Institute of Advanced Industrial Science and Technology / GSJ

Hiroshi Takenaka

Dept. Earth and Planet. Sci., Kyushu Univ.

A program was coded for performing a 3D numerical simulation of fault zone waves (fault zone head waves, direct P phases propagating within the low velocity zone (LVZ) and fault zone guided waves) to delineate detailed structure of fault zones. 3D numerical simulation is necessary to determine the velocity and Q structures and geometry of LVZ, when the fault structure is relatively complex or the free surface plays an important role in the waveforms with shallow sources.

We solved the equation of motion and stress-strain relation numerically in velocity-stress scheme by using the staggered-grid finite-difference method with a second-order approximation for the time derivative and fourth-order approximation for the spatial one. We used the free surface boundary condition for the earth's surface and absorbing boundary condition for the other model boundaries. In the present study, we focused on the high frequency fault zone waves up to 25 Hz originated from P phase with shallow source. We computed the synthetics for fitting the real seismograms recorded by a linear seismometer array at the depth of 300m across the Mozumi-Sukenobu fault with explosion sources which was performed by Ito *et al.* (2001).

We performed the simulations for the two cases of the source location: (i) in the center of the LVZ and (ii) 100m outside from the boundary of the LVZ so that they are accordance with the observation. The distances of source and linear array were 2km and 4 km. The synthetics for the case (i) contain the fault zone head waves at the first arrival, and excite the direct P phase with large amplitude and the wave trains following the direct phase especially in LVZ. On the other hand, the synthetics for the case (ii) hardly excite the direct P phase and the wave trains even in LVZ. These properties in the synthetics are consistent with those in the observed seismograms. This program is, thus, expected to be able to determine details of 3D complex fault zone structure, using relatively high frequency components.

P3-2

Displacement and stress Green's functions for a constant slip-rate on a quadrantal fault

Taku Tada¹, Eiichi Fukuyama² and Bunichiro Shibazaki³

1. Domestic Research Fellow, Japan Science and Technology Corporation. Contact address: NIED (see below; Phone: +81-298-60-2071, Fax: +81-298-60-2832, E-mail: kogutek@bosai.go.jp)
2. National Research Institute for Earth Science and Disaster Prevention (NIED), 3-1 Tennodai, Tsukuba, Ibaraki 305-0006, Japan (Phone: +81-298-51-1611, Fax: +81-298-54-0629, E-mail: fuku@bosai.go.jp)
3. Building Research Institute (BRI), 1 Tatehara, Tsukuba, Ibaraki 305-0802, Japan (Phone: +81-298-64-6757, Fax: +81-298-64-6777, E-mail: bshiba@kenken.go.jp)

In numerically calculating the elastodynamic field created by slip on a fault in a 3-D medium, the fault plane is often discretized into a set of small square elements, on each of which the slip is assumed to follow certain types of spatio-temporal variation profiles. One of the simplest and most popularly used categories of such assumption is that of the so-called "piecewise-constant slip-rate", which states that the slip-rate takes a constant value everywhere and at every moment within a given square element during a given discrete time window. The elastodynamic field in the medium can then be calculated by convolving the discretized spatio-temporal profile of the fault slip with the Green's functions corresponding to a constant slip-rate that takes place on each discrete fault element during each discrete time window.

In mathematical terms, a constant slip-rate profile on a discrete space-time element with a square shape can be synthesized by a superposition, with appropriate offsets in space and time and with appropriate sign reversals, of eight identical profiles of slip-rate that takes a constant value everywhere on a quadrantal part of the fault and at every moment after the onset of slip (e.g., Fukuyama and Madariaga, 1998). In the present study we have derived the rigorous expressions for the Green's functions which represent the displacement and stress response of an infinite, homogeneous and isotropic medium to a constant slip-rate on a quadrantal fault that continues perpetually after the slip onset. Our expressions for the stress Green's functions are a substantial simplification over those obtained by Aochi, Fukuyama and Matsu'ura (2000), and are expected to help reduce the computation time required in numerical simulations. The consistency with similar Green's functions for the 2-D problem, given by Tada and Madariaga (2001), has also been verified.

Our present theory can be extended, with a few modifications, to the case where the discrete elements have triangular shapes. The use of triangular elements widens the scope of simulation studies significantly, since faults of any arbitrary geometry can be modeled approximatively by joining small triangular elements together. In the poster presentation we plan to show some examples of results of numerical simulation studies on the dynamics of slipping faults carried out by using the rigorous Green's functions for a constant slip-rate on discrete fault elements of either square or triangular shapes.

Formation of the geometry of fault system due to dynamic interactions among fault elements

R. Ando¹, T. Tada² and T. Yamashita¹

1. Earthquake Research Institute, Univ. Tokyo, Yayoi, Bunkyo, 113-0032, Japan (Phone: +81-3-5841-5728, +81-3-5841-5699, Fax: +81-3-5841-5693, E-Mail: ando@eri.u-tokyo.ac.jp, tyama@eri.u-tokyo.ac.jp)
2. JST Research Fellow, Nat'l Res. Inst. Earth Sci. Disas. Prev., Tukuba, Ibaraki, 305-0006, Japan (Phone: +81-3-298-60-2071, Fax: +81-298-60-2832, E-Mail: kogutek@bosai.go.jp)

While geometrical complexity of fault system is not fully understood, some progress is made in recent studies. It is shown in those studies that interactions among fault segments play an important role in the formation of fault system geometry.

In order to investigate the effect of interactions on the formation of fault system geometry and dynamic rupture process, we newly develop the numerical scheme using a boundary integral equation method (BIEM), and simulate the dynamic rupture process assuming interactions among fault segments and non *a priori* constraint on the fault tip path. We assume fracture criterion that the fault tip extends in the direction where the shear traction takes local maximum.

We obtain qualitative properties of the effects of the interactions on the formation of fault geometry. First of all, we find the characteristic distribution area of planes on which the shear traction takes local maxima, called *traction reversal area*, around an in-plane shear fault. Next we find that the resulting fault geometry significantly depends on its initial distribution and approaching or separating of each fault tip is simulated. We also find that the resulting geometry highly depends on the fault tip velocity, which implies quasi-static analyses not inappropriate for the understanding of dynamic processes. From the simulation of the spontaneous rupture transfer process of the interactive faults, we find that the arresting of the rupture could occur in the interactive fault system, because of abrupt bending of fault tip, and the released shear traction is negative on the bent segment of the fault. Comparing our results with the 1992 Landers, California, earthquake, we find similarity on heterogeneous distribution of the slip on the fault, the geometry of the fault trace, and the time delay of the rupture transfer. One of the differences between our bending fault system and the straight fault system is the existence of stopping phase due to the time delay of rupture transfer, which appearing in our bending fault system.

We also simulate the spontaneous dynamic rupture process in fault zone; fault zone is approximated by arrays of micro-cracks in our study. We find that the rupture process depends on the initial micro-crack geometry rather than simply on the micro-crack density, and rupture arresting could occur due to the interactions among micro-cracks.

Our results show that spontaneous fault bending and interactions among faults could be a significant factor of the complexity of earthquakes.

P3-4

Simulation of earthquake rupture process using geological information: Application to the Uemachi fault

Yuko KASE¹, Haruo HORIKAWA¹, Haruko
SEKIGUCHI¹,
and Kenji SATAKE¹

1. Active Fault Research Center, National Institute of Advanced Industrial Science and Technology, AIST Tsukuba Central 7, AIST, Tsukuba, Ibaraki 305-8567, Japan (Phone: +81-298-61-3640, Fax: +81-298-61-3803, E-mail: kasep@ni.aist.go.jp)

In order to understand fault behaviour and predict strong ground motion, it is important to simulate realistic rupture processes of future earthquakes. We introduce geological information into model parameters of dynamic rupture simulations: fault model and stress field. We simulate rupture on the Uemachi fault.

A fault model is obtained from structure of basement and fault traces. The Uemachi fault is a thrust fault. The dip and rake angles are 60 and 90 degrees, respectively. The length of the fault is about 45 km, and the fault is composed of two main segments. Unfortunately, surface traces are not always clear, and the subsurface fault structure deeper than a few kilometers is unknown. There is no information on a possible rupture initial point. For the reasons given above, we carried out many simulations, varying distance and offset between two segments and location of an initial crack.

Principal stresses are assumed to be proportional to depth. A minimum principal stress is assumed to be equal to the overburden load, since the Uemachi fault is a thrust fault. EW maximum principal stress axis is assumed from a tectonic stress. We varied depth-dependence of a maximum principal stress and a ratio of strength excess to stress drop (the S value; Andrews, 1976, JGR), and calculated dynamic rupture processes using a finite difference method. We obtained the vertical dislocation of about 3 m on the earth's surface, which is consistent with a geological observation.

Two different rupture length are obtained: rupture terminating at the fault stepover and that propagating across the stepover. Whether rupture propagates across the fault stepover depends on a location of an initial crack. In a simulation using the obtained values of distance and offset between two segments observed on surface trace, a rupture does not propagates across the fault stepover. We need to improve the fault model and stress field by using further geological information, and to examine more possible earthquake rupture processes on the Uemachi fault.

P4-1

Experimental study of the shear failure process of rock in seismogenic environments

A. Kato¹, S. Yoshida¹, H. Mochizuki¹, M. Ohnaka²,

1. Earthquake Research Institute, Univ. of Tokyo, Yayoi 1-1-1, Bunkyo-ku, Tokyo, 113-0032, Japan
(Phone: +81-3-5841-5731, Fax: +81-3-5689-7234, E-mail: akato@eri.u-tokyo.ac.jp,
shingo@eri.u-tokyo.ac.jp, h-mochi@eri.u-tokyo.ac.jp)
2. Professor emeritus of Univ. of Tokyo, and Univ. College London, (E-mail: ohnaka@fd.catv.ne.jp)

There is commanding evidence that the earthquake rupture process combines frictional slip failure on a pre-existing fault with fracturing of intact rock. It is thus crucial to investigate the constitutive properties concerning the fracturing of intact rock in seismogenic environments as well as slip failure on pre-existing surfaces. In order to investigate the constitutive properties of intact granite in simulated seismogenic environments, we have conducted a series of fracture experiments using a triaxial apparatus which enable us to independently control the rate of loading piston, temperature, confining pressure, and interstitial pore water pressure in seismogenic environments. Tsukuba-intact granite (length=40mm, diameter=16mm) was deformed under temperature-pressure conditions that simulate crustal depth down to 17 km at various strain rates ranging from 10^{-5} /s to 10^{-7} /s (the slip velocity ranges from 10^{-4} mm/s to 10^{-6} mm/s).

Based on the experimental results conducted at a strain rate of 10^{-5} /s, we successfully evaluated the dependence of constitutive law parameters prescribing the slip-dependent law on temperature and effective normal stress in a quantitative manner. It was found that the critical slip displacement D_c for intact Tsukuba-granite remains almost constant below 300C while D_c increases with increasing temperature above 300C, and the increasing rate of D_c against temperature tends to be large at higher effective normal stress. The breakdown stress drop for intact granite is roughly constant (80 MPa) below 300C while it decreases linearly with temperature. The reduction rate of breakdown stress drop against temperature becomes large at higher effective normal stress. Although the peak shear strength increases linearly with increasing effective normal stress below 300C, the increase in the rate of peak shear strength against the effective normal stress (internal frictional coefficient) becomes small above 300C. These variations of constitutive law parameters are consistent with the microscopic observation that the mechanical behavior of Tsukuba-granite in the temperature range above 300C is mainly brittle and slightly plastic at a strain rate of 10^{-5} /s. The plastic deformation in shear zone is attributed to thermally activated processes such as dislocation glide of biotite and quartz grains.

After clarifying how constitutive properties depend on temperature and effective normal stress, the effect of slip velocity on constitutive properties was investigated by experiments conducted in wet seismogenic environments at strain rates ranging from 10^{-5} /s to 10^{-7} /s (the slip velocity ranges from 10^{-4} mm/s to 10^{-6} mm/s). It was found that the peak shear strength logarithmically diminishes with decreasing slip velocity, and shows similar results under dry conditions observed in previous studies. Both D_c and breakdown stress drop also decrease logarithmically with decreasing slip velocity. It was found that the effect of slip velocity on constitutive properties is not greatly significant and is barely affected by temperature and effective normal stress in seismogenic environments.

As a whole, it was revealed that the stability of shear failure is enhanced by the increase of temperature, effective normal stress, and slip velocity above 300C. The effect of slip velocity on the stability is not strong by comparison with the effect of temperature and effective normal stress on the stability. The increase in stability above 300C is probably one of mechanisms that govern the lower limit of seismicity in the crust, and one of the factors that prevent a slow slip event from becoming a catastrophic rupture.

P4-2

Hydrodynamic controls on fault strength during rapid slip: laboratory constraints

Christopher WIBBERLEY*, Shinichi UEHARA and Toshihiko SHIMAMOTO
*Dept. of Geology and Mineralogy, Graduate School of Science, Kyoto University, Kyoto
606-8502, Japan *e-mail: cwibber@ip.media.kyoto-u.ac.jp*

Fluid pressure evolution during rapid slip has been shown theoretically to be capable of dictating strength changes and overall stress release during earthquakes. In particular, frictional heating of pore fluid can cause a rapid fluid pressure increase, resulting in a large drop in effective stress and therefore strength of the deforming zone. This process of thermal pressurization depends on firstly the relationship between frictional strength and heat production, and secondly the relationship between heat production and the fluid pressure response. Applications of such theoretical models are hindered by the lack of data on the appropriate physical properties of the slip zone and surrounding material which control these relationships. Highlighted by previous theoretical works is the uncertainty in appropriate permeability values that will seriously affect the fluid behaviour during slip.

This presentation firstly reports on the current status of work on permeability and poroelastic properties of fault zone materials, concentrating on gouges from zones of rapid slip. Whilst data from several fault zones show that fault gouges have relatively low permeabilities in comparison to surrounding fault rocks, slip zone permeabilities are lower still. Compressibilities of gouges do not vary much between samples, but are sensitive to pressure and only show elastic behaviour after compaction to an initial peak pressure. The data are used to estimate hydraulic diffusivity with water as the pore fluid.

Previous models of thermal pressurization and other responses to rapid slip are assessed using the data. It is shown that gouge from the principal slip zones of faults typically have hydraulic diffusivities lower than estimated thermal diffusivity, provided that the gouges have been subjected to previous peak effective pressures in the region of 80 - 120 MPa. Given these conditions, pressurized fluid is unlikely to escape at a faster rate than it can be heated by the thermal pulse. These hydrodynamic constraints are from laboratory data on core-scale samples and lateral continuity of hydrodynamic properties requires verification in the field. Asperities and cemented fault rocks that can behave by fracture dilatancy may limit the ability of pressurization to occur along the rupture plane, suggesting that dynamic fluid pressure rises are only likely to occur if the rupture plane is confined to the previous low permeability central slip zone.

P4-3

Preliminary report on a small-scale granitic mylonite zone in the Hirabayashi NIED core penetrating the Nojima fault

Koji Shimada¹, Takashi Arai², Satoshi Hirano³, Ryuji Ikeda⁴,
Kenta Kobayashi⁵, Tatsuo Matsuda⁴, Kentaro Omura⁴,
Hidemi Tanaka⁶ and Tomoaki Tomita⁷

1. Department of Earth Sciences, Waseda Univ., Shinjuku, Tokyo, 169-8050, Japan

(Phone: +81-3-5286-1510, Fax: +81-3-3207-4950, E-mail: kojishim@mn.waseda.ac.jp)

2. Shinshu Univ., 3. JAMSTEC, 4. NIED, 5. Niigata Univ., 6. Univ. Tokyo, 7. Univ. of Tsukuba

The core penetrating the active Nojima fault recovered from 1000 m to 1838.8 m depth at Hirabayashi (here after, the NIED core) has been investigated according to material and geologic methods by many authors (e.g. Tanaka et al., 2001, Matsuda et al., 2001). The NIED core consists of three fracture zones at depths of about 1140 m, 1300 m and 1800 m, and granodioritic to tonalitic protolith. All fracture zone was characterized by cataclastic fault rocks accompanied with alterations such as pseudotachylyte, fault gouge, cataclasites, and weakly pulverized and altered rocks. No evidence of intracrystalline plastic deformation has been observed in these fault rocks.

Recently, a small-scale granitic mylonite zone has been discovered at the depth of 1828.3 m by thin section observations. The polished slab piece of the mylonite is the deepest in the analyzed section of the 1800 m fracture zone (1774.9 m to 1828.4 m depth). Although precise extent of the mylonite zone has not been clarified yet, the mylonitic foliation depicted by preferred orientation of mafic minerals suggests that the zone is less than 1 m in thickness. Under the microscope, a centimeter-scale sigmoidal elongation-trajectory of recrystallized quartz aggregates is traceable. A quartz c-axis fabric in the high-strain zone shows the type-I crossed girdle pattern which suggests low- to medium-grade metamorphic conditions during the mylonitization. The maximum principal strain axis is nearly horizontal, and the mylonitic foliation dips moderately on the basis of weak asymmetry in the c-axis fabric.

We present a revised fault rock distribution map of the 1800 m fracture zone and mylonitic microstructures, and discuss the relationship between the existence of the mylonite zone and initiation of the cataclastic faulting of Nojima fault.

P4-4

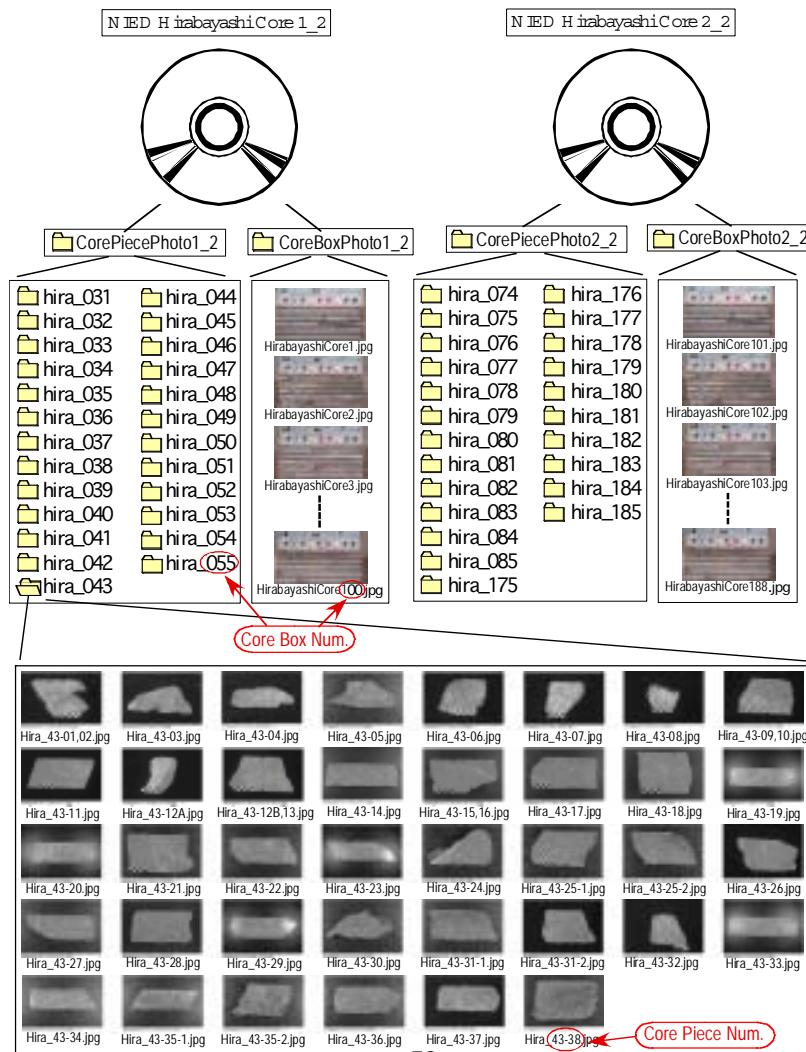
Photographs of NIED Nojima Fault Drilling Cores at Hirabayashi Site: CD-ROM Volumes

Kentarō OMURA^{*1}, Takashi ARAI^{*2}, Satoshi HIRANO^{*3}, Kenta KOBAYASHI^{*4}, Tatsuo MATSUDA^{*1}, Koji SHIMADA^{*5},
Hidemi TANAKA^{*2}, Tomoaki TOMITA^{*6}, and Ryuji IKEDA^{*1}

^{*1}National Research Institute for Earth Science and Disaster Prevention (NIED), 3-1, Tennodai, Tsukuba, Ibaraki, 305-0006, Japan, (omura@bosai.go.jp), ^{*2}University of Tokyo, ^{*3}Japan Marine Science and Technology Center, ^{*4}Niigata University, ^{*5}Waseda University, ^{*6}University of Tsukuba

We collected fault zone cores continuously from 1000m to 1838m depth of Nojima Fault which activated during the 1995 Hyogoken Nanbu Earthquake by drilling through the fault about one year after the earthquake. Cores are all granitic rocks including porphyritic intrusive rocks in spots and remarkably fractured zones consisting of cataclastic rocks at three depths around 1140m, 1300m and 1800m. Core samples in fracture zones were so damaged that we fixed the surface of each core piece with an epoxy resin and cut it vertically into two halves. A cutting surface of one of two halves was fixed again by epoxy resin and was polished into plane surface (polished piece). The other half of core was used for chemical analysis or making thin section, e.t.c.. Total about 2210 polished pieces were made by cores from three fracture zone intervals: 1054 - 1189.6m, 1276.7 - 1336.7m and 1774.9 - 1828.4m. We took photographs of all cores placed in core boxes and all polished pieces' surfaces. Those photographs were converted into digitized images (JPEG format) and stored in two volumes of CD-ROM.

The each CD-ROM volume include two folders; one contain core box photographs, the other consist of folders corresponding core box in fracture zones, which contains polished pieces photographs. The latter folder, in addition, contains table (Microsoft Excel file) that correspond the core piece number to the depth. Those digitized image of fracture zone cores are suitable for mesoscopic observation and quantitative image processing. The CD-ROM volumes will be distributed to applicants soon after the Workshop.



Author Index

=A=

Aki, K. S2-3
 Ando, M. **S1-8** S4-12 P2-2 P2-5
 Ando, R. **P3-3**
 Aochi, H. **S3-2**
 Aoki, H. P2-3

Arai, T. S4-6 P4-4 P4-5

=B=

Beilecke, T. S2-9
 Bernard, P. S1-7
 Bizzarri, A. S3-3
 Borm, G. S1-7 S2-9
 Boullier, A. M. S1-4 **S4-8**
 Bram, K. S2-9

=C=

C  lerier, B. S1-4
 Celik, C. P2-6
 Chen, W. M. S4-12
 Chester, F. M. **S4-11**
 Chester, J. S. S4-11
 Cocco, M. **S3-3**
 Cornet, F. H. **S1-7**

=D=

Day, S. M. S2-3 P2-1
 Dor, O. S2-4
 Dubois, M. S4-8

=E=

Ellsworth, W. L. **S1-3** S1-6
 Engeser, B. **S1-2**

=F=

Fischer, D. S2-9
 Frank, A. S2-9
 Fujimoto, K. S1-4 S4-2 S4-8 **S4-9** S4-10
 Fukuchi, T. S4-4
 Fukuyama, E. **S3-1** **P2-11** P2-13 P3-2
 Fusejima, Y. **P2-12**

=G=

Gebrande, H. S2-9
 Glover, P. S1-4

=H=

Hickman, S. H. **S1-6**
 Hiramatsu, Y. S2-1
 Hirano, S. S4-6 P4-4 P4-5
 Hirose, T. S4-4
 Honkura, Y. P2-6
 Horikawa, H. P3-4
 Horiuchi, S. S2-5 **S2-6** P2-2 P2-8

=I=

Iio, Y. S1-1 **S2-5** S2-6 P1-1 P2-8
 Ikeda, R. **S0-1** **S1-1** S2-5 S4-3 S4-6 S4-7 P4-4
 P4-5
 Ildefonse, B. S1-4 S4-8
 Imanishi, K. P2-7 **P2-8**
 Imura, R. P2-12
 Ishii, H. P1-1
 Ito, H. S1-4 **S1-5** S2-2 S2-5 S4-3 S4-8 S4-9 S4-10
 S4-12 P2-7 P2-8 P3-1 P4-3

=K=

Kano, Y. S2-1 **P2-9**
 Kase, Y. **P3-4**
 Kato, A. **P4-1**

Kayen, R. P2-4	Monzawa, N. S4-5
Kiguchi, T. S1-4 P4-3	Moore, D. S4-3
Kirschner, D. L. S4-11	Moretti, I. S1-7
Kobayashi, K. S4-6 P4-4 P4-5	Morino, M. P2-12
Kobayashi, Y. S2-5	Moriyama, S. P1-1
Komatsubara, T. P2-12	Muller, R. D. P2-10
Kubo, A. P2-13	=N=
Kück, J. S1-2 S2-9	Nagai, S. S2-1
Kurosawa, H. P2-12	Nishigami, K. S2-1 P1-3 P2-9
Kuwahara, Y. S2-2 P2-8 P3-1 P4-3	=O=
=L=	Ogasawara, H. P1-1 P1-2
Li, Y. G. S2-3 P2-1	Ogawa, Y. S2-8
Lin, C. H. P2-5	Oglesby, D. D. S2-3 P2-1
Lockner, D. A. S4-3	Ohmi, S. S2-5 P2-8
Lüschen, E. S2-9	Ohnaka, M. P4-1
Lussac, C. S1-4	Ohtani, T. S1-4 S4-8 S4-9 S4-10
=M=	Okaya, D. S2-9
Madariaga, R. S3-2	Okubo, M. P2-3
Mamada, Y. P3-1	Olsen, K. B. P2-11
Marone, C. S3-4	Omura, K. S1-1 S4-6 S4-7 P4-4 P4-5
Masuda, K. S4-2	Onishi, M. P2-3
Matsuda, T. S1-1 S4-6 S4-7 P4-4 P4-5	Oshiman, N. P2-6
Matsuzawa, T. P2-8	Oshita, K. P2-3
Mikumo, T. P2-11	Otsuki, K. S4-5
Mishina, M. S2-8	=P=
Mitsuhata, Y. S2-8	Pezard, P. A. S1-4 S4-8
Miyata, T. P2-4	=R=
Mizoguchi, K. S4-4	Rabbal, W. S2-9
Mizuno, K. P2-12	Reches, Z. S2-4
Mizuno, T. S2-1 P1-3	=S=
Mochizuki, M. P4-1	Sakaguchi, A. S4-12

- Sasaki, T. P2-12
- Satake, K. P3-4
- Sato, H. S2-5
- Sato, N. S4-1
- Sekiguchi, H. P3-4
- Sekiguchi, S. P2-8
- Shibazaki, B. **S3-4** P3-2
- Shih, B. J. P2-4
- Shimada, K. S4-6 **P4-4** P4-5
- Shimamoto, T. **S4-4** P4-2
- Shishikura, M. P2-12
- Smithson, S. S2-9
- Stork, A. L. **P2-7**
- Sugiyama, Y. P2-12
- =T=
- Tada, T. **P3-2** P3-3
- Tadokoro, K. S2-1
- Takada, S. P2-4
- Takai, K. S2-6
- Takeo, M. P2-8
- Tanaka, H. S4-3 S4-6 S4-9 S4-10 **S4-12** P4-4 P4-5
- Tanaka, T. **P2-3**
- Tanaka, Y. P2-4
- Tank, S. B. **P2-6**
- Toda, S. **S2-7**
- Tolak, E. P2-6
- Tomita, T. S4-6 P4-4 P4-5
- Tuncer, M. K. P2-6
- =U=
- Ueda, A. S4-9
- Uehara, S. P4-2
- Ujiie, K. S4-12
- =V=
- Vardoulakis, I. S1-7
- Vidale, J. E. S2-3 P2-1
- =W=
- Wang, C. Y. S4-12
- Wibberley, C. **P4-2**
- Wilson, J. E. S4-11
- Wohlgemuth, L. S1-2
- =Y=
- Yabe, Y. S4-1
- Yamamoto, E. S2-5
- Yamamoto, K. S2-5 **S4-1**
- Yamashita, T. **S3-5** P3-3
- Yanagidani, T. P2-9
- Yoshida, S. S3-4 P4-1
- Yoshioka, T. P2-12
- =Z=
- Zamora, M. S1-4
- Zhao, S. J. **P2-10**
- Zheng, S. S2-6 **P2-2**
- Zoback, M. D. S1-6
- =Group=
- Nankai Trough Seismogenic Zone Research Group
P1-4
- SA Group **P1-1**

original on February, 26, 2002
revised on March 11, 2002

International Symposium on
Physics of Active Fault Organization Committee

Ryuji IKEDA	Chair
Eiichi FUKUYAMA	Co-chair
Kentaro OMURA	Co-chair
Shigeki HORIUCHI	Co-chair
Mizuho ISHIDA	Co-chair
Tatsuo MATSUDA	
Atsuki KUBO	
Kaori TAKAI	
Yukiko HAYASHI	

Sponcered by National Research Institute for Earth Science and Disaster Prevention